Academic year 2024 – 2025

Master Thesis

From MENA to Europe: System-optimal hydrogen and derivative imports under finance and infrastructure constraints

Full Name of Student: Lucas Christopher Mandl-Ehmann

Core Provider: Hanze University of Applied Sciences

Specialisation: Hanze University of Applied Sciences

Host Organization: German Aerospace Center (DLR)
Curiestr. 4, 70563 Stuttgart
Germany

Submission Date: 30.11.2025

Originality declaration

By this letter, I declare that I have written this thesis completely by myself, and that I have used no other sources or resources than the ones mentioned.

The sources used have been stated in accordance with the EUREC Project Guidelines. I have indicated all quotes and citations that were literally taken from publications, or that were in close accordance with the meaning of those publications, as such. Moreover, I have not handed in an essay, paper or thesis with similar contents elsewhere. All sources and other resources used are stated in the bibliography.

In case of proof that the essay, paper or thesis has not been constructed in accordance with this declaration, the School of Engineering considers the essay, paper or thesis as negligence or as a deliberate act that has been aimed at making correct judgment of the candidate's expertise, insights and skills impossible.

In case of plagiarism the examiner has the right to exclude the student from any further participation in the particular assignment, and also to exclude the student from further participation in the MSc program at the School of Engineering of Hanze University of Applied Sciences, Groningen. The study results obtained in the course will be declared null and void in case of plagiarism (also see Article 14 of the Teaching and Examination Regulations).

Name: Lucas Mandl-Ehmann

Place: Stuttgart, Germany

Date: 30.11.2025

Signature:

Acknowledgments

I would like to express my sincere gratitude to my supervisors at the Institute of Networked Energy Systems at the DLR, Manuel Wetzel and Thomas Pregger, for their continuous support, constructive feedback, and many valuable discussions throughout this project. Their practical insights and guidance were essential for linking the modelling work to real-world questions and keeping the study focused and relevant.

I am equally grateful to my academic supervisor, Frank Pierie, for his scientific guidance, critical comments and encouragement over the course of this thesis. His input has helped me greatly to improve the clarity and robustness of this work.

Abstract

Decarbonising the European energy system is likely to require large-scale imports of renewable hydrogen and synthetic fuels, for which the Middle East and North Africa (MENA) region is a prime candidate supplier due to its resource endowment and proximity. This thesis provides a system-level techno-economic assessment of long-term (2030-2050) hydrogen and synfuel trade between the European Union (EU) and MENA, asking what cost-optimal trade architecture emerges and how it is shaped by cross-regional infrastructure constraints and country-specific financing conditions. A brownfield, spatially explicit energy-system optimisation model is extended to couple the EU and MENA via existing and expandable electricity and gas networks, a broad portfolio of hydrogen and synfuel pathways (including DAC-based synthetic methane and Fischer-Tropsch fuels), and perfect-foresight optimisation for 2030, 2040 and 2050. The scenario set comprises a baseline with uniform financing and unconstrained infrastructure (BASE), a no-trade case (AUTARKY), two transport variants with delayed or absent cross-regional hydrogen pipelines (TRANS_delay, TRANS_no_pipeline), and a WACC case with differentiated costs of capital in MENA.

Within the explored scenario space, the cost-optimal configuration under uniform financing and unconstrained infrastructure is MENA-centred: renewable generation and conversion capacity shift towards MENA, while Europe remains structurally import-dependent for hydrogen, synthetic methane and Fischer-Tropsch fuels. Hydrogen primarily redistributes energy within and between regions, FT fuels serve as long-distance carriers and synthetic methane provides large-scale seasonal flexibility via cavern storage. Removing cross-regional molecular trade demonstrates the technical feasibility of European self-sufficiency, albeit at a substantially higher cost, whereas infrastructure constraints that delay or remove hydrogen pipelines reduce trade volumes and alter the carrier mix without eliminating the economic rationale for EU-MENA exchange. Differentiated, higher costs of capital in MENA reduce export volumes, concentrate investment in a few low-risk exporters, reshore parts of the supply chain to Europe and yield the highest total system costs of all variants, underscoring financing conditions as a critical driver of who trades, with whom and at what cost. Methodologically, the thesis demonstrates the value of combining a brownfield network representation, a broad carrier portfolio and regionally differentiated financing assumptions in an integrated energy-system model, and concludes that an EU-MENA hydrogen and synfuel partnership is structurally attractive but highly sensitive to infrastructure development and the management of financing risk.

Table of contents

1. Introduction 10
2. Modelling framework and methodology 12
   2.1 Energy system optimisation model: REMix framework 12
   2.2 Adapted REMix model 12
   2.2.1 Geographic model area and network representation 12
   2.2.2 Technology portfolio and carrier representation 13
   2.2.3 Temporal scope and investment accounting 14
   2.3 Input data sources and harmonisation 15
   2.4 Validation of model adaptations and extensions 16
   2.5 Scenarios as a robustness test for the EU-MENA system 16
   2.6 Result metrics and evaluation dimensions 16
3. Model inputs and techno-economic assumptions 18
   3.1 Geographical aggregation and network topology of the EU-MENA system 18
   3.2 Final energy demand assumptions 19
   3.3 Techno-economic assumptions for energy technologies 20
   3.3.1 Hydrogen production pathways and process configurations 20
   3.3.2 Synthetic methane production pathway 21
   3.3.3 Fischer-Tropsch fuel production pathway 21
   3.3.4 Energy storage technologies 22
   3.3.5 Energy transportation technologies 22
   3.4 Scenario assumptions and common settings 23
4. Model results 25
   4.1 BASE and AUTARKY: integrated system architecture and value of trade 25
   4.1.1 Pathway ramp-up dynamics in the BASE scenario 32
   4.1.2 AUTARKY scenario: system reconfiguration without cross-regional trade 33
   4.1.3 System costs and regional cost decomposition 36
   4.1.4 Political implications: import dependence and sovereignty 41
   4.2 Outcome sensitivity to infrastructure constraints 42
   4.2.1 TRANS_delay 43
   4.2.2 TRANS_no_pipeline 44
   4.2.3 CO_2 price levels, regional differentials and system cost 46
   4.3 Outcome sensitivity to finance constraints 47
5. Discussion 50
   5.1 Uncertainty in underlying assumptions 50
   5.2 Results in the context of a comparison study by Krüger et al. 52

5.3 Political relevance for an EU-MENA energy partnership 52
6. Conclusion 54
References X
Annex XVIII

Table of Figures

Figure 2-1 Geographical representation of the adapted model 13
Figure 2-2 Technological system boundary of the adapted model 14
Figure 2-3 Temporal scope and investment horizon of the optimisation model 15
Figure 2-4 Connection between scenarios and SQ/RQ 16
Figure 2-5 Methodology overview 17
Figure 3-1 Reduced EU-MENA network topology 19
Figure 3-2 Regional baseline water stress levels in 2030, based on values from [52] 20
Figure 4-1 Total RES capacity 2030 (left) and 2050 (right) (BASE scenario) 25
Figure 4-2 Total electrolysis (left) and reverse osmosis (right) capacity (BASE, 2050) 26
Figure 4-3 MENA electrolysis and storage utilisation (BASE, 2050) 26
Figure 4-4 EU electrolysis and storage utilisation (BASE, 2050) 27
Figure 4-5 Total methanation (left) and FT synthesis (right) capacity (BASE, 2050) 27
Figure 4-6 Net annual hydrogen flows; top 80% (BASE, 2050) 28
Figure 4-7 Net annual methane flows; top 80% (BASE, 2050) 29
Figure 4-8 Net annual network utilisation (BASE, 2050) 29
Figure 4-9 EU final methane demand and storage utilisation (BASE, 2050) 30
Figure 4-10 Net annual FT fuel flows; top 80% (BASE, 2050) 31
Figure 4-11 Annual supply chain composition based on total installed capacities (BASE) 32
Figure 4-12 FLH of HVAC and HVDC grid 2030 (left) and 2050 (right) (BASE) 33
Figure 4-13 Change in RES (left) and Electrolysis (right) capacity in AUTARKY compared to BASE (2050) 33
Figure 4-14 Change in methanation (left) and FT production (right) capacity in AUTARKY compared to BASE (2050) 34
Figure 4-15 Selected storage capacity BASE vs. AUTARKY (2050) 34
Figure 4-16 EU hydrogen cavern storage utilisation AUTARKY (2050) 34
Figure 4-17 Net annual network utilisation AUTARKY (2050) 35
Figure 4-18 MENA and Turkey hydrogen storage utilisation AUTARKY (2050) 35
Figure 4-19 Gross annual network flows BASE vs. AUTARKY (2050) 36
Figure 4-20 MENA total system cost by group and aspect BASE 37
Figure 4-21 EU total system cost by group and aspect BASE 37
Figure 4-22 EU (left) and MENA (right) mean methane marginal demand duration curves BASE 38
Figure 4-23 EU and MENA marginal demand duration curves BASE (2050) 39
Figure 4-24 Marginal electricity production cost Δ 2030 (left) and 2050 (right) BASE 40
Figure 4-25 Marginal hydrogen production cost Δ 2030 (left) and 2050 (right) BASE 40
Figure 4-26 EU autarky penalty decomposition by sector BASE 41
Figure 4-27 Import dependency by country (top 15) BASE (2050) 42
Figure 4-28 Change between BASE and 2023 reference import dependencies (country-specific import dependency data from [74]) 42
Figure 4-29 Installed RES and electrolysis capacity TRANS_delay vs. BASE 43
Figure 4-30 EU autarky penalty by sector TRANS_delay 44
Figure 4-31 Total installed RES (top left), hydrogen (top right), methanation (bottom left) and FT fuel production (bottom right) capacities TRANS_no_pipeline (2050) 45

Figure 4-32 Regional DAC capacity AUTARKY (left) and TRANS_no_pipeline (right) in 2050 46
Figure 4-33 Total installed RES (top left), hydrogen (top right), methanation (bottom left) and FT fuel production (bottom right) capacities WACC (2050).....48
Figure 4-34 Net annual energy flow through EU-MENA network links (2050).....49

List of Tables

Table 2-1 Accounting indicator categories.....15
Table 3-1 Overview of main characteristics for the analysed energy carriers 20
Table 3-2 Saltwater desalination using reverse osmosis, techno-economic input data.....21
Table 3-3 Catalytic methanation plant, techno-economic input data 21
Table 3-4 Low temperature Fischer-Tropsch fuel production, techno-economic input data21
Table 3-5 Methanol-to-Kerosene route, techno-economic input data.....22
Table 3-6 Solid Adsorption Direct Air Capture, techno-economic input data 22
Table 3-7 TCO for selected transport technologies.....23
Table 3-8 Common modelling settings.....23
Table 3-9 Scenario variants 24

Nomenclature

EU ..... European Union
MENA ..... Middle East and North Africa
IPCC..... Intergovernmental Panel on Climate Change
DLR ..... Deutsches Zentrum für Luft- und Raumfahrt (German Aerospace Center)
NeoFuels ..... Research project providing demand scenarios for hydrogen and synfuels
H_2 ..... Hydrogen
H_2O ..... Water
CH_4 ..... Methane
NG ..... Natural gas
LNG ..... Liquefied natural gas
LH_2 ..... Liquefied hydrogen
CO_2 ..... Carbon dioxide
FT fuel ..... Fischer-Tropsch synthetic fuel (liquid hydrocarbons)
RFNBO ..... Renewable fuel of non-biological origin
RES ..... Renewable energy sources
PV ..... Photovoltaic
AEC ..... Alkaline electrolysis cell / alkaline electrolyser
PEM ..... Proton-exchange membrane electrolyser
SOEC ..... Solid-oxide electrolysis cell
DAC ..... Direct air capture (of CO_2)
SWRO ..... Seawater reverse osmosis (desalination)
MTH ..... Methanol-to-hydrocarbon route for FT fuel production
HVAC ..... High-voltage alternating current (electricity transmission)
HVDC ..... High-voltage direct current (electricity transmission)
REMix ..... Renewable Energy Mix energy system model framework
ESOM ..... Energy system optimisation model
GAMS ..... General Algebraic Modeling System
TSC ..... Total system cost
TCO ..... Total cost of ownership
CAPEX ..... Capital expenditure
O&M ..... Operation and maintenance
FOM ..... Fixed operation and maintenance
WACC ..... Weighted average cost of capital
VOLL ..... Value of lost load
FLH ..... Full-load hours

kWh ..... Kilowatt-hour
MWh ..... Megawatt-hour
GWh ..... Gigawatt-hour
TWh ..... Terawatt-hour
MW ..... Megawatt
GW ..... Gigawatt
TW ..... Terawatt
€/MWh ..... Euro per megawatt-hour
€/t ..... Euro per metric tonne

1. Introduction

Global warming is unequivocally anthropogenic, with extensive impacts on current and future societies and the environment [1]. Consequently, climate-change mitigation has become a central pillar of the current global policy landscape, with increasing efforts to phase out fossil fuels and build resilient energy systems [2].

The European Union (EU) presents itself as a frontrunner in global decarbonisation, setting ambitious targets to become climate-neutral by 2050 [3]. Given the EU's commitments, the deep decarbonisation of hard-to-abate sectors, responsible for a substantial share of energy-related greenhouse-gas emissions, becomes essential [4, 5]. Renewable hydrogen[1] and renewable fuels of non-biological origin (RFNBOs, hereafter synfuels) are widely regarded as promising energy carriers for decarbonising these hard-to-abate sectors [7].

At present, however, the domestic cost competitiveness of renewable hydrogen and synfuels is hindered by high production costs [7]. The high energy intensity of hydrogen pathways, coupled with limited surplus renewable electricity as well as immature technologies keeps EU supply prices elevated [7]. Importing hydrogen and synfuels from regions where production-cost advantages may outweigh transportation costs and conversion losses is therefore a plausible option. Reflecting this, and alongside energy diversification efforts, the EU's near-term hydrogen strategy envisages the import of 10 million tonnes of renewable hydrogen and synfuels by 2030 [8].

Despite concrete near-term targets, the EU hydrogen strategy [9] remains vague about renewable hydrogen and synfuel sourcing strategies beyond 2030; phase three focuses on technological maturity and large-scale deployment, but does not specify long-term sourcing pathways [9]. The long-term role of imports from outside the EU therefore remains politically undetermined, marking a need for further system studies on sourcing strategies.

A review of 41 selected studies (see Annex 1) reveals a similar lack of consensus regarding the role of imports in the future EU energy system. Current studies forecast widely varying hydrogen-import shares, from single-digit percentages (e.g., [10]) to dependencies exceeding 50% (e.g., [4]), while consistently finding that synfuels are generally cheaper to import rather than to produce domestically, as transport costs constitute a smaller share in the final supply price [11]. This disparity is often driven less by disagreement on direction than by modelling choices [12].

First, the envelope of technologies reviewed is often narrow. Many assessments only consider a limited number of energy carriers (e.g., [13], [14] or [15]) or simplify transport chains (e.g., [16], [17] or [18]). In a multi-energy system, where all energy demands must be met simultaneously, a narrow energy carrier scope can overlook competition for resources and technologies among carriers, which in turn can misrepresent the role of an energy carrier in a broader system and produce artificially low supply cost estimates [11].

Secondly, even when transport is modelled comprehensively, greenfield assumptions are common, omitting considerations of existing infrastructure [19]. Approaching a potential trade network from brownfield conditions – using, repurposing or expanding upon existing infrastructure – can, however, expose or disprove infrastructure bottlenecks and represent more realistic transportation conditions, as alternative technologies might be needed to

[1] The definition for renewable hydrogen follows the guidelines set by the European Commission [6]. As such the hydrogen must be produced using renewable electricity.

avoid these constraints when considering limited build rates. Since transportation can account for up to 54% of the final supply price, a detailed analysis is warranted [12].

Thirdly, financing risks are frequently oversimplified. Uniform financing conditions forego country-sensitive risk premiums, which have been shown to raise final supply costs by multiples (see [20] and [21]). Incorporating accurate financing conditions into future system studies is therefore of high priority [22].

Some recent work begins to address individual elements of these gaps (e.g., [23] and [24]), but to the author's knowledge, no study simultaneously combines a brownfield network representation, a broad hydrogen and synfuel carrier portfolio and country-sensitive financing assumptions for an integrated system with the Middle East and North Africa (MENA) region as trade partner. The MENA region is attractive given its abundant renewable energy potential and geographic proximity to key entry points into the European energy grid [16].

Against this backdrop, this thesis provides a system-level techno-economic assessment of long-term (2030-2050) EU-MENA trade in hydrogen and synfuels. It constructs a brownfield energy system optimisation model (ESOM) that couples the European Union as primary importer with the MENA region as a potential exporter and analyses the resulting trade architecture under alternative infrastructure and financing conditions.

The thesis primarily aims (i) to generate decision-relevant insights on the viability of the MENA region as a hydrogen and synfuel trade partner for the EU, and, secondarily, (ii) to quantify how methodological choices regarding infrastructure and financing affect system outcomes.

The analysis is guided by the following main research question (RQ):

> *What cost-optimal architecture of hydrogen and synfuel trade between the EU and the MENA region emerges up to 2050, and how is it shaped by cross-regional infrastructure constraints and country-specific financing conditions?*

To structure the analysis, three sub-questions (SQ) are addressed:

1. What configuration of generation, conversion, storage and transport assets between the EU and the MENA region emerges under a cost-minimising central-planner perspective when cross-regional trade is unconstrained and financing conditions are uniform?
2. How do limitations on cross-regional transport infrastructure alter this cost-optimal architecture in terms of trade volumes, siting of assets and total system costs?
3. How do country-specific costs of capital for renewable, hydrogen and synfuel investments in the MENA region alter the spatial distribution of investment, trade flows and the regional allocation of system costs compared to the uniform-financing baseline?

To navigate these questions, Chapter 2 describes the modelling methodology and system boundary. Chapter 3 details the exogenous inputs and scenario configurations. Chapter 4 reports the model results and answers Sub-questions 1-3. Chapter 5 discusses the findings in the context of literature and policy implications. Chapter 6 concludes the thesis by summarising the main findings and formulating an answer to the main research question.

2. Modelling framework and methodology

To answer the research questions posed in the introduction, this thesis employs a model-based approach, with scenarios utilised as the main exploration method. The following chapter will justify the use of REMix as an appropriate model choice (Chapter 2.1), followed by the methodological description of the adapted REMix model (Chapter 2.2), data sourcing methods (Chapter 2.3) and the employed validation strategy (Chapter 2.4). Chapter 2.5 then outlines the use of scenarios as the main analysis method before finally describing the applied evaluation criteria (Chapter 2.6).

2.1 Energy system optimisation model: REMix framework

Energy-system optimisation models are key tools for developing future energy scenarios [25]. For this thesis, the model must (i) represent multiple hydrogen and synfuel production pathways, (ii) capture spatially explicit EU-MENA trade corridors and (iii) distinguish regional subsystems to track cross-border flows.

The *REMix* framework, developed at the Institute of Networked Energy Systems of the German Aerospace Center (DLR), meets these requirements. It translates user-defined energy systems into a GAMS-based optimisation model and has historically been used to assess infrastructure needs in continental systems with high shares of variable renewable energy sources (RES) [26].

For this study, an existing intra-European REMix model is extended to include the MENA region as well as additional hydrogen and synfuel supply chains, detailed in Chapter 3. An overview of the underlying model can be found in [27] and [28].

2.2 Adapted REMix model

As described in Chapter 2.1, the existing REMix model instance is adapted to fit the needs of this thesis. The following section will first present the geographical abstraction of the EU-MENA system in the adapted REMix model, then describe the technological system boundary and lastly define the temporal scope and accounting approach on which the model is optimised.

2.2.1 Geographic model area and network representation

Inside the adapted REMix model, the EU-MENA system is abstracted as a set of regional nodes connected by technology-specific links. Each country is represented by at least one node, though smaller countries may be grouped to control model complexity. Node locations and interconnections are derived from existing high-voltage electricity and natural-gas transmission networks (see Annex 3) using grid reduction methods outlined in [28]. Within each node, supply, demand and storage are aggregated, without modelling sub-regional energy transmission to limit model complexity.

To ensure full system connectivity, a minimal number of new interconnections are introduced where legacy infrastructure is insufficient. These additions are constrained to preserve the brownfield character of the system. External imports into the model boundary are disallowed, except for a limited volume of natural gas (NG) to reflect current trends [29]. Figure 2-1 visualises an abstract representation of a small set of model nodes configured in the above-described way.

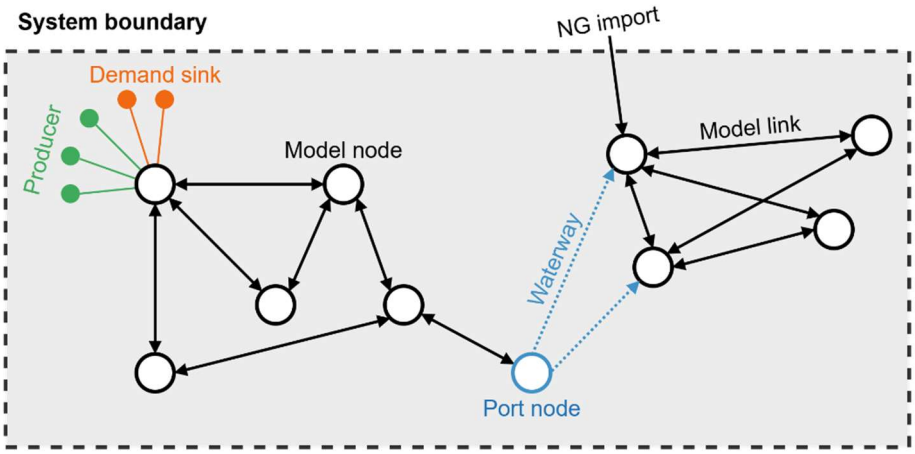

Figure 2-1 Geographical representation of the adapted model

2.2.2 Technology portfolio and carrier representation

The operational supply chain represented in the adapted model comprises four stages: (i) electricity generation, (ii) conversion to hydrogen and synfuels, (iii) transport and (iv) end-use. This choice reflects a standard ESOM focus on system operation and investment decisions across the physical energy chain, while excluding upstream raw-material extraction, plant manufacturing and end-of-life processes [30, 31]. While the most important assumptions will be highlighted here, a list of all relevant assumptions is presented in Annex 4.

The underlying REMix instance already includes a broad portfolio of renewable and fossil power plants, hydrogen production via electrolysis and steam-methane reforming, and storage options for electricity and gases.

To reflect the EU-MENA focus of this thesis, the technology envelope is extended along three dimensions. First, seawater reverse-osmosis (SWRO) desalination is added to provide feedwater for electrolysis in water-scarce locations such as many MENA countries [32], capturing the additional energy demand associated with water supply. Second, two synthetic-fuel pathways are introduced: (i) catalytic methanation to produce synthetic methane (CH_4) that serves as natural gas replacement or crucial petrochemical feedstock [33] and Fischer-Tropsch (FT) synthesis to produce liquid hydrocarbons, which serve hard-to-abate sectors such as aviation and shipping [34]. Third, all hydrogen derivatives in the model rely on CO_2 from direct air capture (DAC), consistent with the long-term phase-out of fossil point sources after 2041 in European regulation [35].

Other hydrogen-based derivatives, such as methanol and liquid organic hydrogen carriers (LOHCs), are excluded due to inconsistent demand data and limited economic competitiveness of synfuel reconversion pathways [36].

Maritime and land transport are introduced as additional transfer options for synfuels and liquefied hydrogen. To remain within the linear-programming limits of the base model, these modes are represented through a business-case abstraction rather than explicit unit dispatch. In practice, trucking or shipping would require binary availability decisions coupled to travel-time constraints, leading to mixed-integer formulations that would greatly increase the complexity of the resulting optimisation problem. A dedicated logistics operator that manages the discrete scheduling is therefore assumed to exist, allowing for linear scaling of transfer flows via distance-dependent variable costs and time delays. The transport costs are derived using a total-cost-of-ownership (TCO) approach. Land transport TCO are

abstracted using road-based cost assumptions rather than rail, reflecting both the greater operational flexibility of trucks in serving dispersed demand and the intention to adopt a conservative estimate of transport costs without introducing additional rail infrastructure and scheduling detail.

As the final stage of the supply chain, energy carriers are utilised domestically or in the importing region based on exogenously defined demand profiles. Where absent, technology-specific storage options are introduced to enable the temporal decoupling of production and demand.

Figure 2-2 schematically illustrates the system boundary and included processes. External resources enter from outside the system boundary, while by-products leave the system boundary. CO_2 emissions are captured over the total supply chain via CO_2 emissions costs, but not further constrained. Energy transportation to domestic demand clusters is separated from cross-nodal energy transport. All numerical parameters and regional datasets are reported in Chapter 3.

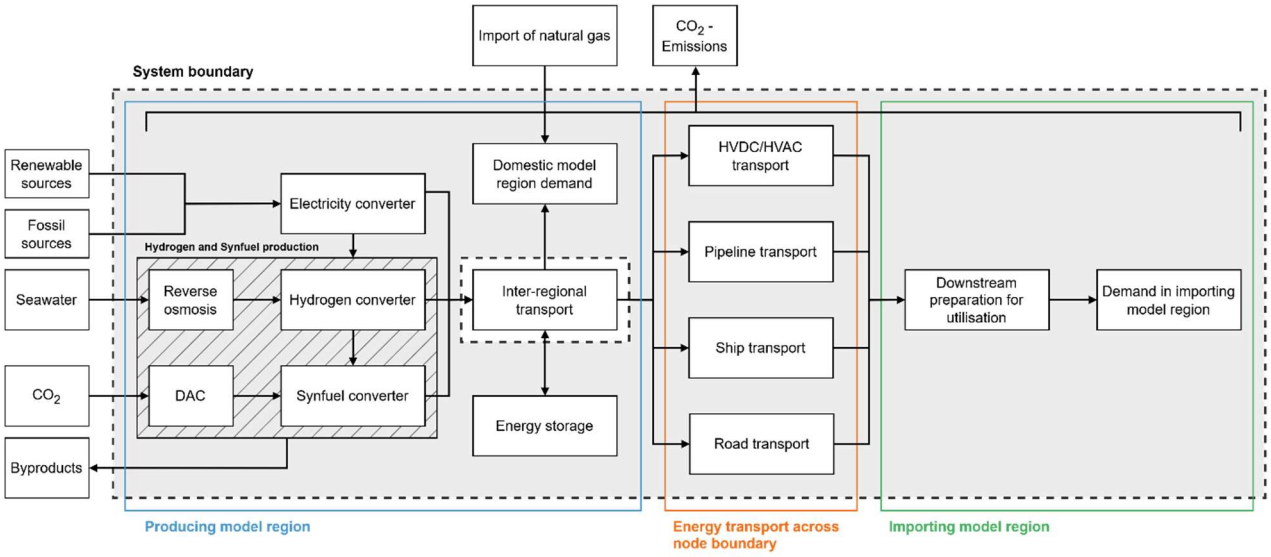

Figure 2-2 Technological system boundary of the adapted model

2.2.3 Temporal scope and investment accounting

To capture long-term trade dynamics between the EU and the MENA region, the adapted REMix model is configured as a perfect-foresight optimisation across the target years 2030, 2040 and 2050. To limit the required optimisation time, each year is resolved at three-hour resolution (2,920 time slices), preserving daily and seasonal variability. While myopic intertemporal coupling is a possible alternative, perfect foresight provides clearer insights into ramp-up dynamics and infrastructure deployment, relevant for the evaluation of pathway build-out [19]. To keep problem sizes tractable, the time step between model years is increased from five to ten years relative to the baseline model.

The model optimises the system by minimising the total system cost (TSC), defined as the discounted sum of the accounting indicators listed in Table 2-1 over the time horizon. Indicators outside of this defined set are not captured in the model. Similarly, no additional policy constraints (e.g. annual emission limits) exist within this study. Capital expenditures are annuitised using a uniform cost of capital of 8% and discounted to the base year using a socio-economic discount rate of 2%. The mathematical formulation of the objective function is

provided in Annex 2. A more detailed description of the generic accounting model can be found in [28]. Figure 2-3 illustrates the temporal system boundary and accounting flow, as future annual accounting indicators are considered in current investment and dispatch decisions and then summed annually to yield the TSC.

Table 2-1 Accounting indicator categories

Accounting indicator	Interpretation
Investment cost	Calculated from the net balance of capacity expansion and decommissioning.
Fixed O&M	Capacity-bound fixed operational cost.
Variable O&M	Variable cost indicators based on mode and volume technology activations.
Fuel cost	Sourcing cost for fossil feedstocks.
CO_2 cost	Sum of CO_2 emissions and CO_2 credits from DAC (priced in as the inverse CO_2 emissions cost).
Water cost	Cost of buying feedstock water.
Loss-of-load cost	Slack-cost of curtailed energy demand.

The accounting indicators not only determine the total system cost, but also underpin the marginal system costs reflected in nodal prices. Nodal marginal prices arise as the dual values of the nodal balance constraints and represent the marginal change in TSC associated with supplying one additional unit at a given node and time slice. Technologies are dispatched in merit order according to their marginal costs, which can be decomposed into the same cost components as in Table 2-1, until the nodal price equals the cost of the marginal technology. Under inelastic demand, load is fully met as long as the nodal price remains below the value-of-lost-load (VOLL) penalty, at which point curtailment becomes optimal.

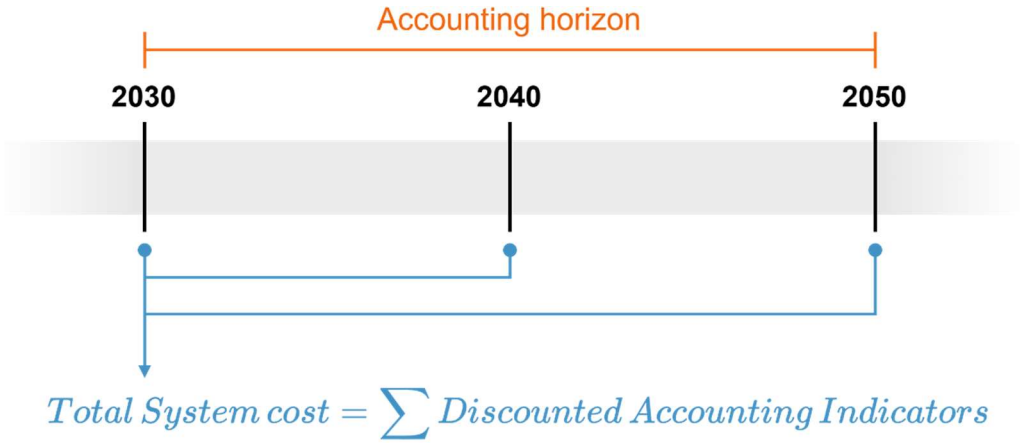

Figure 2-3 Temporal scope and investment horizon of the optimisation model

2.3 Input data sources and harmonisation

The input data for the adapted REMix model comprise parameter values from literature research and project-internal datasets. To ensure comparability across sources, all monetary values are converted to euros and harmonised to a common base year (2025) using [37]. Demand projections for European final energy carriers are taken from the *Clean Planet for All* [38, 39] scenario set, while MENA demand is derived from a dataset that was developed and recently published as part of a DLR research project [40]. These data form the basis for energy system modelling in the ongoing DLR research project *NeoFuels* [40], which

provides the context for this thesis. Further details on data selection and aggregation are provided in Chapter 3.

2.4 Validation of model adaptations and extensions

Validation efforts in this thesis focus on ensuring the correct implementation of additions to the underlying REMix model. The base model's use for continental energy systems has been documented in prior studies (e.g., [27, 28]); the core model formulation is therefore treated as given. The new technologies and transport abstractions are integrated following the existing modelling logic and verified using face and trace validation, complemented by structured walkthroughs as described in [41]. Concretely, the model is validated by discussing the model and the model results within the Institute of Networked Energy systems (structured walkthrough and face validation) at the DLR and by confirming, that supply chain energy balances and capacity expansions stay within model limits throughout the model years (trace validation). Additionally, the model results are compared against the results of a study of similar scope by Krüger et al. [24].

A full behavioural validation of the long-term scenario outcomes is beyond the scope of this thesis but is partially addressed in the Discussion by comparing qualitative patterns to existing studies.

2.5 Scenarios as a robustness test for the EU-MENA system

To test the robustness of model outcomes, this thesis employs scenarios as the main model analysis method. The scenarios are constructed as counterfactuals to a central reference model configuration, varying only a limited number of scenario levers at a time. They thus aid in interpreting the optimisation not as a single prediction, but rather an exploration of how the cost-optimal system changes under varying assumptions, separating underlying storylines from variable-dependent outcomes.

Specifically, a central reference model configuration, representing an unconstrained system (SQ1), is first formulated and then tested via transportation (SQ2) and finance (SQ3) constraints. This allows the impact of trade, infrastructure and financing assumptions on the EU-MENA hydrogen and synfuel system to be quantified. Together with the central reference case, the main research question (RQ) can then be answered (Figure 2-4). A detailed scenario description is provided in Chapter 3.4.

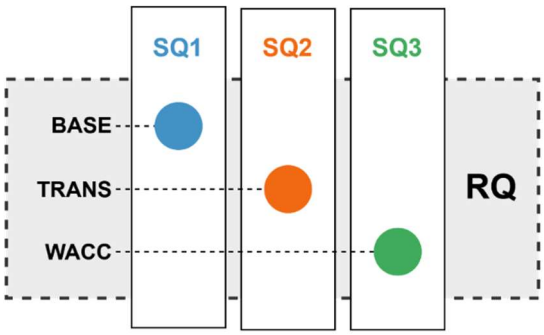

Figure 2-4 Connection between scenarios and SQ/RQ

2.6 Result metrics and evaluation dimensions

To enable consistent comparison across scenarios, results are interpreted through three lenses: technical, economic and political, using metrics comparable across regions, carriers and model years.

The physical model configuration is described using (i) maps of installed generation, conversion, storage and network capacities (ii) annual energy flows and full-load hours on technologies and links to identify utilisation and bottlenecks, and (iii) build rates and carrier-specific trade balances across production, trade and delivery stages. Where useful, these are complemented by time series of storage levels and technology activation.

System economics are analysed using (i) nodal marginal prices and their differentials across regions and carriers, including mean marginal-price duration curves to diagnose scarcity and congestion, (ii) marginal production-cost deltas relative to the lowest-cost node and (iii) total and specific system costs decomposed by stage (generation, conversion, storage, transport and demand) and group (Table 2-1). Scenario effects are summarised via the autarky penalty [13], defined as the difference in total system cost between a no-trade configuration and the current scenario configuration, which makes comparative advantages explicit.

The political dimension is captured via import dependency, defined as net imports relative to regional final demand for a given carrier and year. Plotting cumulative import dependency by country and carrier, alongside associated export volumes, allows assessment of whether cost-optimal outcomes are compatible with current concerns around energy independence and exposure to external suppliers.

The methodology can be summarised as shown in Figure 2-5, displaying the exogenous input assumptions, optimisation model structure and model results used to answer the research questions.

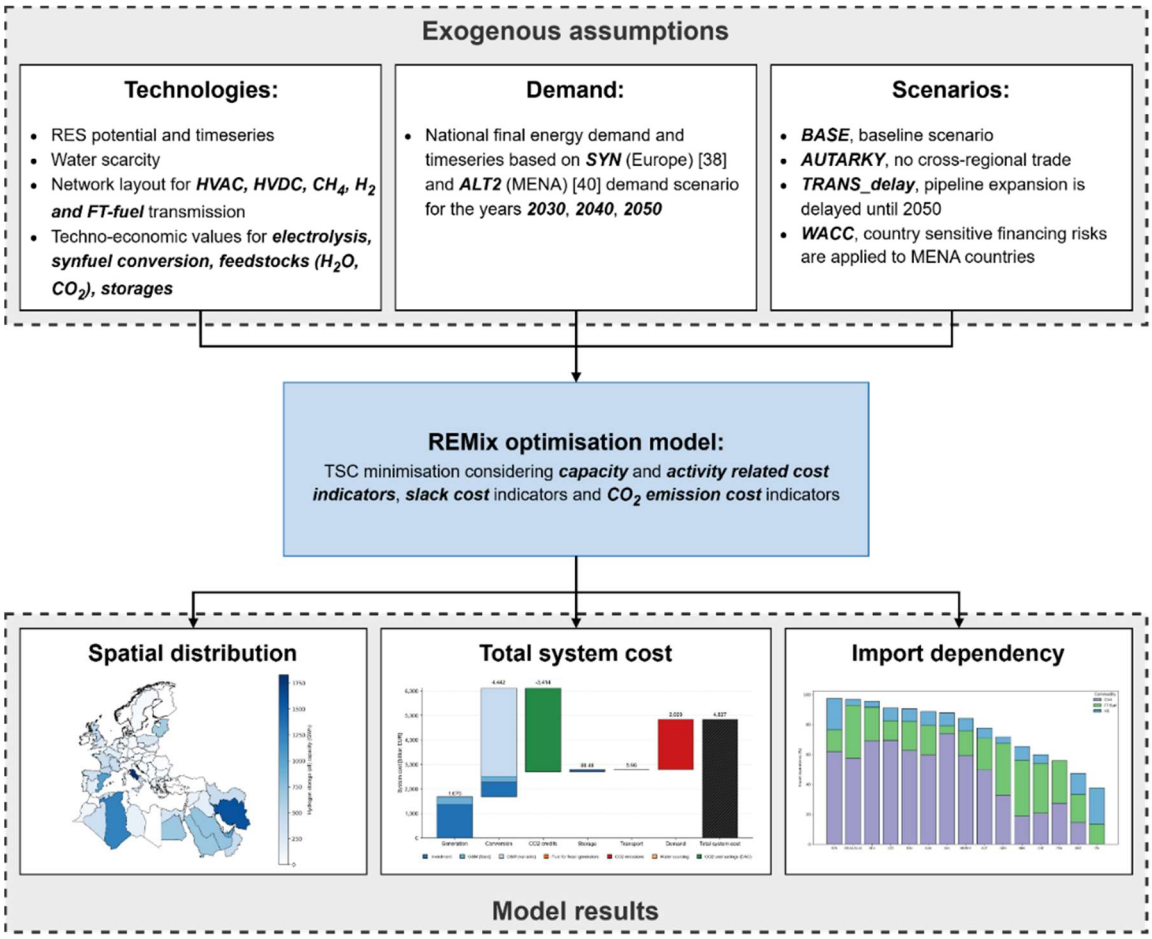

Figure 2-5 Methodology overview

3. Model inputs and techno-economic assumptions

This chapter specifies the exogenous inputs to the adapted REMix model. It defines the geographical aggregation and network topology, summarises techno-economic parameters for added technologies, consolidates economic boundary values and validation checks, and outlines the specific scenario configurations.

3.1 Geographical aggregation and network topology of the EU-MENA system

Building on the generic node-link representation described in Chapter 2.2.1, this section specifies the geographical scope of the adapted model, the data sources and the additional transport abstractions introduced for land and maritime trade.

The geographical scope is expanded to include the countries Algeria, Egypt, Iran, Iraq, Israel, Jordan, Kuwait, Lebanon, Libya, Morocco, Oman, Qatar, Saudi Arabia, Syria, Tunisia and the United Arab Emirates, in addition to the European countries represented in the base model. Turkey is added to the model as a transit region connecting Europe and the Middle East. While transmission and storage capacities can be built in Turkey, demand is not modelled. Each of these countries is mapped to one or more model regions, which are subsequently assigned to the regional nodes described in Chapter 2.2.2. An overview of the region-node mapping is provided in Annex 5.

The network topology and node placement are derived using the sci2Grid_gas [42] and OpenStreetMap [43] dataset for gas and electricity transmission capacities, they are thus modelled based on existing network capacities. The post-processed network maps can be found in the Annex 6. Link lengths are, unless otherwise stated, determined from the straight-line distance between node centroids.

To represent overland transport of hydrogen and synfuels beyond the existing pipeline grid, the model is expanded to include a simplified land network. Land links are derived from a reduced network representation that removes network connections crossing large bodies of water.

Maritime trade is captured through dedicated waterway links that connect selected port locations. The underlying model instance already contains 28 port nodes representing major European ports with existing or planned liquefied natural gas (LNG) terminals. For the MENA region, no additional port nodes are introduced, reflecting the high level of water stress (see Chapter 3.3) and the assumption that major production and demand centres are co-located near the coast. Waterway links nonetheless originate and terminate at concrete port locations with existing or planned LNG infrastructure. For Saudi Arabia, Syria and Tunisia, suitable ports are selected based on data from [44], since no operational or planned LNG terminals exist within these countries. A complete list of all port locations is provided in Annex 7. Shipping distances between ports are calculated using the *SeaRoute* software [45], which approximates the shortest feasible maritime route between port coordinates.

In addition to the onshore nodes introduced in Chapter 2.2.2, an offshore hub is added in the North Sea to explore the potential of future offshore hydrogen and synfuel production, as suggested in recent studies on offshore green hydrogen concepts (e.g., [46]). Furthermore, two dedicated natural-gas import hubs are included in Ukraine and Azerbaijan to represent the aforementioned external natural gas suppliers to Europe.

With these additions, the final geographic scope comprises 65 model regions, 96 model nodes and 272 model links, shown in Figure 3-1, with an enlarged version available in Annex 8.

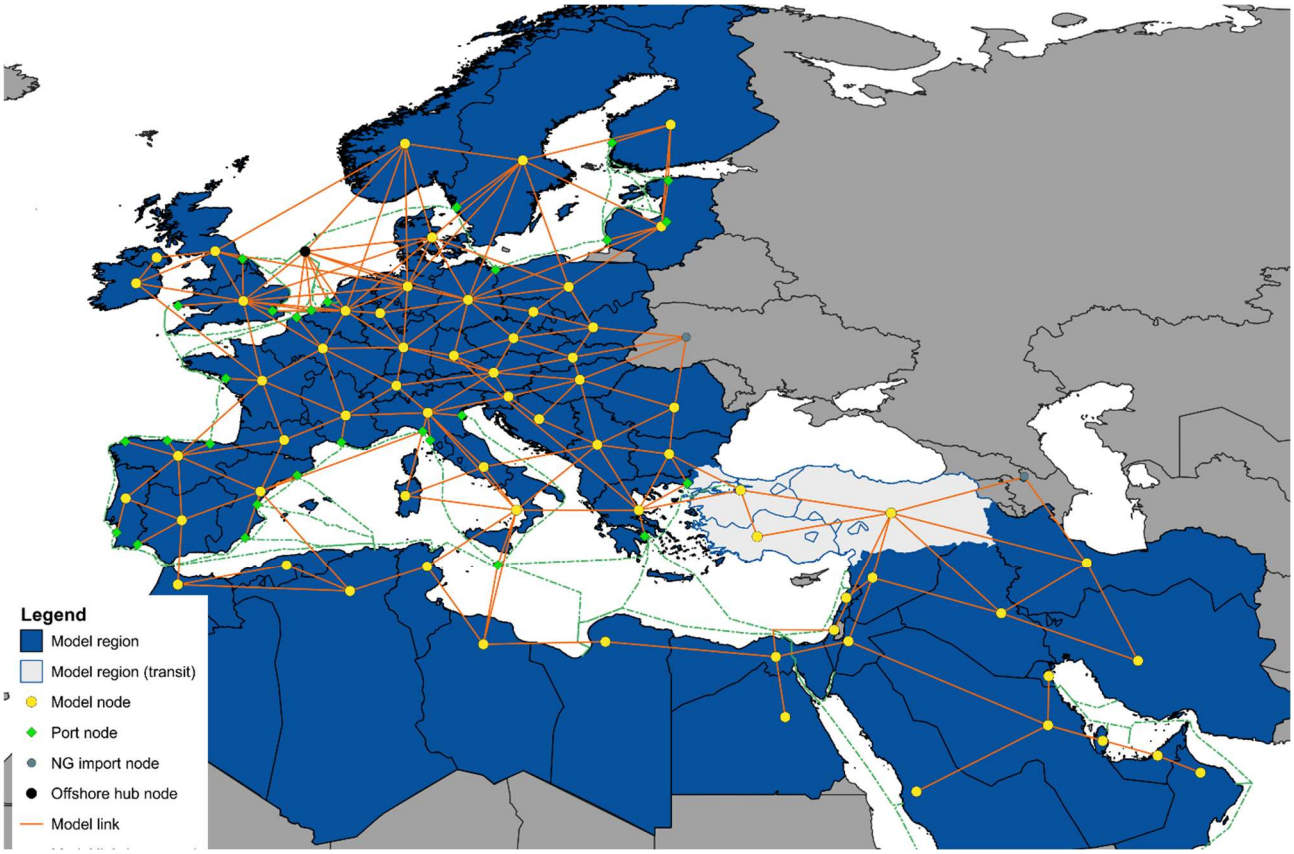

Figure 3-1 Reduced EU-MENA network topology

3.2 Final energy demand assumptions

Final energy demand trajectories for Europe are taken from the Clean Planet for All “P2X” scenario [38], broken down into country-specific “Syn” scenarios as a result of a DLR-coordinated project [39]. The scenario achieves an almost complete reduction in CO_2 emissions in the EU by 2050 and is a mixed scenario in terms of demand for electricity, hydrogen and synthetic hydrocarbons with rather high demand for synfuel in the transport sector and synthetic methane in stationary applications. For the MENA region, the demand dataset “ALT2” developed by Braun et al. [40] is used. The ALT2 scenario for MENA combines moderate efficiency and RES expansion strategies in all sectors of the energy system with the assumption that all remaining fossil fuels will be completely replaced by green fuels by 2050, thereby achieving the goal of 100 % climate-neutral energy supply. Both projections therefore represent high-uptake cases for hydrogen and synfuels across all sectors and are treated as exogenous inputs that are identical across all model scenarios. The demand sectors covered include industry, transport, buildings and services.

Annual carrier-specific demands are disaggregated into hourly profiles following the methodology in [28], preserving daily and seasonal variability in each model region. Table 3-1 shows key characteristics of the analysed carriers on a lower heating-value (LHV) basis. Demand and supply results are reported in GWh, unless otherwise stated.

Table 3-1 Overview of main characteristics for the analysed energy carriers

Energy carrier	Physical State	Energy content [kWh/kg]	Source
Electricity	n/a	n/a	n/a
Natural gas	Gas	13.10	[47]
Hydrogen	Liquid, gas	33.33	[47]
Methane	Gas	13.90	[47, 48]
FT-fuel	Liquid	12.11	[49]

3.3 Techno-economic assumptions for energy technologies

This section summarises the techno-economic assumptions for the main energy technologies represented in the model. All parameters are treated as exogenous and remain identical across all scenarios. Weather years for RES generation are taken, as described in [28], from the REA6 weather reanalysis [50] (2012, 2013 and 2014) and mapped onto the model years in chronological order. Detailed numerical values and data sources are provided in Annex 9.

3.3.1 Hydrogen production pathways and process configurations

Hydrogen can be produced via Alkaline Electrolysis (AEC), Proton-Exchange Membrane electrolysis (PEM) and Solid Oxide Electrolysis (SOEC). The techno-economic data assumptions are provided in Annex 9.

In most European regions, freshwater availability is assumed not to constrain electrolysis and water supply is therefore represented through a simple cost term of 1 €/m³ [51]. In the MENA region, however, high water stress makes desalination a prerequisite for large-scale electrolysis [32]. Regional baseline water stress levels in 2030 are used to identify water-scarce model regions (Figure 3-2). In water-stressed regions (Annex 10), seawater reverse-osmosis (SWRO) desalination is added as a dedicated process that provides feedwater.

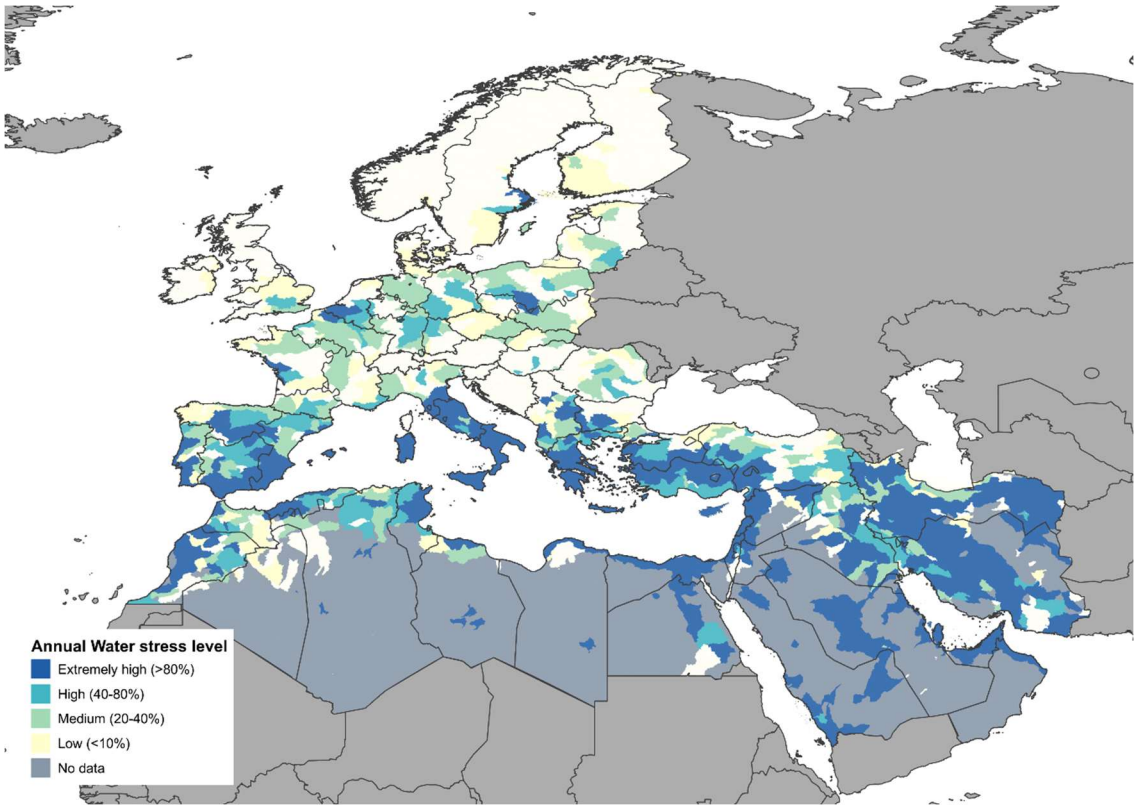

Figure 3-2 Regional baseline water stress levels in 2030, based on values from [52]

The techno-economic parameters for the SWRO technology are displayed in Table 3-2. To calculate the electricity requirement, the method in [53] is used. Salinity is assumed to be uniform at 38 ppm based on samples from [54], leading to a specific energy requirement of 3.1 MWh/t_{H2O}.

Table 3-2 Saltwater desalination using reverse osmosis, techno-economic input data

Parameter	2030	2040	2050	Source
Electricity demand [MWh/t_{H2O}]	3.1			[53]
Lifetime [a]	30			[53]
Capacity factor [-]	1			Assumption
Capital expenditure cost [k€/(t_{H2O}/h)]	43	35	28	[55]
Fixed operation costs [%$_{CAPEX}$]	4			[53]

3.3.2 Synthetic methane production pathway

Synthetic methane production in this study is implemented through the catalytic methanation technology pathway (Table 3-3). Depending on the need for SWRO, the process efficiency fluctuates between 32.6% (2030, including SWRO) and 40.9% (2030, excluding SWRO). Towards 2050, the process efficiency is assumed to improve to 35.5% and 47.5% respectively.

Table 3-3 Catalytic methanation plant, techno-economic input data

Parameter	2030	2040	2050	Source
Hydrogen demand [MWh/MWh$_{CH4}$]	1.198			[48]
CO_2 demand [t/MWh$_{CH4}$]	0.216			[48]
Electricity demand [MWh/MWh$_{CH4}$]	0.023			[48]
Lifetime [a]	30			[48]
Capacity factor [-]	1			Assumption
Capital expenditure cost [k€/MW]	704	622	541	[48]
Fixed operation costs [%$_{CAPEX}$]	3			[48]
Variable operation costs [€/MWh$_{CH4}$]	0.32			[48]

3.3.3 Fischer-Tropsch fuel production pathway

FT fuel production is modelled via two routes: (i) low-temperature FT synthesis of long-chain hydrocarbons from synthesis gas and (ii) a methanol-to-hydrocarbon (MTH) route.

The FT synthesis process is modelled as a low-temperature configuration (Table 3-4), as it favours the formation of liquid and wax products [49]. The overall process efficiency is calculated to be 28.07% (2030) to 31.4% (2050) and 35.3% to 42.4% when SWRO is excluded. Other studies place the efficiency of such supply chains around 40.4% without SWRO [48].

Table 3-4 Low temperature Fischer-Tropsch fuel production, techno-economic input data

Parameter	2030	2040	2050	Source
Hydrogen demand [MWh/MWh$_{FT}$]	1.327			[49]
CO_2 demand [t/MWh$_{FT}$]	0.322	0.297	0.272	[49]
Electricity demand [MWh/MWh$_{FT}$]	0.007			[49]
Lifetime [a]	25			[49]

Capacity factor [-]	1			Assumption
Capital expenditure cost [k€/MW]	1,621	1,064	508	[56]
Fixed operation costs [€/MW_{FT}]	16.61	11.12	9.68	[49]
Variable operation costs [€/MWh_{FT}]	5.493	4.186	2.747	[49]

The MTH route is modelled analogously to the methanol-to-kerosene process (Table 3-5), where methanol is synthesised via direct catalytic hydrogenation of CO_2, before further upgrading to kerosene-range hydrocarbons [57]. The overall process efficiency ranges from 30.1% to 32.9% and 37.8% to 44.0% (without SWRO). The energy and mass balances for all three production pathways are provided in Annex 11.

Table 3-5 Methanol-to-Kerosene route, techno-economic input data

Parameter	**2030**	**2040**	**2050**	**Source**
Hydrogen demand [MWh/MWh_{FT}]	1.23			[48]
CO_2 demand [t/MWh_{FT}]	0.274			[48]
Electricity demand [MWh/MWh_{FT}]	0.007			[48]
Lifetime [a]	30			[48]
Capacity factor [-]	1			Assumption
Capital expenditure cost [k€/MW]	941	821	700	[48]
Fixed operation costs [€/MW_{FT}]	32.27	28.13	24.00	[48]
Variable operation costs [€/MWh_{FT}]	0.003			[48]

Table 3-6 shows the techno-economic assumptions for the supplementary DAC technology.

Table 3-6 Solid Adsorption Direct Air Capture, techno-economic input data

Parameter	**2030**	**2040**	**2050**	**Source**
Electricity demand [MWh/t_{CO2}]	1.725	1.489	1.284	[58]
Lifetime [a]	25	30		[58]
Capacity factor [-]	1			Assumption
Capital expenditure costs [k€/(t_{CO2}/h)]	3,690	2,583	2,214	[58]
Fixed operation costs [k€/(t_{CO2}/h)]	147.6	98.4	86.1	[58]

3.3.4 Energy storage technologies

In addition to the storage options present in the underlying REMix instance (electricity and gaseous energy carriers), three dedicated storage types are added: CO_2 storage, H_2O buffer storage and a general hydrocarbon storage that can hold FT fuels. The assumed techno-economic parameters are documented in Annex 10.

3.3.5 Energy transportation technologies

As outlined in Chapter 3.1, the technology portfolio is extended to include maritime and land transport of liquid hydrocarbons and liquefied hydrogen (Table 3-7).

Truck and trailer costs for road transport are based on Basma and Rodríguez and related sources [48, 59–63], yielding specific road transport costs of 3.33 €/GWh*km for synfuel and 15.30 €/GWh*km for liquefied hydrogen. Ship transport parameters are taken from the *Mærsk Mc-Kinney Møller Center TCO model* and design studies for large LH_2 tankers [64, 65], resulting in specific costs of 0.80 €/GWh*km (2030) to 0.62 €/GWh*km (2050) for synfuel

and 0.45-0.40 €/GWh*km for hydrogen, declining linearly. Detailed assumptions on vehicle sizes, speeds, utilisation, loading times and hydrogen liquefaction are documented in Annex 10.

Table 3-7 TCO for selected transport technologies

Transfer technology	Transported energy carrier	TCO [€/GWh*km]
Land transport	Synfuel	3.33
Land transport	Liquefied hydrogen	15.30
Seaborne transport	Synfuel	0.80-0.62
Seaborne transport	Liquefied hydrogen	0.45-0.40[2]

3.4 Scenario assumptions and common settings

This section defines the scenario set used to analyse the role of EU-MENA hydrogen and synfuel trade in the decarbonised energy system. All scenarios share the same exogenous demand trajectories, technology cost assumptions, resource series and network representation described above.

A common CO_2 price path is applied in every case, rising from 100 €/tCO_2 in 2030 to 200 €/tCO_2 in 2040 and 350 €/tCO_2 in 2050. CO_2 emission values apply uniformly to all combustion emissions within the model boundary. To ensure clean attribution of effects, key modelling settings and build-rate restrictions, taken from the underlying model, are held constant across scenarios, as summarised in Table 3-8. The expansion of long-distance natural gas pipeline capacity is explicitly limited, to incentivise the model to efficiently use the legacy pipeline network and thus test the role of the brownfield pipeline network under different scenario assumptions.

Table 3-8 Common modelling settings

Category	Setting
Objective and discounting	TSC minimisation with Investment cost annuitisation and applied socio-economic discount rate (2%).
Baseline cost of capital	Uniformly applied (8%), except in WACC scenario.
CO_2 emissions cost	120 €/t (2030), 195 €/t (2040), 350 €/t (2050).
Portfolio availability	Full technology envelope available.
Electricity exchange	Permitted via HVAC and HVDC grid, but limited through capacity boundaries.
External NG import	Azerbaijan: 321,800 TWh (2030, 2040), 0 TWh (2050) Ukraine: 169,400 TWh (2030, 2040), 0 TWh (2050)
Build-rate limitations	• CH_4 pipelines: no expansion • New hydrogen pipelines: +1 GW/year • Retrofitted hydrogen pipelines: +1 GW/year • HVDC: +1 GW/year • HVAC: +0.5 GW/year

The BASE case provides the central reference scenario. Financing conditions are represented by a uniform cost of capital of 8% for all regions and technologies. The full technology

[2] Excluding Liquefaction cost.

portfolio is available and no delays are implemented. BASE thus reveals the unconstrained cost-optimal configuration when technology choice and trade are bound only by resource potential, costs, carbon pricing and generic rollout limits.

To quantify the value of cross-regional molecular trade, AUTARKY disables all cross-regional trade in non-electric carriers between the EU and MENA region, while inter-regional trade is still possible. Cross-regional electricity trade continues to be possible, based on the high perceived value of electricity trade within integrated energy studies found in prior studies [27]. High volumes of electricity trade are therefore likely, even in otherwise autarkic scenarios. Comparing AUTARKY with BASE under the same CO_2 price path reveals the additional investment and operating costs required to meet demand when cross-regional exchange is not possible.

Transport availability and timing are then probed through the TRANS scenario variants. TRANS_delay enforces a delayed roll-out of new and repurposed hydrogen pipelines, exploring the role of legacy transmission infrastructure and transportation methods currently available within the EU-MENA trade system. TRANS_no_pipeline disables legacy and new cross-regional hydrogen pipeline capacity altogether, effectively limiting the trade to Fischer-Tropsch fuels and electricity, thus exposing the role of FT fuel trade between the EU and MENA region.

Finally, WACC replaces the uniform 8% cost of capital in the MENA region with country-specific values for renewable generation, electrolysis and synfuel investments, while all European investments retain the 8% rate used in BASE. All other parameters are kept as in BASE. This design isolates the impact of differentiated financing conditions on spatial investment patterns, trade flows and the regional distribution of total system costs, making clear where the optimal configuration is driven more by capital-cost differentials than by resource quality, demand or the carbon price signal itself. The cost of capital values are sourced from Terrapon-Pfaff et al. [21], taken from the “WACC_bau” scenario (see Annex 12). Table 3-9 summarises the main scenario parameters.

Table 3-9 Scenario variants

		TRANS_			
Scenario	**BASE**	**_delay**	**_no_pipeline**	**AUTARKY**	**WACC**
EU-MENA trade assumptions					
EU-MENA exchange	Enabled	Enabled	Enabled	Disabled	Enabled
Exchange portfolio	All	All	Electricity, FT fuel	Electricity	All
Exchange delay	None	Until	None	None	None
Build rates	CH_4: no expansion H_2, HVDC: +1 GW/year, HVAC: +0.5 GW/year				
Accounting assumptions					
Accounting objective	Total system cost (TSC) minimisation				
Discount rate	Socio-economic discount rate of 2%				
Cost of capital	8%	8%	8%	8%	Variable
CO_2 emission cost	120/200/350 €/t				

4. Model results

This chapter presents the main optimisation results for the integrated EU-MENA system and addresses the three sub-questions introduced in Chapter 1. Chapter 4.1 analyses the unconstrained BASE configuration and the contrasting AUTARKY case, thereby answering Sub-question 1 on the value of cross-regional EU-MENA trade. Chapter 4.2 is used to test the robustness of the optimal system architecture and costs against infrastructure and financing constraints, thus addressing sub-questions 2 and 3. Additionally, a qualitative CO_2 price analysis is conducted within Chapter 4.2, based on observations made in the analysis. Given the high number of model regions, the following chapter focuses on overarching scenario storylines only. Enlarged figures, detailed numerical results, and additional plots are provided in the Data Annex.

4.1 BASE and AUTARKY: integrated system architecture and value of trade

The BASE scenario results reveal a clear emerging storyline. In an unconstrained EU-MENA system, production shifts decisively from Europe to the MENA region. The system balance is mainly achieved through energy carrier transport, with methane storage in Europe being utilised as the main seasonal balance tool.

Starting in 2030 and staying largely consistent until 2050, RES are predominantly sited in the MENA region. By 2050, 96.3% of annual electricity generation is provided by solar PV and onshore wind, with a strong bias towards solar PV (11.8 TW) compared to 2.8 TW onshore wind. Of the global total, 88% of solar PV and 64% of onshore wind capacity is sited in MENA (Figure 4-1) by 2050. The remaining renewable energy is mostly provided by concentrated solar power, concentrated in the United Arab Emirates. The outsourcing of RES can primarily be explained by the 57% higher average capacity factor for MENA-based solar PV plants. The effect for onshore wind plants is more moderate (+23%) given high-value sites in and around the North Sea in Europe. While this decisive solar PV bias might seem surprising given the high wind potential of countries like Tunisia, Algeria or Morocco [66], previous studies have shown that a solar-fed hydrogen supply chain is systematically preferred; even in wind-rich settings [67].

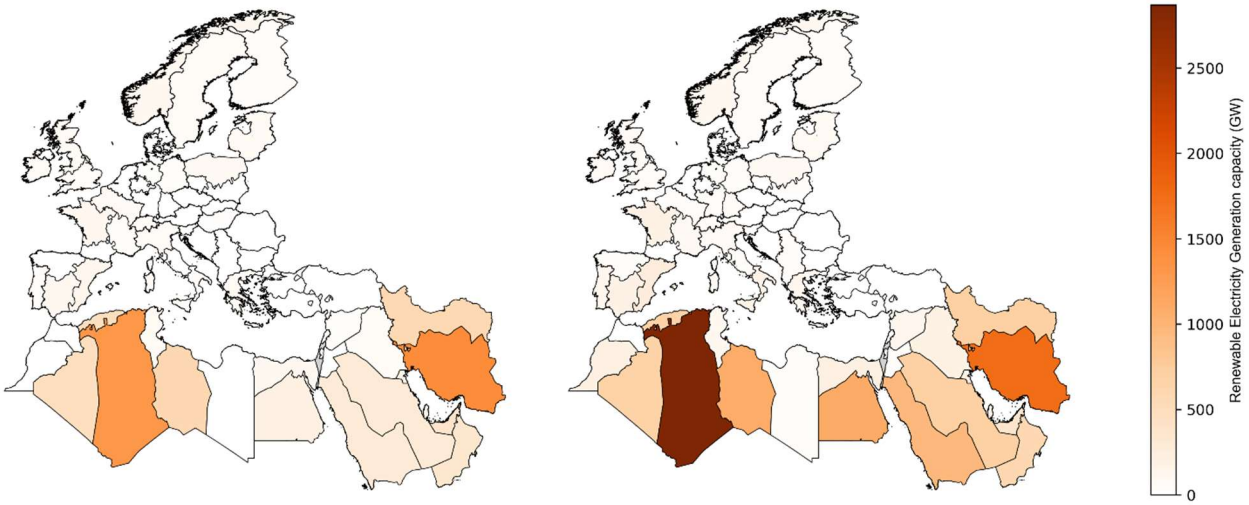

Figure 4-1 Total RES capacity 2030 (left) and 2050 (right) (BASE scenario)

Given the high electricity demand of hydrogen electrolysis, it is unsurprising that electrolysis capacity siting closely mirrors the RES deployment pattern (Figure 4-2). In 2050, hydrogen

electrolysis consumes 45% of the global electricity output (SWRO included). Nearly all of the installed electrolysers are alkaline, reflecting ESOM tendencies to strongly favour the technology with the lowest levelised cost, even if the advantage is only marginal [68]. This so-called “penny switching” effect is often quantified through computationally intensive parameter variation techniques such as a Monte Carlo analysis [68]. Given the available time for this project, no such analysis could be performed, leaving it for future research. Moreover, process-coupling synergies (e.g., reusing excess methanation heat for solid-oxide electrolysis) can likewise not be captured in the chosen spatial and demand model configuration, further encouraging concentrated investments in singular technologies.

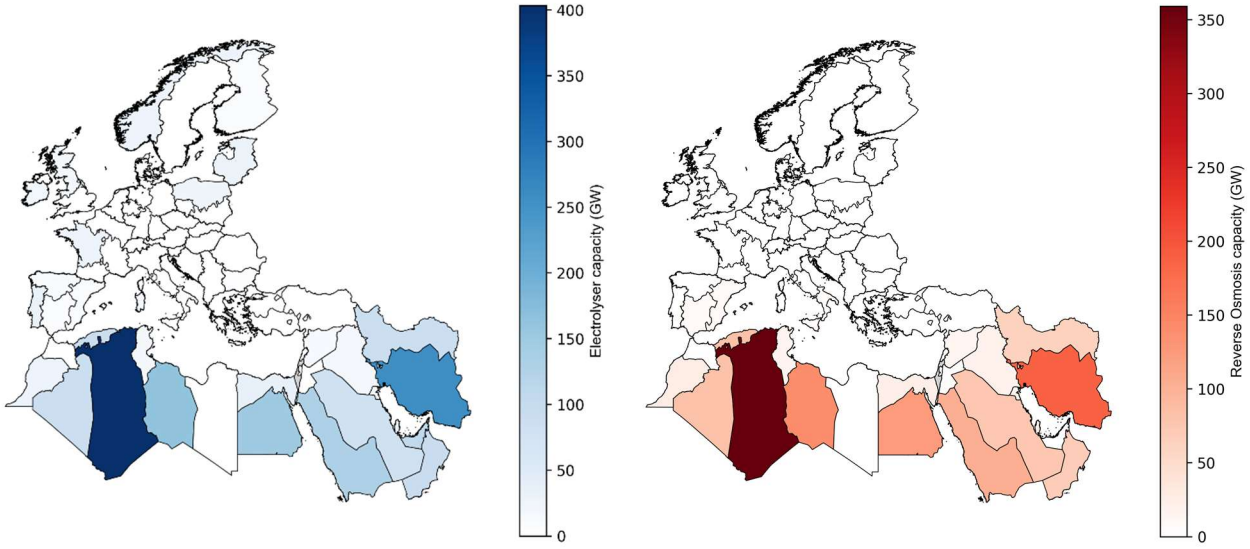

Figure 4-2 Total electrolysis (left) and reverse osmosis (right) capacity (BASE, 2050)

When analysing the electrolysis dispatch (Figure 4-3), it becomes apparent that hydrogen in the BASE system is rapidly refined into synfuels or exported to the EU. In the MENA region, electrolysis follows the diurnal profile of solar-dominated electricity conversion, with tank storage (9.0 TWh) smoothing operation, absorbing midday peaks and releasing hydrogen during off-peak hours.

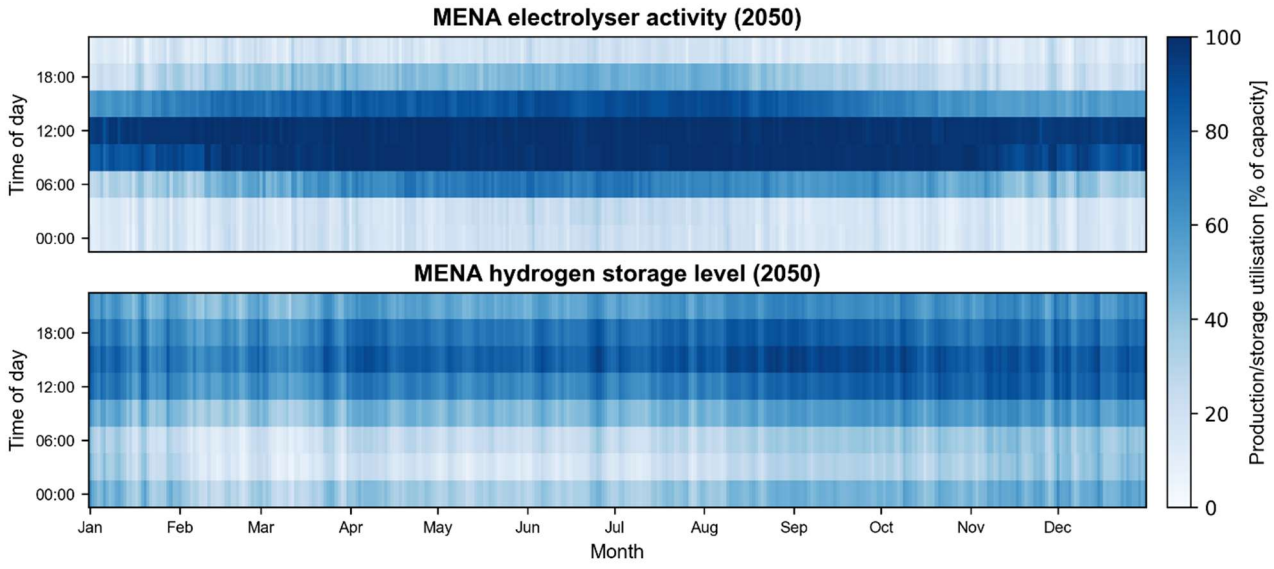

Figure 4-3 MENA electrolysis and storage utilisation (BASE, 2050)

In Europe, a larger contribution from wind power (Annex 13) yields a flatter electrolysis activity profile with less pronounced midday peaks, only really visible in the summer (Figure 4-4). Hydrogen cavern storage (8.8 TWh) nonetheless acts to buffer short- and medium-term demand and is not used as a seasonal storage.

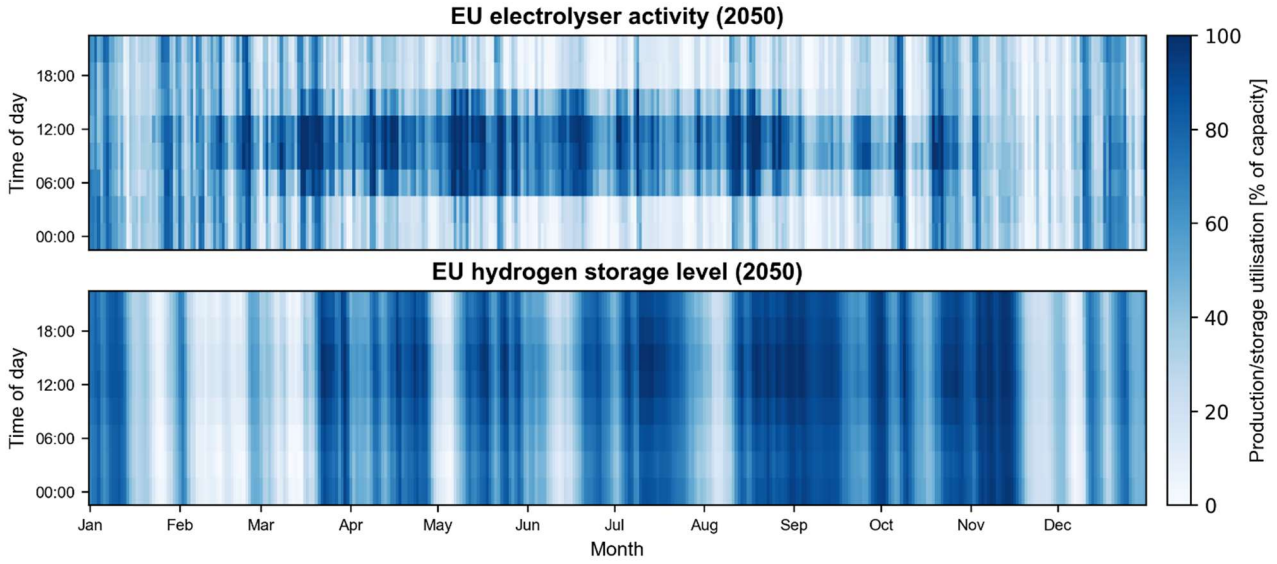

Figure 4-4 EU electrolysis and storage utilisation (BASE, 2050)

Consistent with the siting of electricity and hydrogen assets, synfuel production hubs are concentrated in the MENA region (Figure 4-5). By 2050, the total installed synthesis capacity reaches 974 GW, of which 84% is located in MENA. At this point, it is useful to highlight Iran, in which the model places more synfuel converters than would be expected based solely on local resource availability.

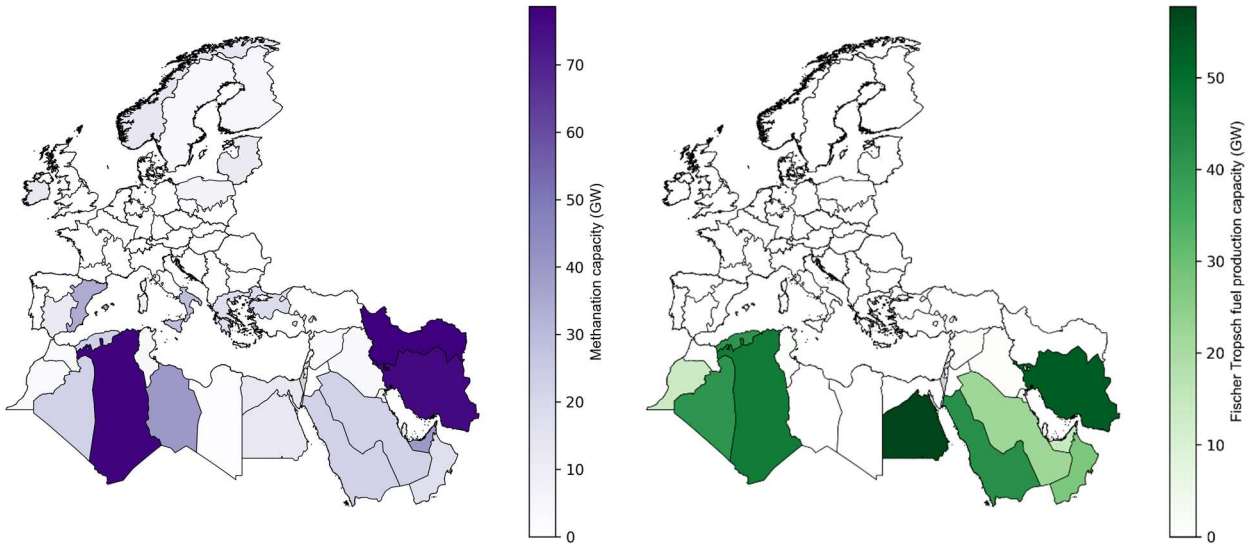

Figure 4-5 Total methanation (left) and FT synthesis (right) capacity (BASE, 2050)

The analysis of net annual hydrogen (Figure 4-6) and methane flows (Figure 4-7) explains the specific siting of generation and conversion capacity in MENA countries such as Algeria, Egypt and Iran. In an unconstrained system, these countries are located at key entry-points into the EU energy network, namely Italy and Spain. Both countries function as bundling points for MENA hydrogen and methane.

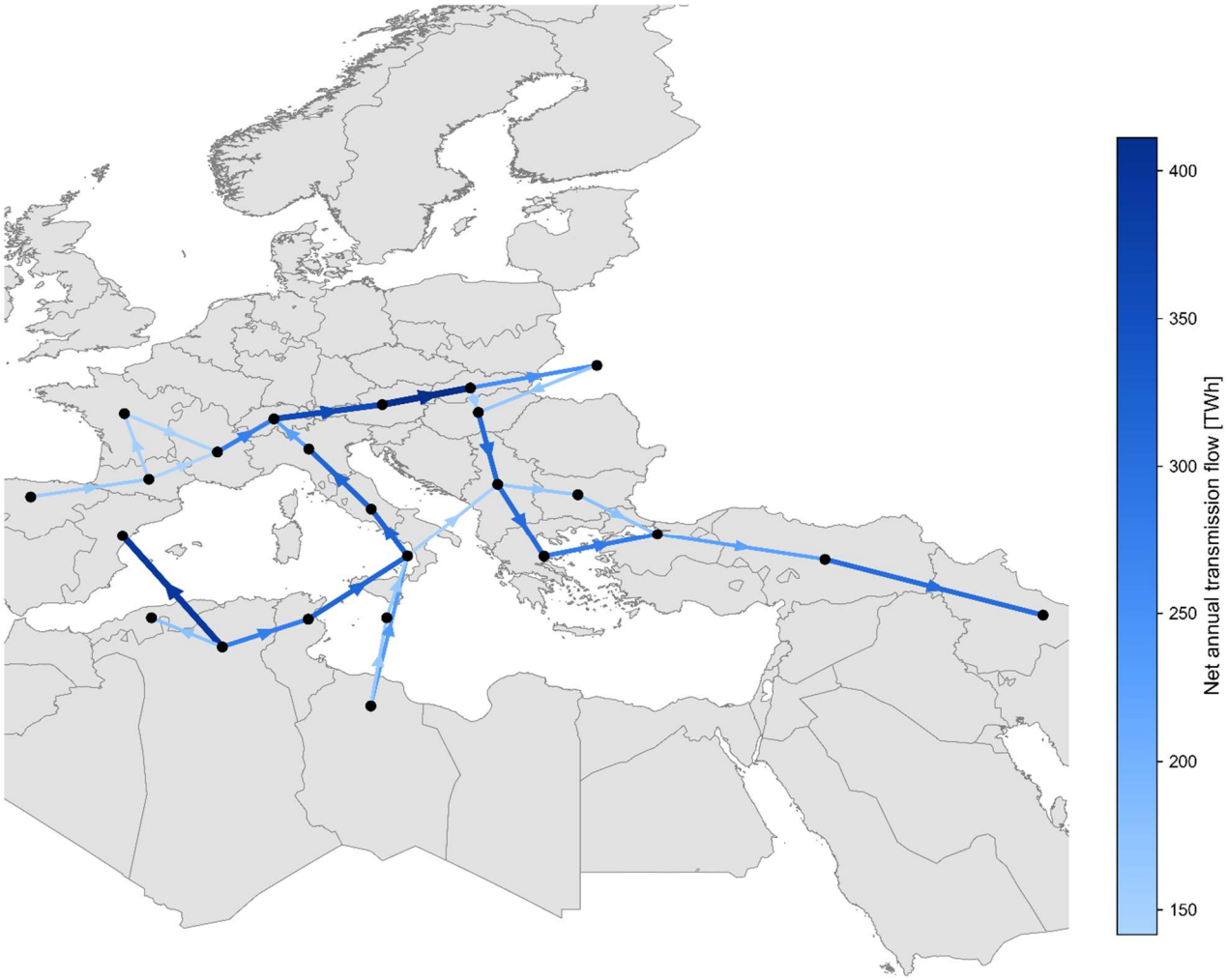

Figure 4-6 Net annual hydrogen flows; top 80% (BASE, 2050)

While hydrogen mainly serves as a spatial redistribution vector, with retrofitted pipelines distributing hydrogen within Europe and newly built hydrogen pipelines installed along import and export spines to increase cross-regional trading capacity (see Annex 13), the bulk of energy is transported through high-capacity legacy methane pipelines (as seen in Figure 4-7 and Figure 4-8), thus acting as the main balancing instrument within the system.

This observation is even more clear when analysing the network utilisation, shown in Figure 4-8. Each bubble represents a pipeline connection, with the horizontal axis denoting annual transported volume and the vertical axis indicating full-load hours. Bubble sizes scale with pipeline capacity.

High-volume methane distribution corridors occupy the upper-right region of Figure 4-8, combining very large flows with near full utilisation (>8,000 FLH), signalling near-congestion utilisation of existing legacy infrastructure. Methane entry points into Europe cluster mainly in the upper-left region, with similarly high utilisation but substantially lower transport capacity. Retrofitted hydrogen pipelines form a broad mid-range cluster (~4,000-7,000 FLH), underlining their role as intra-European redistribution backbones that still retain operational flexibility. By contrast, newly built hydrogen pipelines fall within a narrower band of higher

FLHs but moderate absolute flows, reflecting their role as relatively thin import and export links rather than continent-wide distribution networks.

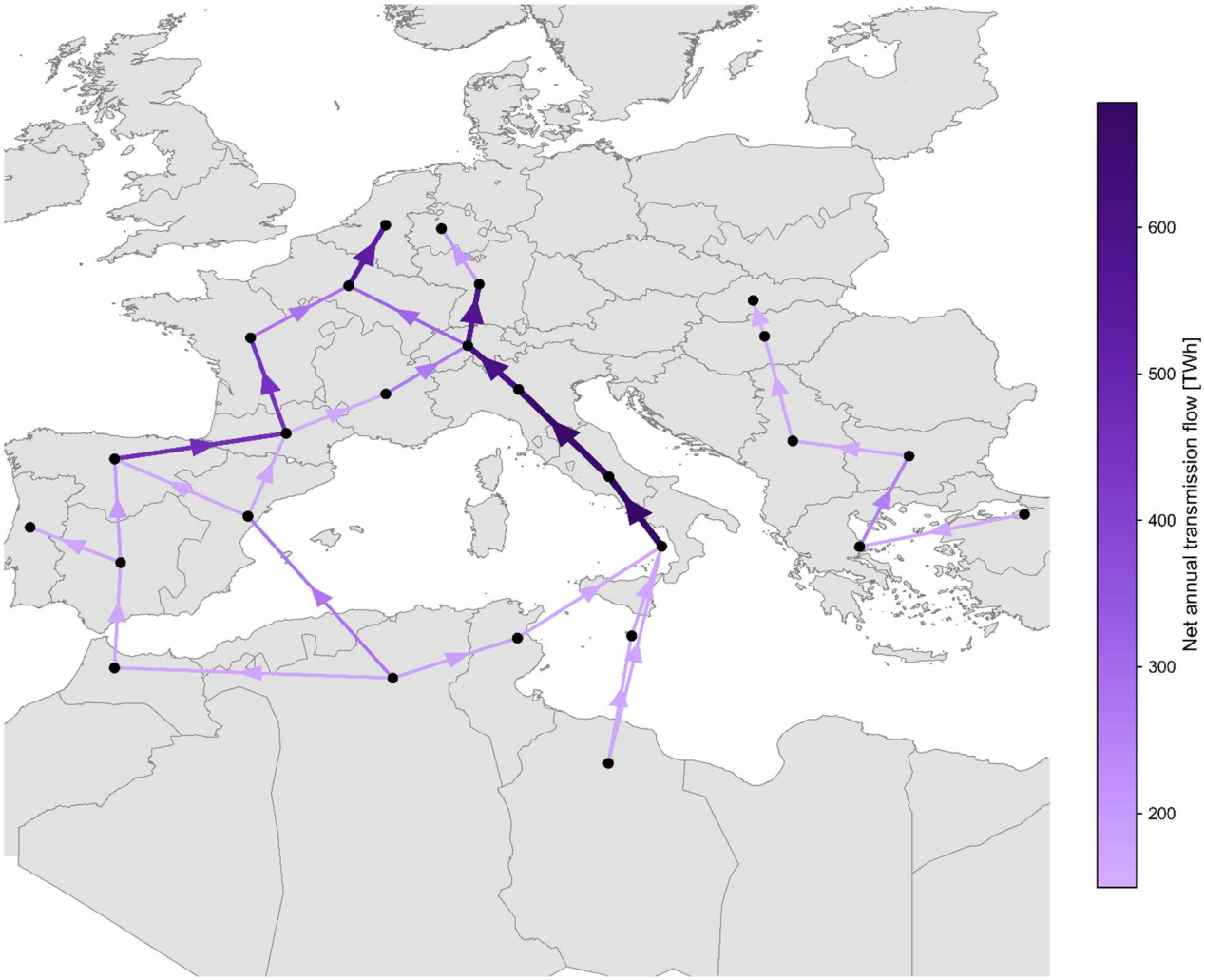

Figure 4-7 Net annual methane flows; top 80% (BASE, 2050)

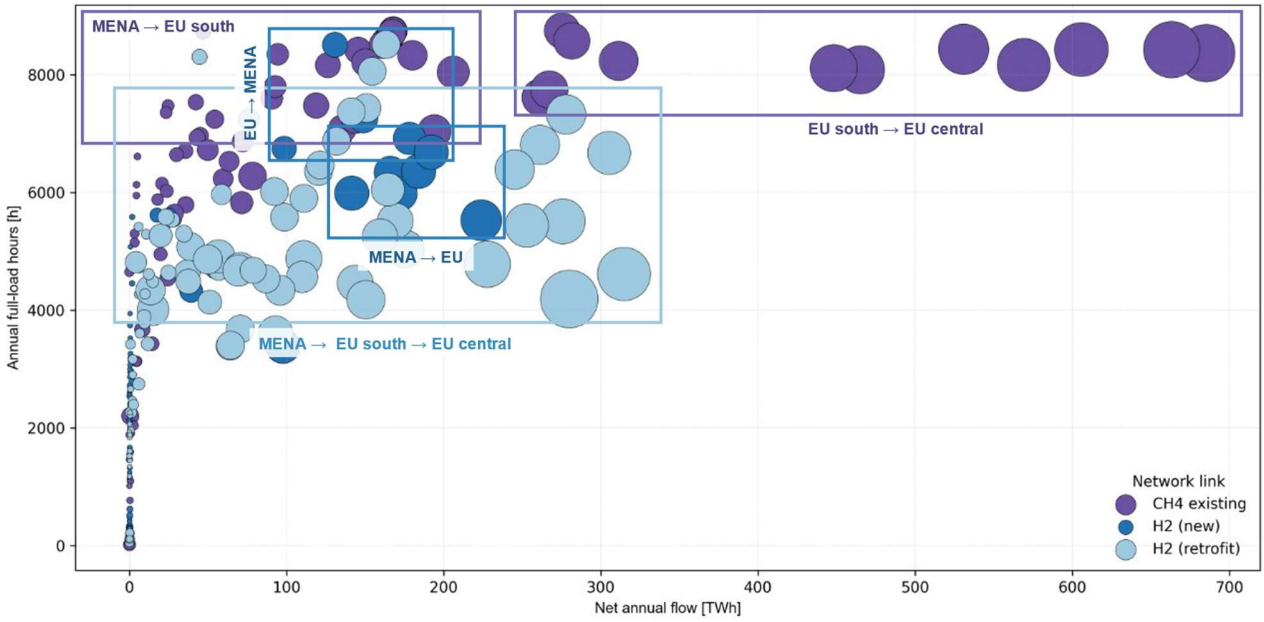

Figure 4-8 Net annual network utilisation (BASE, 2050)

The network link utilisation plot also highlights a crucial hydrogen dispatch decision. The consistently high utilisation of methane links indicates that, if pipeline expansion were allowed, the model would preferentially increase cross-regional methane transport capacity, confirming that transporting and storing methane is structurally preferable. However, because the no-expansion formulation fixes the capacity of legacy cross-regional methane pipelines, these links become a binding system bottleneck. This interpretation is corroborated by the methane pipeline decommissioning pattern. The operational capacity of all EU-MENA links in 2050 matches the legacy capacity, while the average operational legacy capacity across all other links is only 36%.

To compensate these bottlenecks, the model dispatches large methane cavern storages behind the constrained network links in Turkey, Spain and Italy, as well as near demand clusters in Europe (see Annex 13). These facilities absorb summer surpluses, coincident with PV-driven hydrogen conversion, and release gas during winter demand peaks, as shown in Figure 4-9. The required seasonal working-gas requirement amounts to 205 TWh. For context, current European gas storage capacity is ~940 TWh [69], indicating that the modelled requirement lies well within today's aggregate storage envelope.

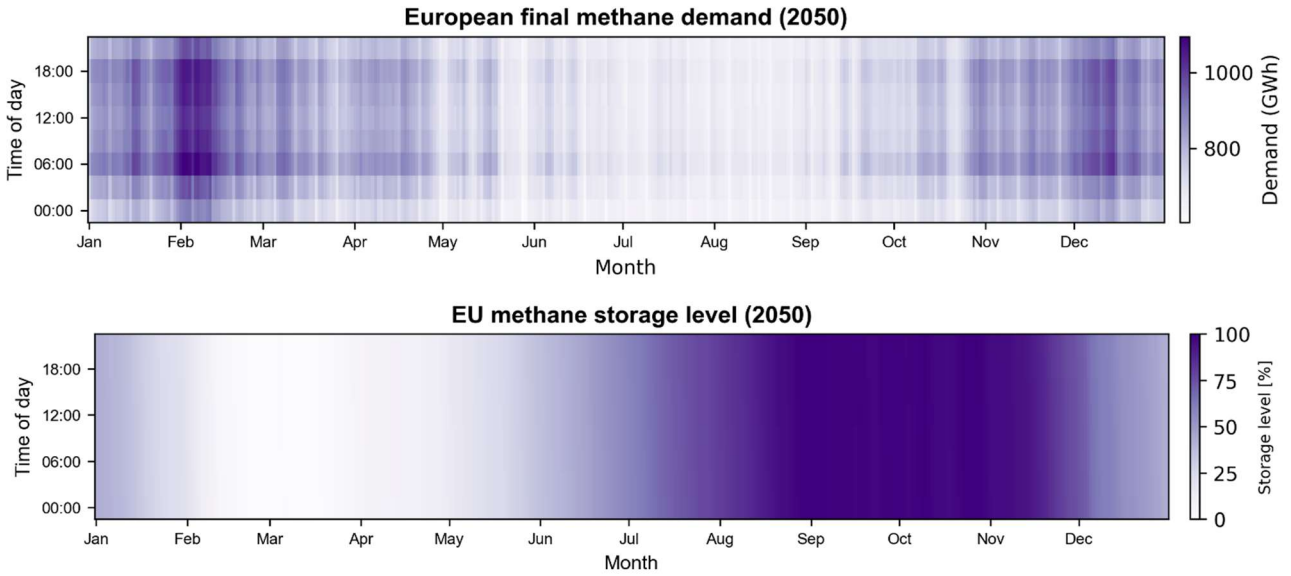

Figure 4-9 EU final methane demand and storage utilisation (BASE, 2050)

Besides methane emerging as an infrastructure constrained commodity, the network flows also highlight European hydrogen exports to Iran. Iran uses the European hydrogen imports to partially cover domestic methane demands, as 26.6% of the required hydrogen for methanation stems from European imports. Iran also emerges as an FT fuel production hub, producing 509% more FT fuel than required for domestic demand.

From there, the resulting synfuels are returned to Europe along two distinct routes. The primary route bundles land-bound FT fuel flows from Iran (33% of incoming network flow) with FT fuel shipments from Egypt (66% of incoming flow), converging in Bulgaria before being transported by land to demand clusters in Central Europe. A secondary route collects FT fuel production in Algeria and routes it into European demand clusters via Spain, providing an additional western entry point that enhances redundancy and partially relieves pressure on the East-Med pathway (Figure 4-10).

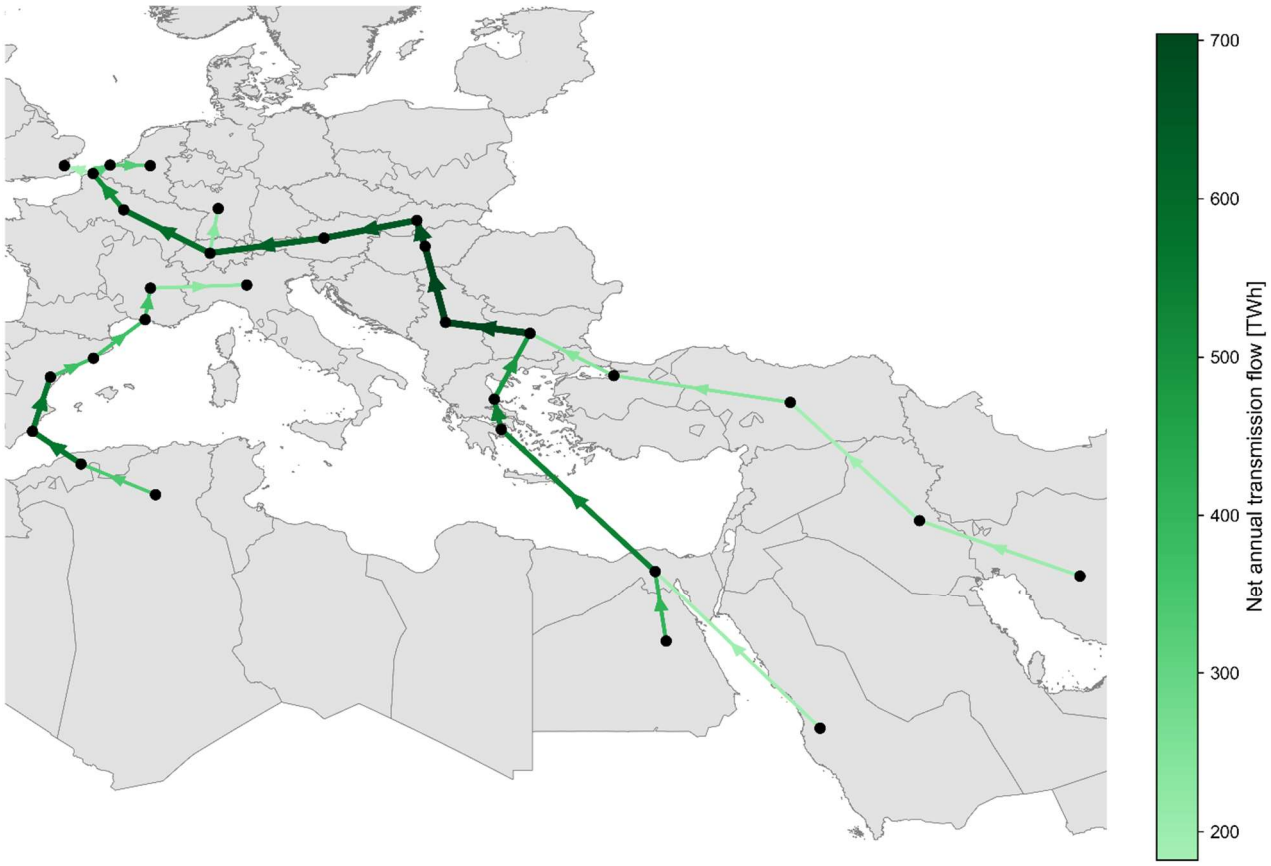

Figure 4-10 Net annual FT fuel flows; top 80% (BASE, 2050)

Taken together, the spatial deployment and dispatch of electricity-derived carriers in the BASE scenario yield a consistent functional differentiation of hydrogen, methane and FT fuels.

Hydrogen predominantly resolves short-term rather than long-term temporal imbalances. In the MENA region, hydrogen production follows the diurnal PV profile and is buffered by short-cycle tank storage, while in Europe it is routed via the retrofitted backbone to industrial and transport sinks and along the Iran export corridor. FT fuels provide long-range spatial connectivity, exploiting existing maritime and land logistics technologies to bypass pipeline bottlenecks. Methane supplies seasonal flexibility. Methane, imported through saturated import pipelines from North Africa, is stored in large cavern storages in gateway countries during the summer and then dispatched through higher volume redistribution pipelines within Europe to service winter demand peaks.

This carrier specialisation induces a hub-and-corridor network topology. Italy and Spain act as seasonal methane buffering gateways. Greece, Bulgaria and Turkey facilitate hydrogen exports and synfuel imports to and from Iran and Egypt. Central Europe appears as the dominant demand sink, dependent on energy imports.

In aggregate, the BASE system achieves diurnal balancing close to RES generation in MENA and seasonal balancing near load centres in Europe, mediated by new and retrofitted hydrogen pipelines, legacy methane infrastructure and liquid synfuel routes that jointly bridge spatial and temporal mismatches between MENA production and European consumption.

4.1.1 Pathway ramp-up dynamics in the BASE scenario

As the previous results mainly centred on highlighting the long-term configuration of the BASE system, this chapter aims to address pathway dynamics not captured in the analysis of the eventual 2050 system configuration.

In general, the supply chain composition follows the same pattern over the model horizon. Most technologies preferred in 2030 continue to be preferred in later model years (Figure 4-11). There are, however, three notable observations. First, fossil generators are gradually decommissioned over the model horizon. Second, other RES, mainly in the form of concentrated solar power, also gradually decline. And lastly, low temperature FT synthesis is only deployed in 2050, representing another example of penny-switching behaviour within the model, as investment costs of low-temperature FT synthesis fall below those of the MTH process for the first time.

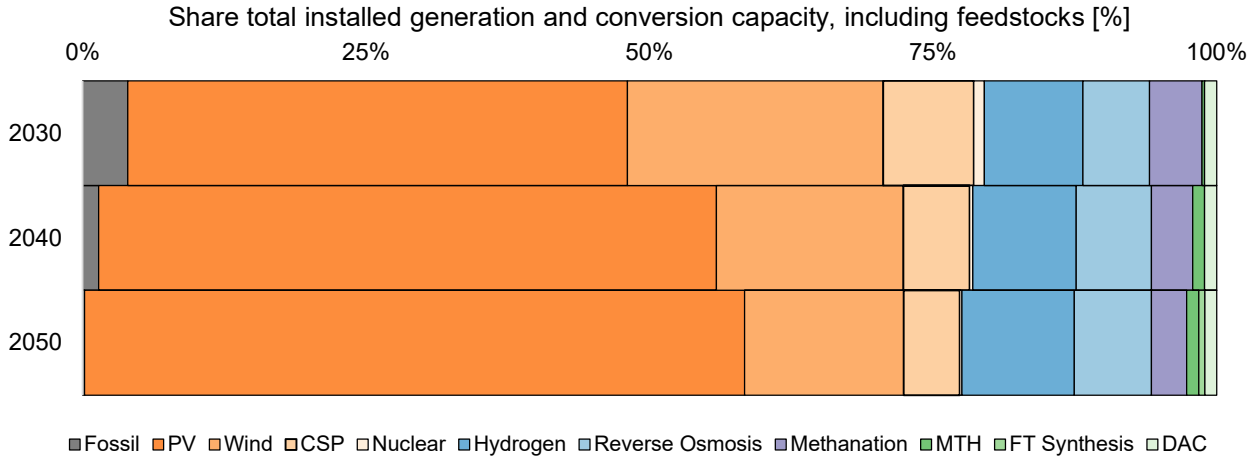

Figure 4-11 Annual supply chain composition based on total installed capacities (BASE)

Consistent with previous studies on integrated EU-MENA energy trade (e.g., [70]), which identify the MENA region as a major and growing electricity exporter, the BASE scenario reproduces a similar pattern.

While gross annual electricity exchanges between MENA and the EU remain of comparable magnitude over the model horizon, reflecting persistently high utilisation of the interconnecting links (Figure 4-12), net annual electricity imports into Europe increase over time. On the Morocco-Spain interconnector, net annual flows towards Europe rise by 13% between 2030 and 2050. Likewise, transmission volumes on the links connecting Turkey with Greece and Bulgaria increase by 72% and 90%, respectively.

By 2050, total net electricity imports from MENA reach 113 TWh, equivalent to 1.7% of European final electricity demand. This indicates that, in the modelled EU-MENA configuration, cross-regional electricity trade remains quantitatively modest relative to overall European electricity consumption.

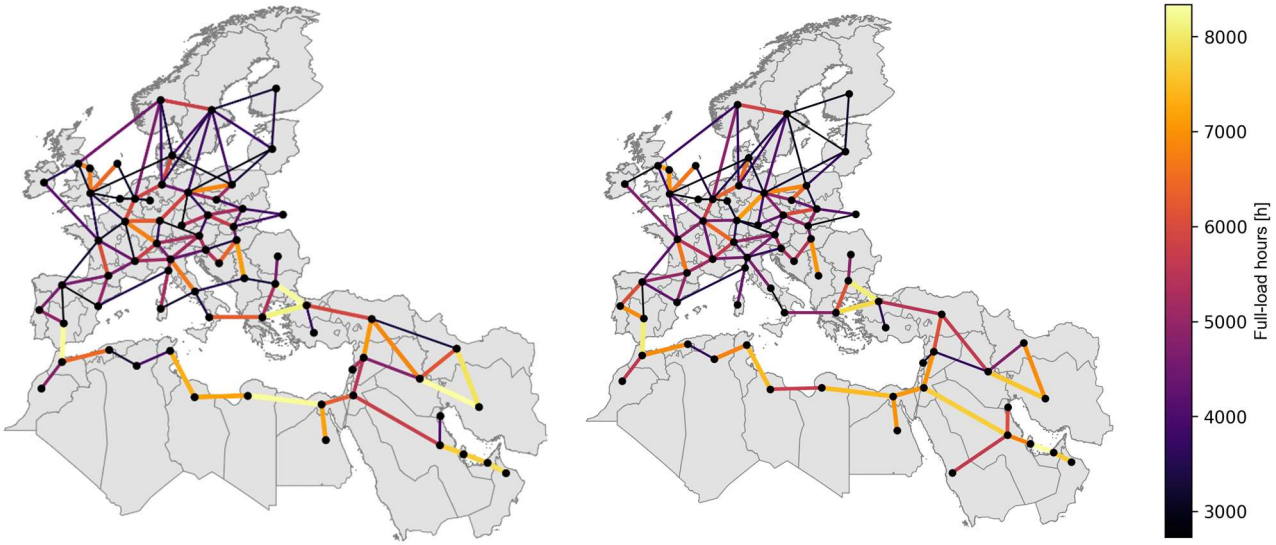

Figure 4-12 FLH of HVAC and HVDC grid 2030 (left) and 2050 (right) (BASE)

Beyond the static 2050 BASE configuration, this chapter has shown that supply chains are largely stable over time with gradual phase-outs of fossil and nuclear generation and a late, cost-driven shift to low-temperature FT synthesis, alongside increasing but still modest EU–MENA electricity imports

4.1.2 AUTARKY scenario: system reconfiguration without cross-regional trade

When energy transport between the MENA region and Europe is disabled, the system re-balances from concentrated investment in MENA towards a more geographically distributed pattern. New production clusters for electricity, hydrogen and synfuels emerge in Spain, the Balkan region and the Nordics, while MENA retains a sizeable but no longer dominant share of generation and conversion capacity (Figure 4-13 and Figure 4-14).

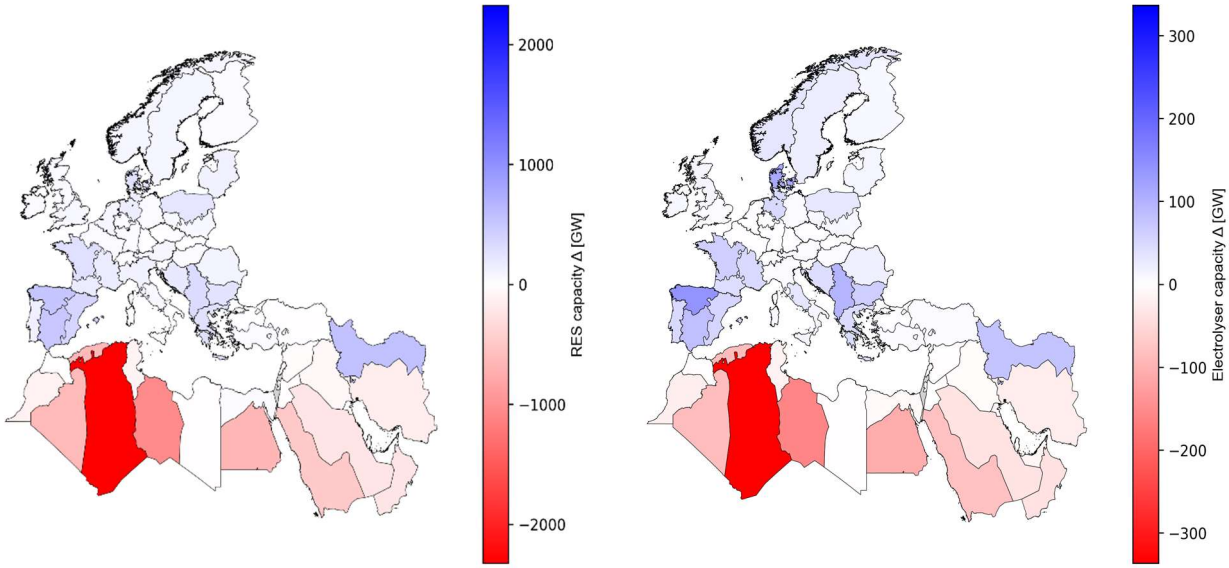

Figure 4-13 Change in RES (left) and Electrolysis (right) capacity in AUTARKY compared to BASE (2050)

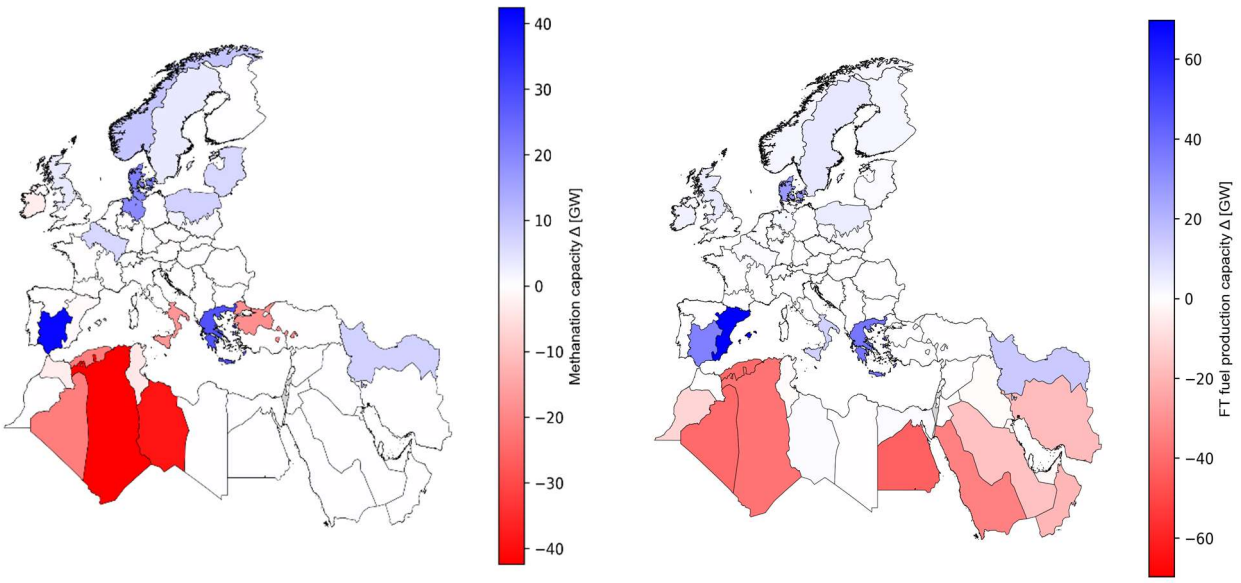

Figure 4-14 Change in methanation (left) and FT production (right) capacity in AUTARKY compared to BASE (2050)

A second prominent adjustment is the expansion and reconfiguration of storage. In BASE, the total working-gas volume across all storages amounts to 225 TWh, increasing by 19% to 268 TWh in AUTARKY. While methane cavern capacity declines moderately, hydrogen cavern storage in Europe grows by nearly 700%, indicating a substantial shift in the way seasonal flexibility is provided (Figure 4-15).

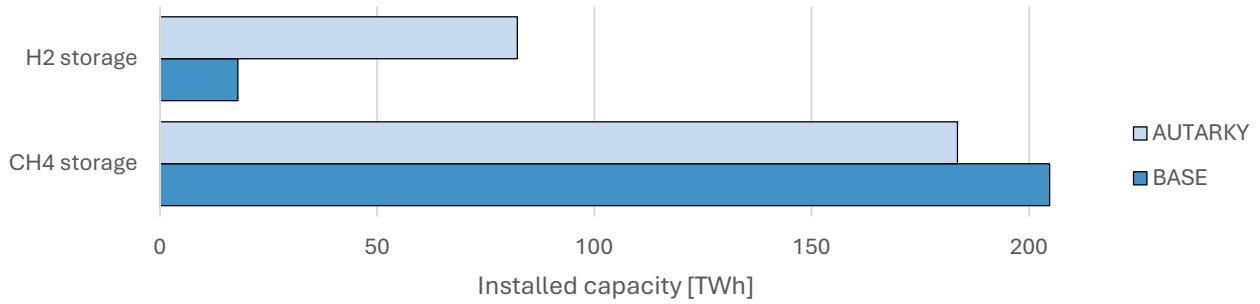

Figure 4-15 Selected storage capacity BASE vs. AUTARKY (2050)

The enlarged hydrogen storage fleet signals a change in hydrogen's role within Europe, from short-term to seasonal storage medium. State-of-charge profiles of European hydrogen caverns exhibit a pronounced annual charging–discharging cycle, in contrast to the shorter-term fluctuations seen in BASE (Figure 4-16). Hydrogen is now systematically accumulated during periods of surplus production and withdrawn to cover winter demand peaks.

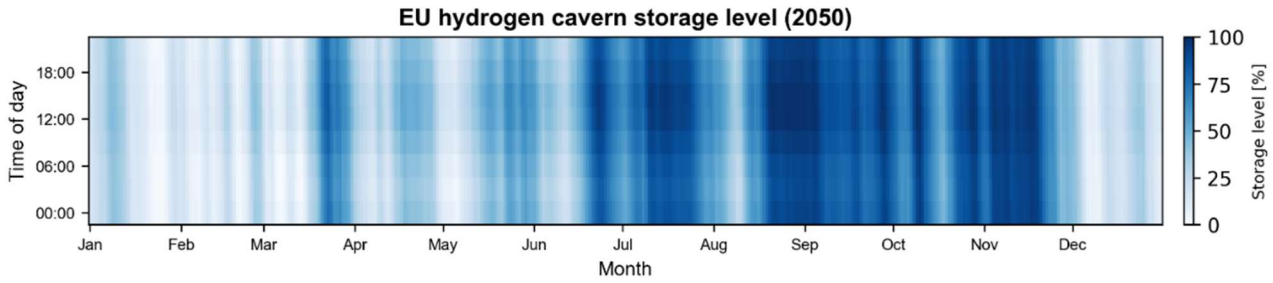

Figure 4-16 EU hydrogen cavern storage utilisation AUTARKY (2050)

This interpretation is consistent with the utilisation of hydrogen and methane pipelines. Both the net annual volume of transported hydrogen and the full-load hours of hydrogen pipelines increase, whereas methane network flows and utilisation decline (Figure 4-17).

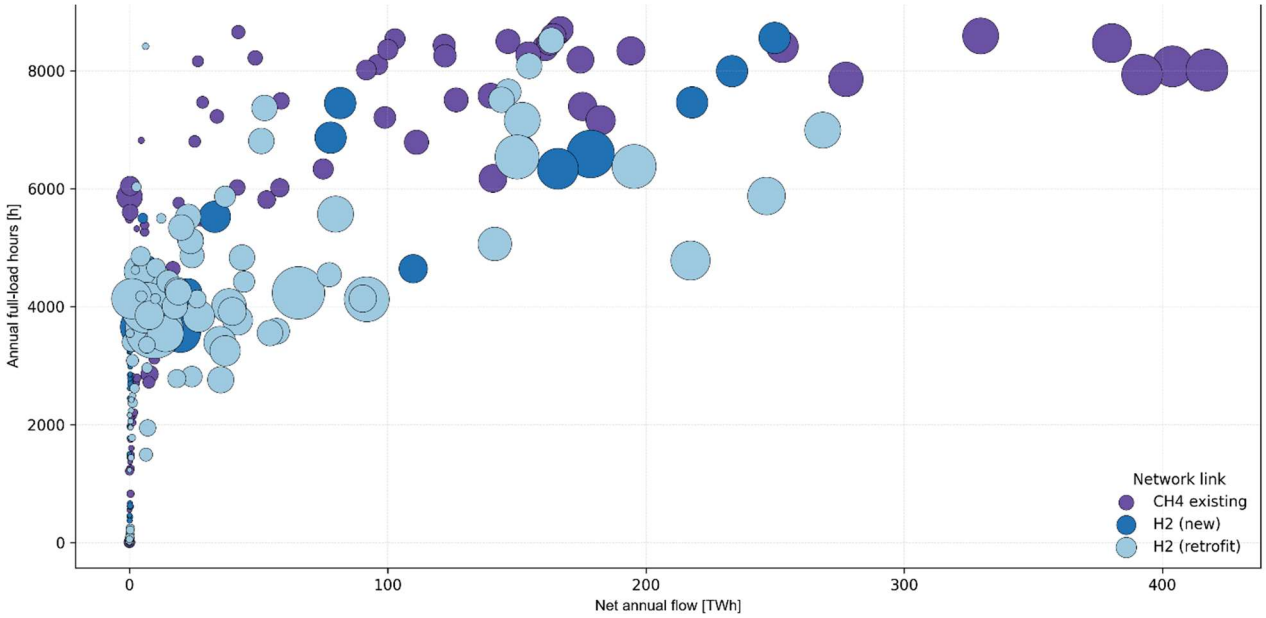

Figure 4-17 Net annual network utilisation AUTARKY (2050)

In the MENA region, hydrogen storage also develops a stronger seasonal character. Additional cavern facilities are installed in Turkey and operated with clear seasonal swings, while hydrogen tanks in other MENA countries continue to smooth short-term imbalances and intra-day variability (Figure 4-18). Together, these assets support a more regionally self-contained balancing of renewable generation.

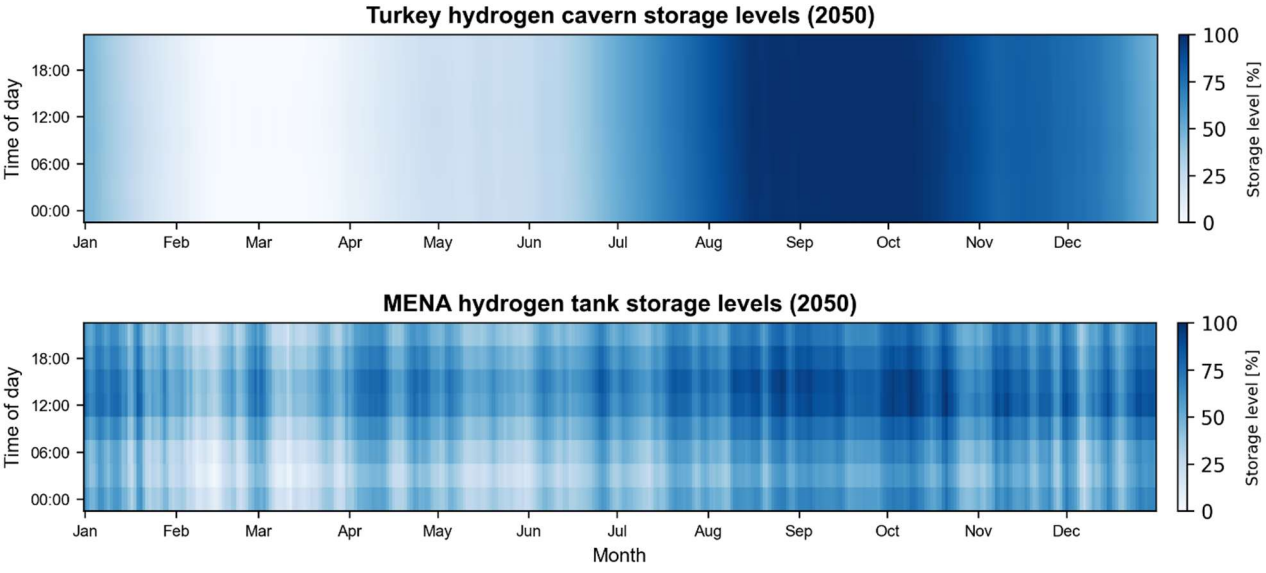

Figure 4-18 MENA and Turkey hydrogen storage utilisation AUTARKY (2050)

In summary, the AUTARKY configuration yields a more balanced spatial distribution of generation and conversion capacity, with an increased reliance on hydrogen-based flexibility rather than methane. Hydrogen becomes a genuine seasonal storage medium, particularly in the MENA region, and its gross annual network flows rise by 15.3% to 10,823 TWh per year. In parallel, gross methane flows decline by 36.1% to 6,705 TWh, reflecting the reduced

role of methane as an imported seasonal buffer. Similarly, FT fuel transport also declines by 52.2%, indicating a relocation of FT fuel production facilities closer to demand clusters (Figure 4-19).

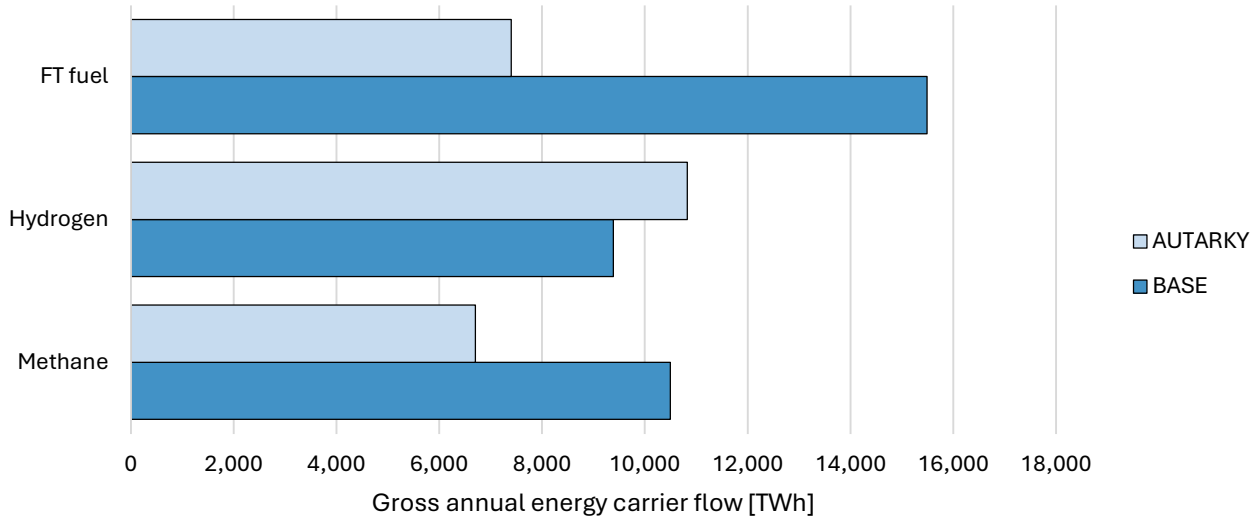

Figure 4-19 Gross annual network flows BASE vs. AUTARKY (2050)

4.1.3 System costs and regional cost decomposition

The technical patterns in BASE and AUTARKY translate into distinct cost structures and regional burdens, which are examined in this section.

The BASE total system cost over the model horizon amounts to 8.50 trillion EUR, corresponding to average annual system costs of 425.21 billion EUR, of which the MENA region carries 241.34 billion EUR, or 56.8%. For context, the EU has historically imported energy carriers at an estimated 200-300 billion EUR per year [71]. The modelled cost level is therefore within the broad range of current European energy import expenditure. Even if future EU-MENA energy partnerships were structured such that Europe shouldered a larger share of the total cost burden, the implied European energy bill would remain comparable to today, suggesting that scope for further savings lies at least as much in cost-sharing arrangements as in additional technological cost reductions.

In the MENA region, total system costs are dominated by energy-use costs, in particular CO_2 emission costs associated with final energy utilisation (42%), followed by electricity generation (35%) and hydrogen/synfuel conversion (21%, including feedstock production). As illustrated in Figure 4-20, a substantial share of these activity-related costs is offset by credits from DAC-based CO_2 capture, making aggregate MENA system costs highly sensitive to the CO_2 price trajectory. In a lower CO_2-price setting, both the gross emissions bill and the countervailing DAC credits would shrink, likely increasing TSC if MENA remains export-focused, as DAC savings currently outweigh domestic emissions cost.

In Europe, the cost structure exhibits a mirror image. Because the bulk of electricity and hydrogen-intensive processing is sited in MENA, European system costs are dominated by the cost of energy use and associated CO_2 emissions, while domestic generation, conversion and network costs account for a smaller share (Figure 4-21). This confirms that, under the BASE configuration, the European system is primarily exposed to the carbon price applied at the point of final energy use rather than to capital cost risks on the generation or

conversion side. At the same time, the spatial decoupling between the location of CO_2 emissions (mostly in Europe) and CO_2 savings (DAC and process capture in MENA) implies that a lower CO_2 price would not primarily reduce global system costs. Instead, it would shift the relative competitiveness of production locations: cheaper emissions would make it more attractive to repatriate synfuel production to Europe, along with the associated DAC, thereby strengthening European energy autarky rather than lowering worldwide mitigation cost.

Across both regions, network expansion contributes only a minor share to total system cost. Synfuel and hydrogen conversion costs are driven mainly by variable operating expenditures rather than upfront investment, consistent with the literature that identifies renewable hydrogen production as the primary cost component in synfuel supply chains (e.g., [72], [73]).

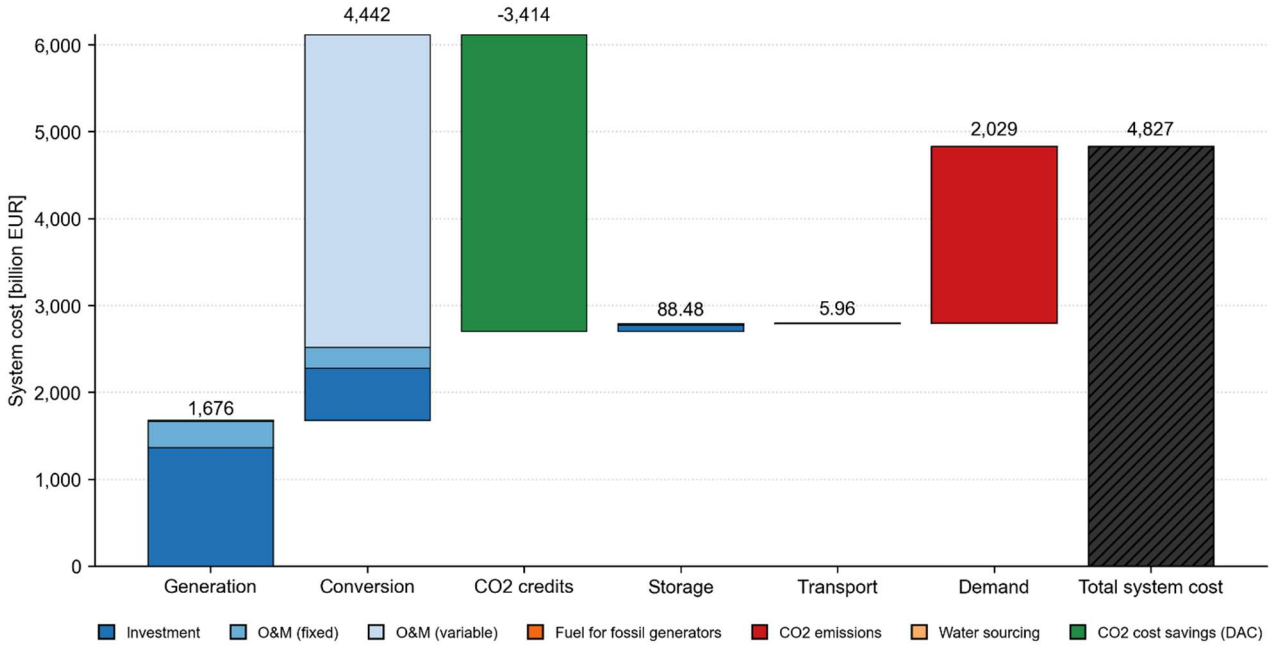

Figure 4-20 MENA total system cost by group and aspect BASE

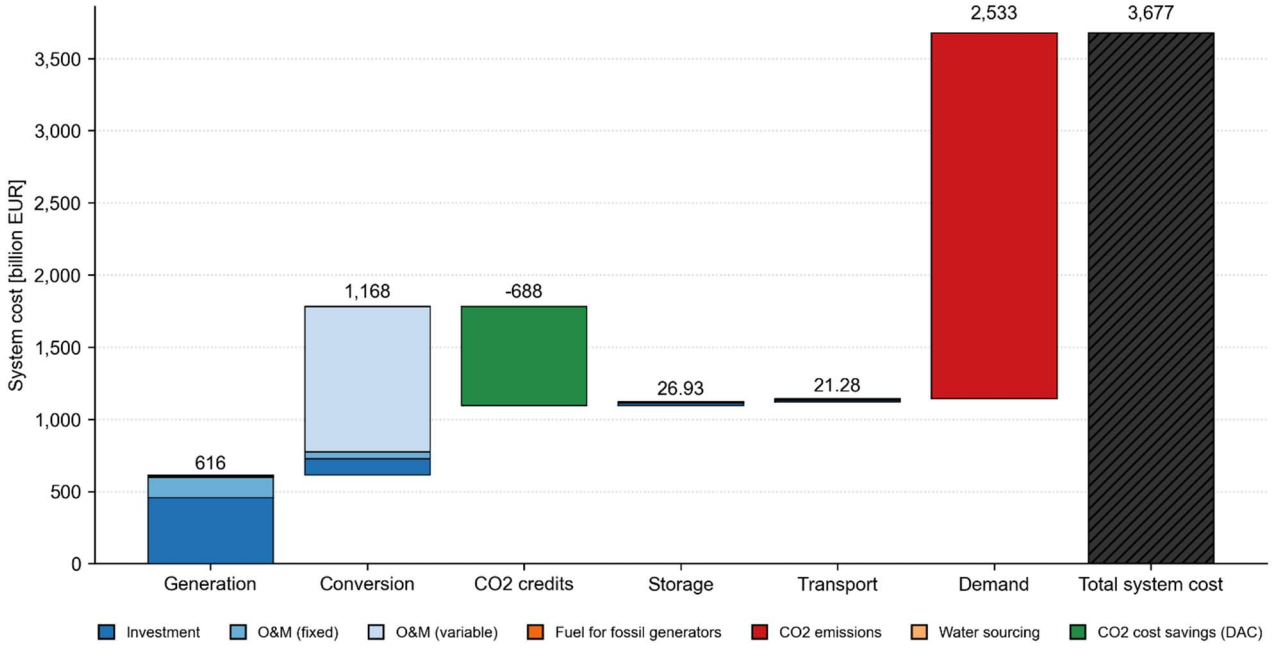

Figure 4-21 EU total system cost by group and aspect BASE

Taken together, the cost decomposition highlights three points. First, the absolute cost level of the BASE system appears politically plausible when benchmarked against historical EU energy import bills. Second, CO_2 prices are the dominant driver of both European and MENA system costs, governing whether the value of low-carbon imports derives more from avoided emissions or from avoided capital expenditure. Third, transport and network infrastructures play an enabling rather than leading role in the cost balance: they are essential to unlock spatial arbitrage, but they do not dominate total system cost.

Marginal price signals

At the system level, marginal demand prices for all synthetic energy carriers increase over time. In both Europe and MENA, the methane marginal-demand duration curves in Figure 4-22 show that the entire 2050 curve is shifted upward by roughly 3-5 EUR/kWh relative to 2030, with only limited intra-annual variation. Once fossil options are phased out and carbon costs are fully internalised, methane thus becomes a uniformly expensive carrier.

Hydrogen and FT fuels (shown in Annex 13) exhibit a similar, though somewhat smaller, price uplift between 2030 and 2050. The relatively flat shape and moderate spread of their duration curves indicate that these supply chains operate close to their long-run average costs: marginal prices are set by capital-intensive assets running at high full-load hours rather than by short scarcity spikes. Price volatility is therefore governed more by structural cost levels than by transient shortages.

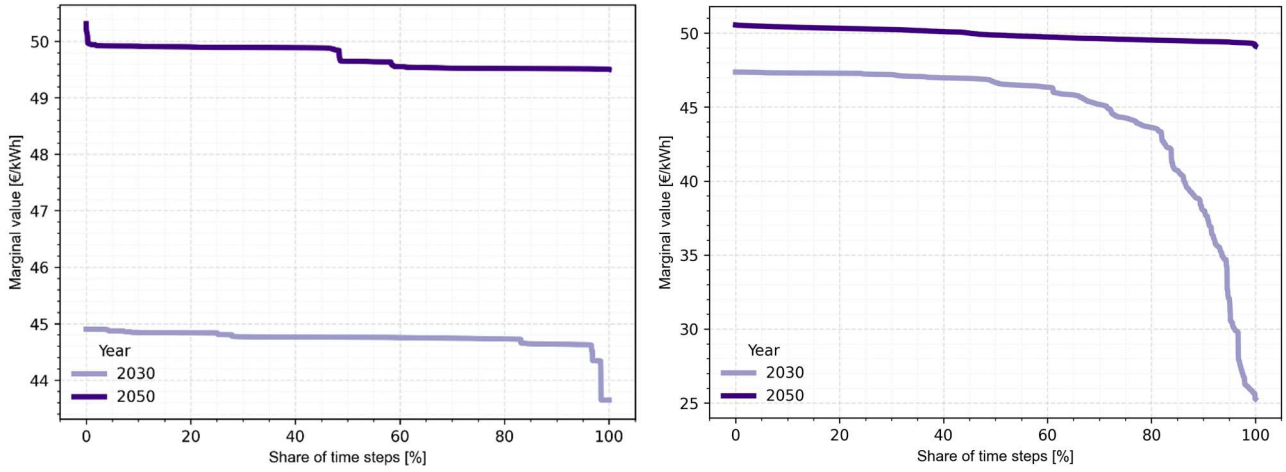

Figure 4-22 EU (left) and MENA (right) mean methane marginal demand duration curves BASE

The comparison between Europe and MENA highlights how regional price differentials evolve as trade and networks expand. In 2030, the methane and hydrogen duration curves for the two regional groups (Annex 13) still show pronounced spreads: MENA exhibits both very low and very high marginal prices, while Europe is clustered within a narrow band. This pattern suggests that MENA still hosts large pockets of unexploited low-cost potential alongside higher-cost domestic uses, whereas Europe already operates close to a single marginal option for each carrier.

By 2050, the corresponding duration curves for methane, hydrogen, electricity and FT fuels lie almost on top of each other (Figure 4-23). Remaining differences are small and confined to a few hours at the extremes of the sorted curves, typically during periods of simultaneous high demand and low renewable availability. This indicates that the bulk of the year is

characterised by almost uniform marginal values across regions, with only brief scarcity episodes preserving a small spatial premium. Transport and storage investments have thus arbitraged away most spatial spreads: energy is moved from low-cost production sites to high-demand regions until marginal values nearly equalise, compressing regional rents on hydrogen and synfuel production and leaving only narrow congestion and scarcity rents at a limited set of highly utilised network elements.

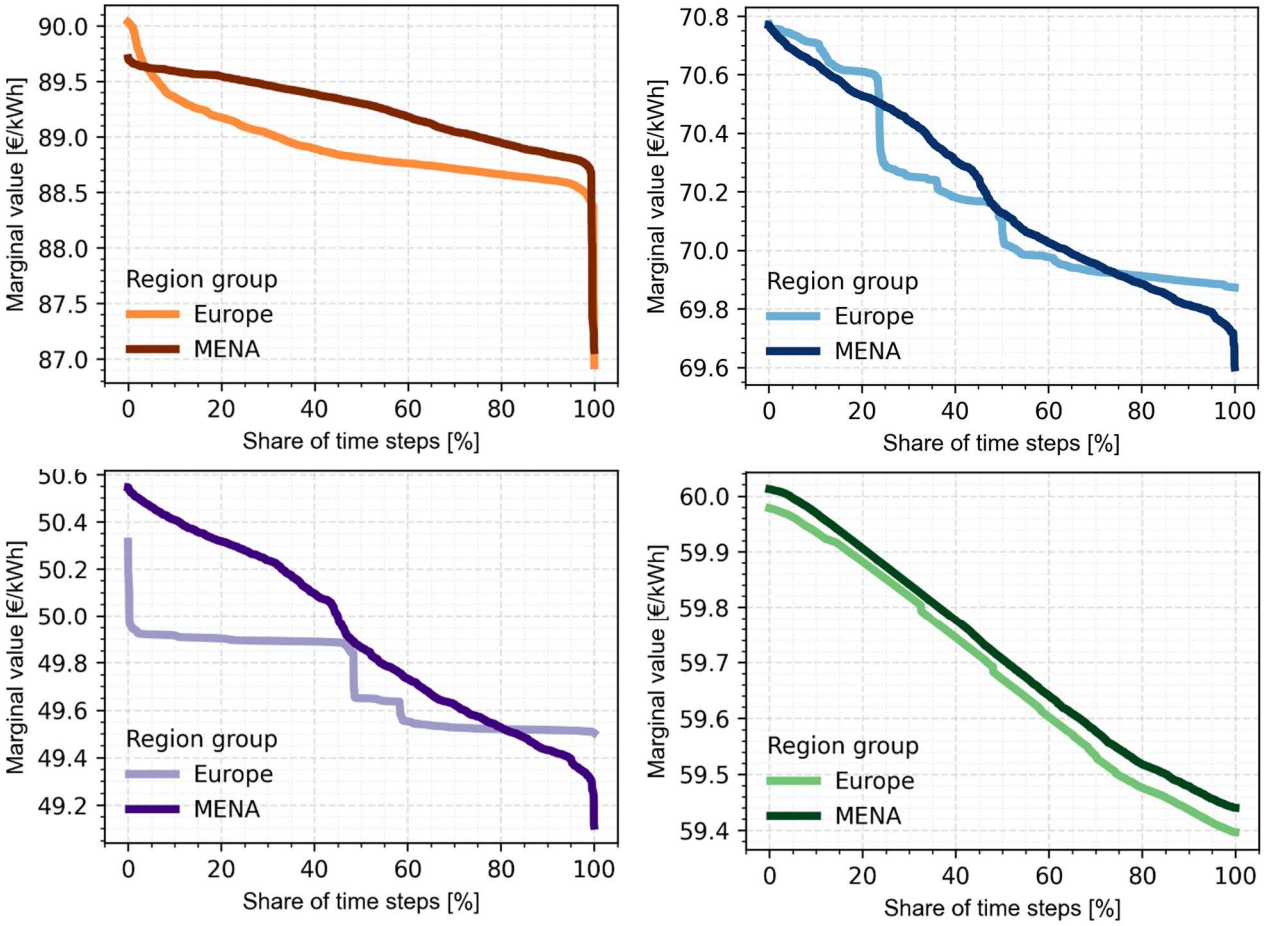

Figure 4-23 EU and MENA marginal demand duration curves BASE (2050)

Spatial patterns in marginal production costs reinforce this picture. For electricity, high-quality MENA resource regions maintain a persistent cost advantage over Europe throughout the horizon. As transportation capacity expands, this gap narrows but does not disappear. Even in 2050, selected MENA nodes remain the lowest-cost electricity producers (Figure 4-24), while high utilisation of the electricity network prevents a full equalisation of nodal production costs. The system therefore retains a structural supply advantage in specific MENA locations that cannot be entirely arbitraged away by finite grid capacity.

For hydrogen, by contrast, marginal production-cost spreads shrink dramatically over time. Initial differences between MENA and Europe of about 1 EUR/kWh decline to only a few cents per kWh by 2050, as shown in Figure 4-25. Methane and FT-fuel production costs (Annex 13) display similar behaviour, with large initial deltas reduced to comparatively small residuals in the mature system. Put differently, renewable electricity remains structurally cheaper in selected MENA sites, but the conversion and logistics system is configured such that derived fuels are delivered at nearly equal marginal costs across both regions.

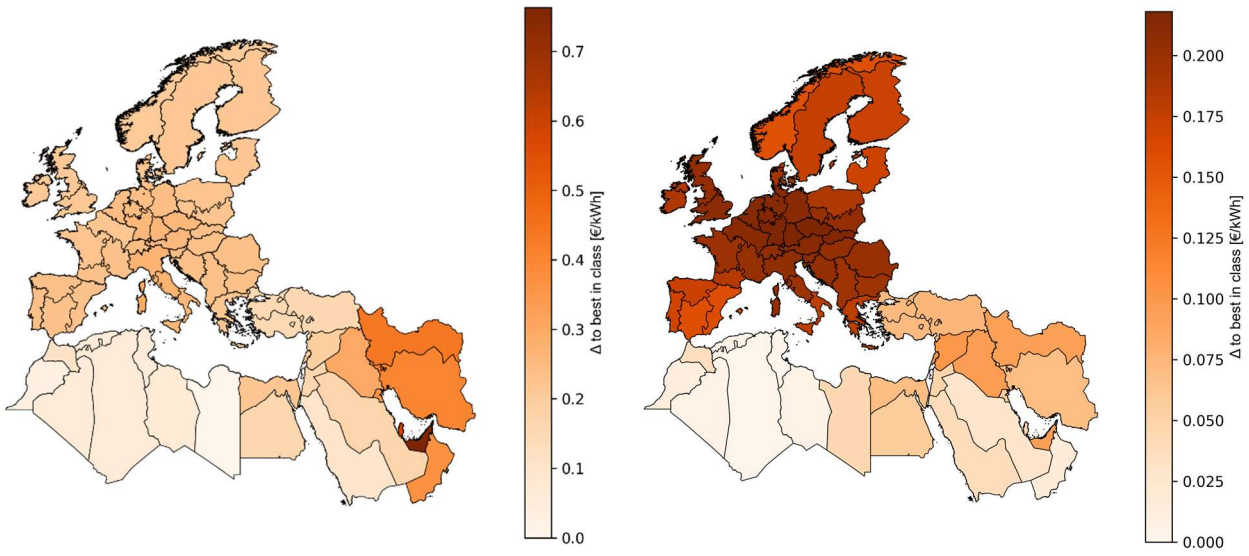

Figure 4-24 Marginal electricity production cost Δ 2030 (left) and 2050 (right) BASE

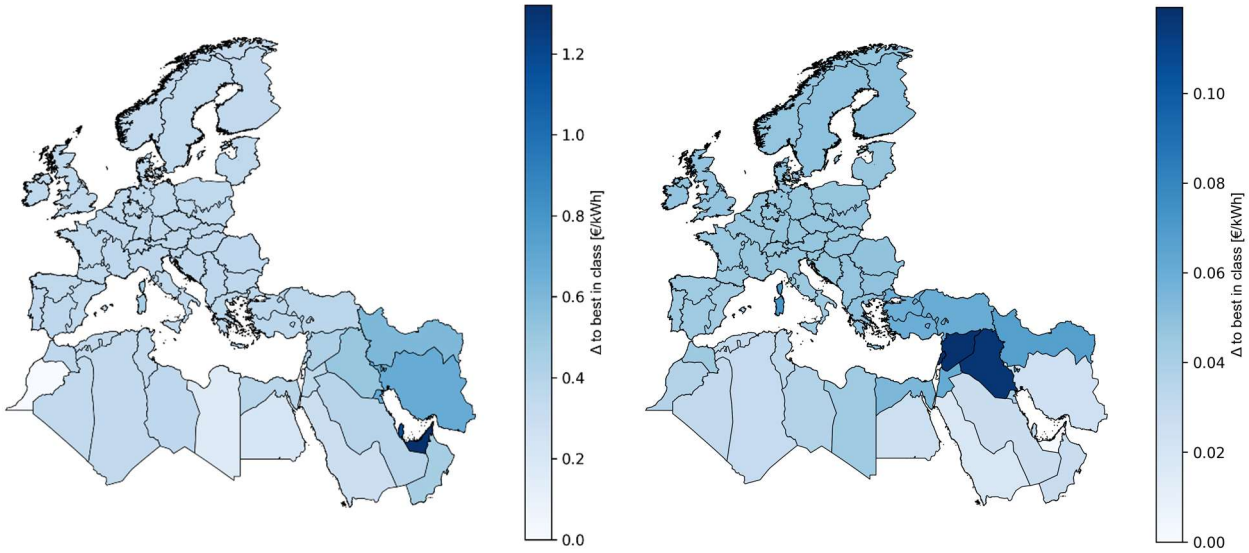

Figure 4-25 Marginal hydrogen production cost Δ 2030 (left) and 2050 (right) BASE

Overall, the demand-duration and production-cost diagnostics indicate that a mature BASE system retains a persistent electricity-cost advantage in selected MENA locations. However, marginal values for hydrogen and synfuels are largely equalised across regions and region-specific price premia in fuel production remain small. Infrastructure expansion converts most resource advantages into lower system-wide costs instead of regional mark-ups.

This reinforces the interpretation of the BASE configuration as a highly integrated EU-MENA energy space, in which Europe strategically outsources capital-intensive generation and conversion while accepting dependence on a limited set of high-utilisation corridors.

Autarky penalty calculation

Against this cost background, the AUTARKY scenario makes the price of foregoing cross-regional molecular trade explicit. Relative to BASE, total system cost in AUTARKY is 2.7% higher, even though the technical configuration changes substantially.

On the European side, the penalty is driven primarily by higher capital deployment in generation and a greater reliance on domestic flexibility (Figure 4-26). In AUTARKY, investments in electricity generators more than double (+107%), and storage dispatch increases by 63%, mainly through the build-out and intensified use of hydrogen cavern storage.

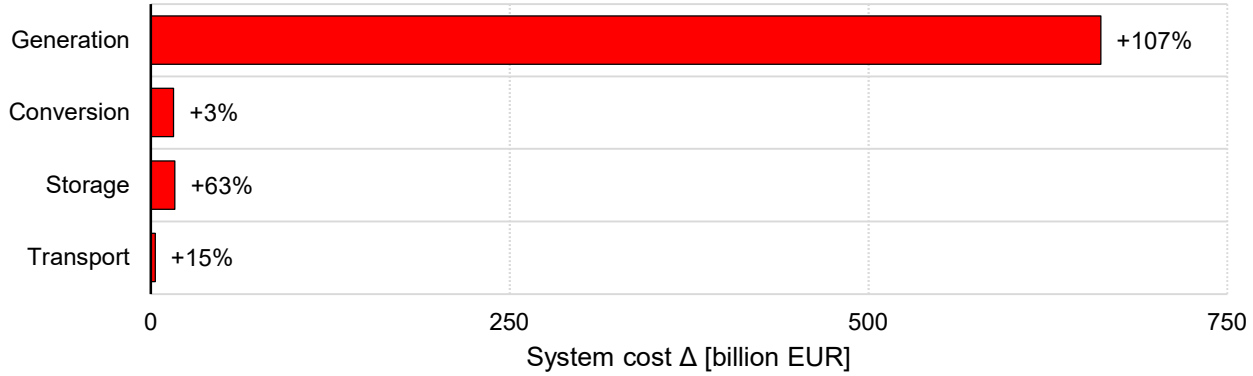

Figure 4-26 EU autarky penalty decomposition by sector BASE

Without access to cheap MENA resources and cross-regional synfuel and methane imports, Europe compensates by reshoring generation and internalising seasonal balancing. Hydrogen caverns take over part of the flexibility previously provided by imported methane and synfuels, shifting the provision of seasonal adequacy from imported molecules to domestically installed assets. Over the full horizon, this translates into a European autarky penalty of 19% relative to BASE, or about 698 billion EUR in additional system cost.

Within the MENA system, the pattern is inverted. Total system cost falls by 9.7% relative to BASE, largely because the region no longer builds an export-oriented generation and conversion fleet. Installed generator capacity declines by 54%, and associated generation expenditures drop accordingly. At the same time, investments into hydrogen storage in Turkey increase storage costs by 21% compared to BASE (Annex 13), as hydrogen caverns there take over a larger share of regional balancing. In economic terms, MENA substitutes capital-intensive export infrastructure with a smaller, more domestically focused system.

4.1.4 Political implications: import dependence and sovereignty

The import dependency of European countries is high in the BASE scenario. As shown in Figure 4-27, several countries cover over 50% of their final hydrogen and synfuel demand through imports. For demand clusters such as Germany, or the Benelux area, import dependency reaches around 95%. In total, Europe covers 47.6% of the total energy demand through imports in 2050. Carrier-specific plots (Annex 13) show that methane and FT fuels are almost entirely import-supplied for top consumers.

Relative to the average EU import dependency of 59.2% in 2023 [71], the aggregate import share in 2050 declines somewhat to 47.6%, but still implies that nearly half of final energy demand is met by imports. However, a per-country comparison of import dependency (Figure 4-28) highlights, that countries with high domestic production potential (e.g., Spain, Greece, Italy) are able to reduce their import dependency, while the import dependency for central European demand clusters such as Germany or the Benelux area actually increases by 2050. exc

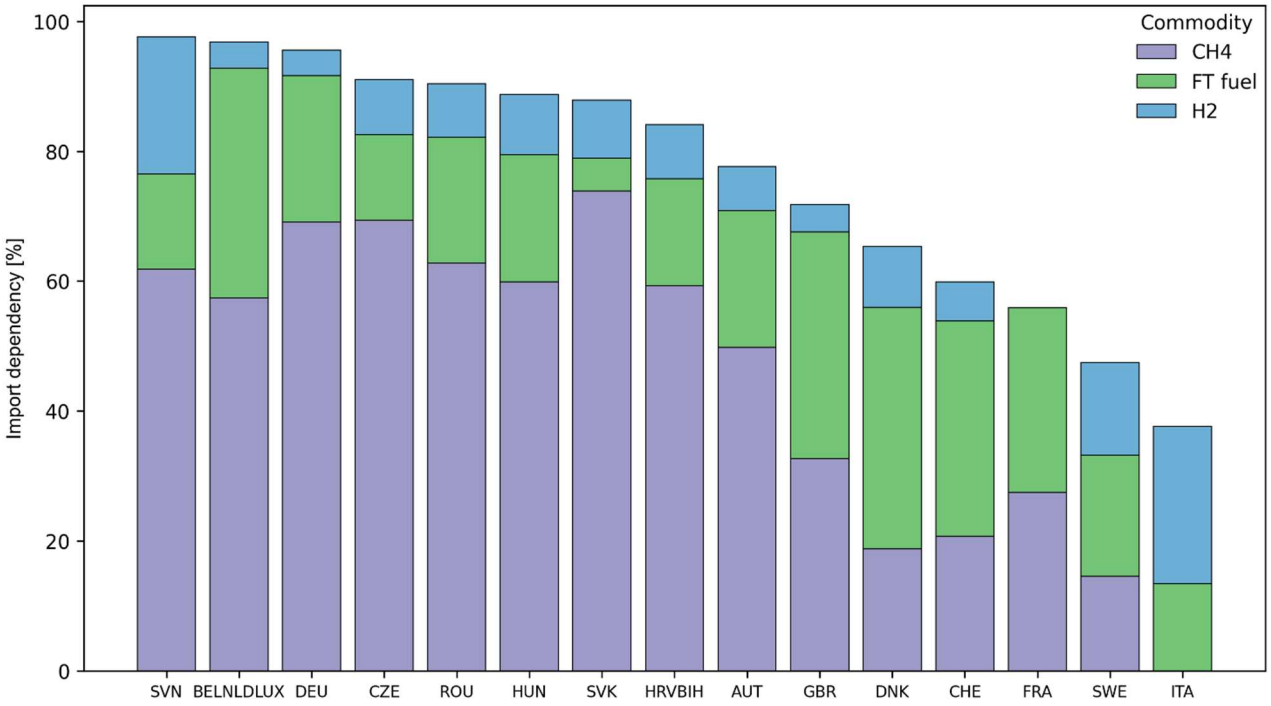

Figure 4-27 Import dependency by country (top 15) BASE (2050)

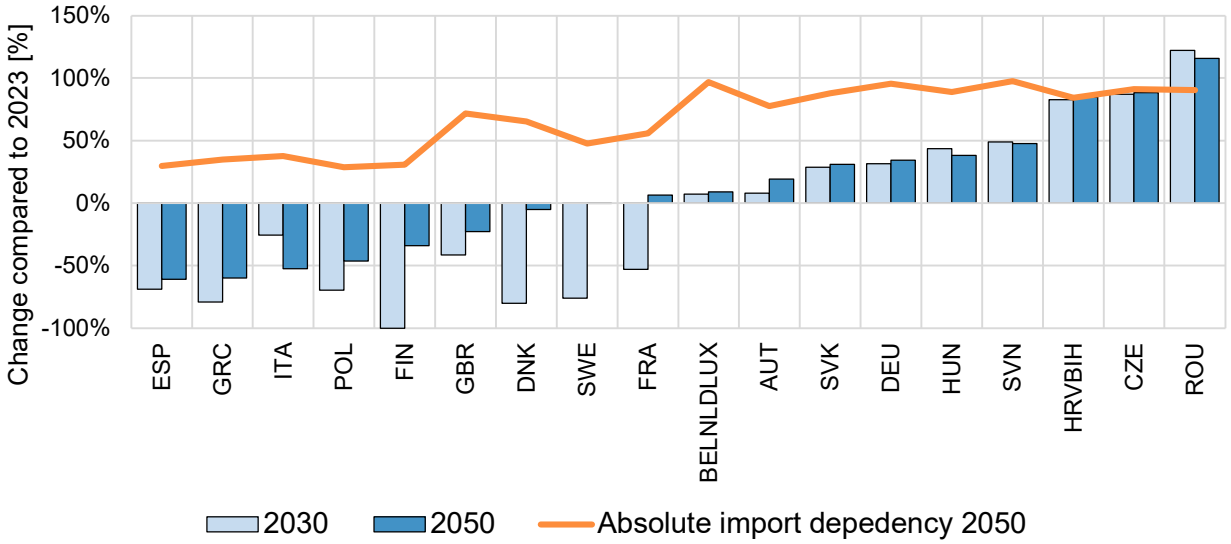

Figure 4-28 Change between BASE and 2023 reference import dependencies (country-specific import dependency data from [74])

Together, these findings answer Sub-question 1. Under uniform financing and unconstrained trade, the model configures a clearly MENA-centred system in which most renewables, electrolysers and synfuel plants are located in North Africa and the Middle East, exporting synthetic methane, hydrogen and FT fuels to a structurally import-dependent Europe. The AUTARKY case shows that Europe can technically reshore supply by massively expanding domestic capacity and seasonal storage, but only at a sizeable total-system-cost penalty, with Europe bearing most of the increase.

4.2 Outcome sensitivity to infrastructure constraints

This chapter now probes the robustness of that MENA-centred pattern against transportation constraints. Sections 4.2.1 and 4.2.2 report dedicated model runs for infrastructure

delay (TRANS_delay) and the removal of cross-regional pipelines (TRANS_no_pipeline), thereby addressing Sub-question 2 on the importance of infrastructure availability and use. Section 4.2.3 then uses the resulting cost structure as a reference point to qualitatively discuss the role of CO_2 price trajectories and DAC credits, without introducing additional model runs.

4.2.1 TRANS_delay

In TRANS_delay, the expansion of cross-regional hydrogen pipelines is prohibited until 2040, with 2050 as the first commissioning year for additional capacities. Methane continues to use legacy pipeline infrastructure and FT fuels are transported by ship and land. The scenario effectively investigates the role of strongly delayed hydrogen trade within the EU-MENA system, highlighting the adequacy of existing infrastructure.

Compared to BASE, interregional electricity grid capacity decreases by 13%, and hydrogen pipeline capacity falls by 78%. The system substitutes long-distance hydrogen transport with more regionalised hydrogen production and storage, while relying on legacy gas and synfuel logistics for cross-border trade.

On the supply side, this shift is visible in the installed capacities of renewable generation and electrolysers (Figure 4-29). By 2050, European electrolyser capacity is 36% higher than in BASE, while synfuel capacities remain essentially unchanged. The model therefore localises hydrogen production within the EU but maintains the MENA region as the main synfuel export hub.

Hydrogen storage follows the same pattern. European hydrogen cavern capacity increases by 184% and hydrogen tank storage by 75% relative to BASE, mirroring the qualitative behaviour of the AUTARKY scenario but at a smaller scale. Methane storage capacity, in contrast, remains an order of magnitude larger than hydrogen caverns, confirming that methane still provides the dominant seasonal buffer. The additional hydrogen storage is primarily used to bridge medium- to long-term imbalances within the European subsystem, partially replacing imported hydrogen flows.

Gross annual energy transfers confirm that most carriers are only moderately affected by the delayed infrastructure. Electricity (-11%), methane (-15%) and FT fuel (-1%) flows remain close to BASE levels, while hydrogen network flows drop by 47%. In contrast to BASE, hydrogen is no longer exported eastward to Iran; instead, hydrogen flows exclusively into the EU to meet domestic demand (Annex 13).

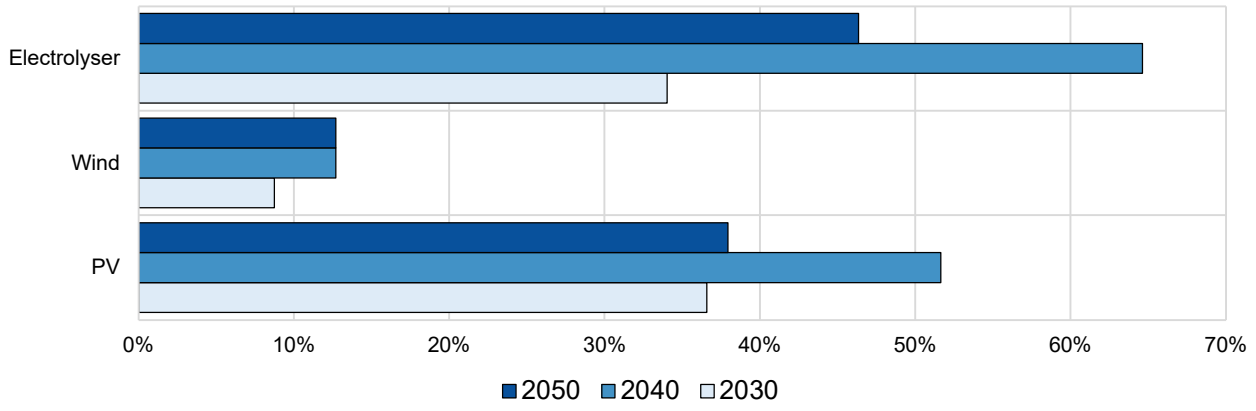

Figure 4-29 Installed RES and electrolysis capacity TRANS_delay vs. BASE

From a cost perspective, TRANS_delay remains clearly preferable to full autarky. Compared to AUTARKY, total system cost is 13.1% lower, corresponding to savings of 506 billion EUR over the model horizon (Figure 4-30). The European system relies on less domestic generation and storage capacity than under autarky and can still draw on MENA resources via methane imports and synfuel trade.

Relative to the unconstrained BASE, however, delaying infrastructure expansion entails a modest penalty. In TRANS_delay, total system cost is 1.4% higher than in BASE, and the European system is 5.2% more expensive, mainly due to 22% higher generation costs and 39% higher storage costs. Early expansion of electricity and hydrogen corridors thus remains economically valuable: it flattens marginal price spreads, reduces the need for domestic flexibility in Europe and enables more efficient use of MENA resource potentials.

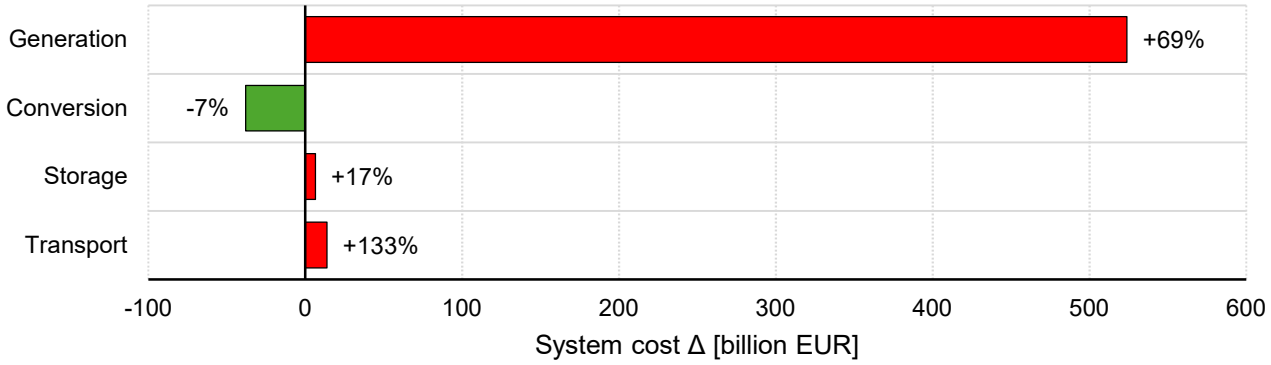

Figure 4-30 EU autarky penalty by sector TRANS_delay

Overall, TRANS_delay demonstrates that even with substantially delayed hydrogen corridors, legacy methane pipelines and synfuel logistics already suffice to sustain a MENA-centred production pattern and reduce the European cost penalty relative to autarky. It also shows, that the additional benefit of early corridor expansion is real but incremental: it reduces, rather than reverses, the strong reliance on MENA-based generation and conversion.

4.2.2 TRANS_no_pipeline

The TRANS_no_pipeline scenario removes all cross-regional methane and hydrogen pipeline connections between MENA and Europe. Long-distance energy trade is thus limited to electricity exchange via HVAC/HVDC and the maritime and land transport of synfuels. Land transport is never constrained, so synfuel trade is always technically possible.

This configuration effectively isolates the system value of FT fuel trade under the most restrictive pipeline setting. As expected from the AUTARKY and TRANS_delay analyses, the European energy system responds with increased domestic RES, hydrogen and methane generation, while FT fuel production remains exclusively sited in the MENA region (

Figure 4-31). European generators and converters cluster, as in AUTARKY, in Spain, Greece and the Nordics.

Compared to full autarky, the European energy system requires 42% less solar PV, 18% less on- and offshore wind and 42% less electrolysis capacity by 2050. This indicates that a considerable share of the additional generators and electrolysers in AUTARKY serve FT fuel production, which in TRANS_no_pipeline is again externalised to MENA. Hydrogen pipeline capacity within Europe declines by 47% (new) and 26% (retrofitted), while hydrogen storage capacities fall by 36% (cavern) and 5% (tanks). The system dispatches 10% more methane

cavern storage (159.2 TWh), underscoring an even stronger reliance on methane as the main seasonal storage vector compared to BASE.

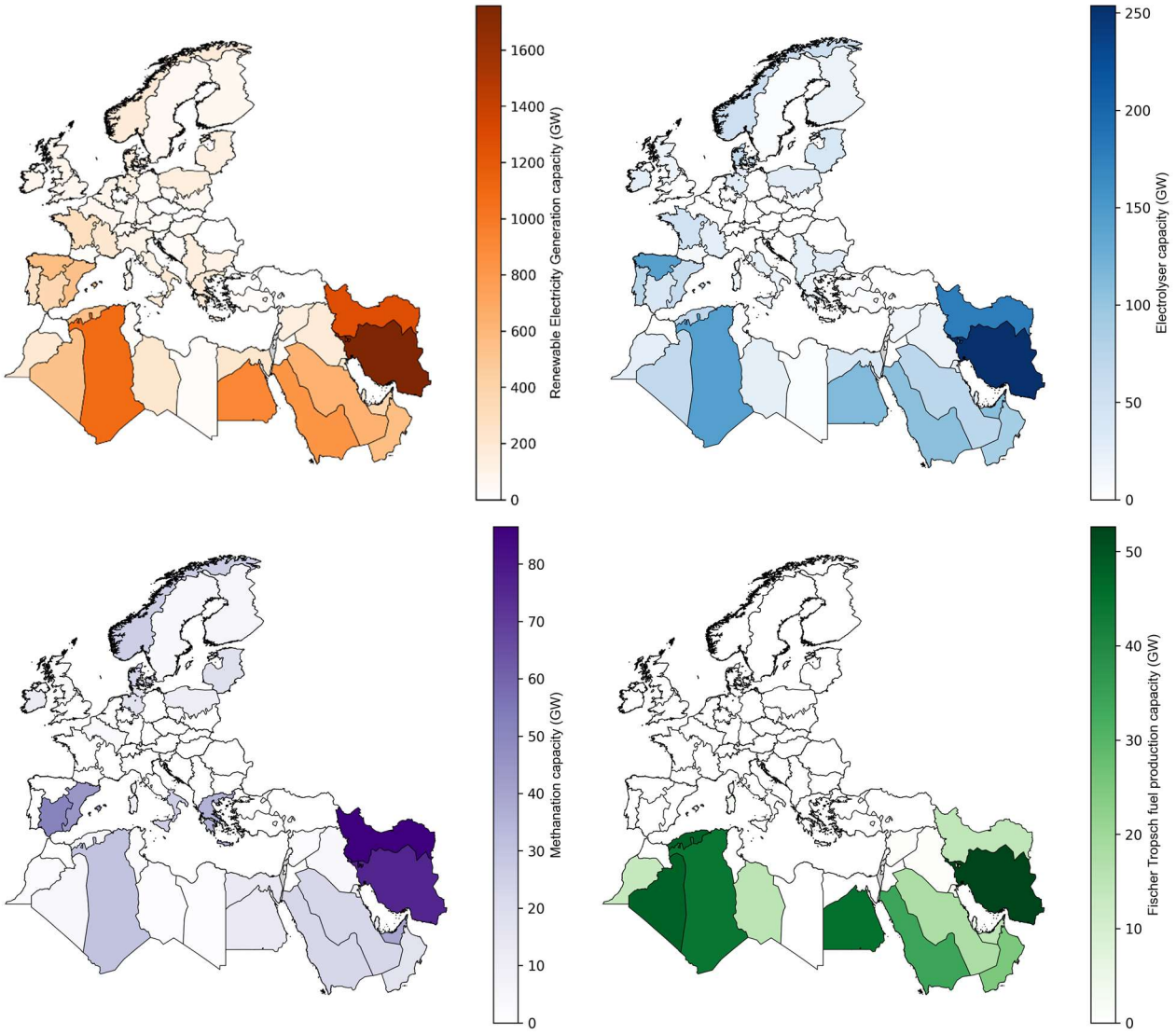

Figure 4-31 Total installed RES (top left), hydrogen (top right), methanation (bottom left) and FT fuel production (bottom right) capacities TRANS_no_pipeline (2050)

The cost decomposition shows a mixed picture. Relative to AUTARKY, European electricity generation costs are 18.2% lower and storage costs 28.1% lower, reflecting the reduced need for domestic capacity. At the same time, conversion-related costs rise by 106.5%, driven by the intense use of methanation pathways.

This apparent paradox is resolved by examining the location of DAC capacity (Figure 4-32). As already visible in BASE, conversion-related system costs are dominated by variable expenditures, a large fraction of which is offset by CO_2 capture credits. With low electricity generation costs and high CO_2 prices, as in MENA, DAC units can generate a net benefit. The value of avoided or removed emissions exceeds the incremental energy and capital costs.

In AUTARKY, part of the DAC fleet is effectively co-located with FT fuel production or other emitters within Europe, so some of these net benefits appear in the European system ledger. In TRANS_no_pipeline, FT fuel production and the associated DAC capacity are

consolidated in MENA. The net-beneficial impact of CO_2 removal is thus booked in the MENA cost balance, while Europe mainly sees the costs of final energy use and residual emissions. The result is that global TSC are still 1.1% lower than in AUTARKY, with MENA as the main beneficiary of CO_2 capture rents. From the European perspective, however, the system is more expensive than under AUTARKY (6.5%), because the region loses access to part of the DAC-related cost relief.

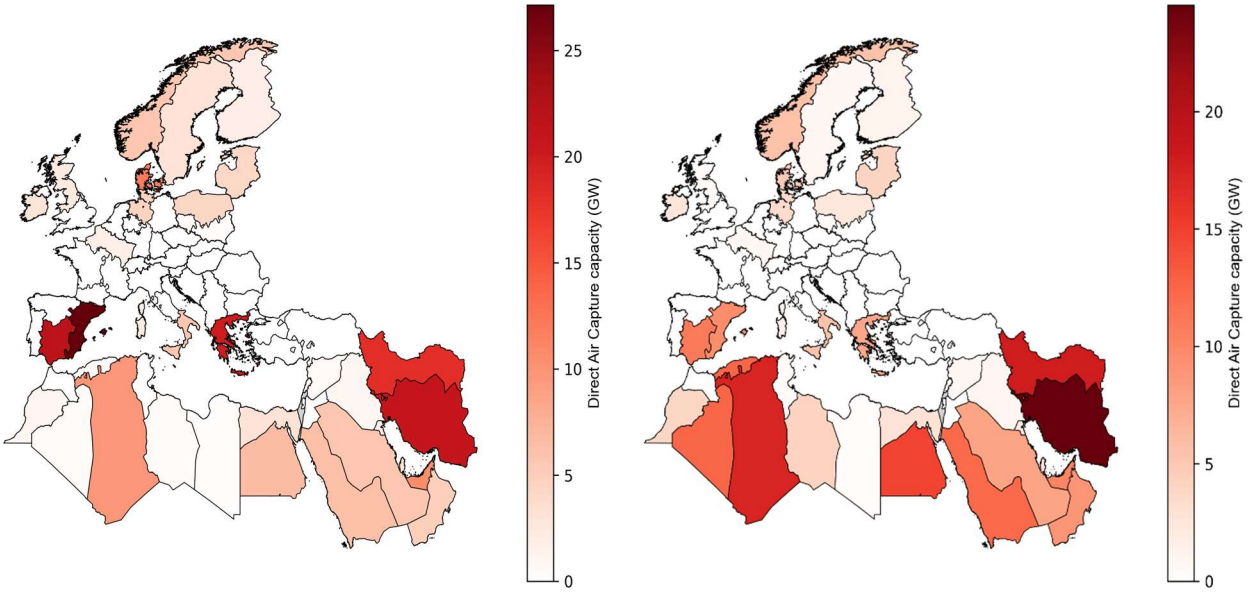

Figure 4-32 Regional DAC capacity AUTARKY (left) and TRANS_no_pipeline (right) in 2050

In short, when pipelines are removed but synfuel trade persists, the system still exploits MENA's superior resource quality and lower conversion costs, and global TSC falls slightly relative to AUTARKY. However, the distribution of benefits becomes asymmetric: MENA captures most of the CO_2-related gains, while the EU bears higher net system costs than under the unconstrained BASE configuration.

The TRANS_delay and TRANS_no_pipeline cases together answer Sub-question 2: infrastructure limits noticeably reshape where capacity is built and how energy moves, but do not overturn the MENA-centred architecture. Delayed or absent cross-regional hydrogen pipelines trigger more electrolysers, storage and reshoring in Europe as well as a more regionalised hydrogen system, yet MENA remains the main synfuel hub as shipping and legacy gas infrastructure can compensate large parts of the constrained or missing infrastructure. Total system costs rise compared to BASE, but the penalty is moderate and remains below the cost of full autarky.

4.2.3 CO_2 price levels, regional differentials and system cost

The TRANS_no_pipeline results underline that CO_2 prices and the treatment of DAC credits shape both the level and the regional allocation of system costs in the current model configuration.

Under the shared baseline CO_2 trajectory, a large share of MENA's activity-related cost is offset by DAC revenues. High CO_2 prices increase the gross emissions bill but also raise the value of captured and removed CO_2. Given cheap renewable electricity in MENA, the DAC revenue effect dominates in exporting countries, so DAC becomes a profitable activity that the model dispatches extensively. Net total system costs in MENA with rising CO_2

prices. On the aggregated EU-MENA level, DAC credits almost fully cancel out emission costs, though substantial CO_2-related payments flow from Europe to MENA.

If the CO_2 price path were lowered uniformly in both regions, two things would likely happen. First, the penalty for residual emissions and inverse value of DAC credits would fall. In a system where DAC is already deployed at scale and is net-beneficial in MENA, the loss of DAC revenue dominates this trade-off. The model would install less DAC, accept more residual emissions and give up a negative-cost asset that previously reduced total system costs. As a result, overall system costs could increase, even though emitting becomes cheaper in accounting terms. Politically, this weakens the business case for large DAC clusters in MENA and reduces the scope for a burden-sharing arrangement in which European CO_2 payments help finance negative emissions in exporting regions.

If CO_2 prices diverge between regions, the allocation of DAC and the distribution of rents could shift. In a system with comparatively lower CO_2 prices in MENA and unchanged prices in Europe, the incentive to deploy DAC in MENA weakens because each tonne of removal earns fewer credits. The optimiser would tend to relocate part of the DAC capacity to Europe, where the high CO_2 price still justifies more expensive removals, and some emission-intensive stages of the value chain could shift back to Europe for the same reason. MENA's net-negative position shrinks, DAC-related rents decline, and Europe takes on a larger share of the physical abatement effort while retaining more of the associated value creation. Given that, at present, only Saudi Arabia and Egypt countries operate government-administered carbon crediting mechanisms [75], and effective CO_2 price levels in the region are generally low, such an asymmetric configuration with lower CO_2 costs in MENA appears more plausible than a fully harmonised regime.

Taken together, these considerations suggest that CO_2 price levels and regional differentials are a structurally important driver of system behaviour in this type of EU-MENA architecture. Within the assumptions of this study, they influence the scale and location of DAC deployment, the regional distribution of costs and rents and the political economy of EU-MENA energy trade, while leaving the qualitative importance of interregional trade in low-carbon carriers intact.

4.3 Outcome sensitivity to finance constraints

Replacing the uniform cost-of-capital assumption in the MENA region with country-specific values leads to three major shifts in the model. First, a partial reshoring of capacity investments back to Europe as well as a concentration of installed capacities in a small number of MENA countries can be observed. Second, the volume of electricity, hydrogen and methane transmission flows is reduced. Third, total system costs increase more than in any other scenario.

Higher financing risks in countries that function as the main entry points into the European energy grid in BASE, such as Algeria, Egypt, Tunisia and Libya, lead to a partial reshoring of production capacity back to Europe. In these countries, WACC values for renewables and synfuels are well above the uniform 8% used in BASE, which makes large export-oriented projects less attractive. Inside the MENA region, new capacity installations concentrate overwhelmingly in Saudi Arabia, where WACC values for renewables, electrolysis and synfuel investments are below the European benchmark (

Figure 4-33). Similarly to BASE, Iran still relies on hydrogen imports to cover domestic methane demand; however, synfuel production is now almost exclusively sited in Saudi Arabia.

Only the production capacity of FT fuels inside the MENA region remains broadly similar to BASE, while electrolysis (-29%) and methanation (-32%) capacity is reduced significantly. The siting of renewable generation, electrolysis and methane production further away from the traditional entry points is also visible when analysing the gross annual transmission flows. Electricity flows decrease markedly (-62.1%), methane flows decline by roughly one third (-31.9%) and hydrogen flows fall more moderately (-11.6%), indicating that the additional transport distance from Saudi Arabia to European entry points is either not financially viable or not possible within the imposed build-rate limitations.

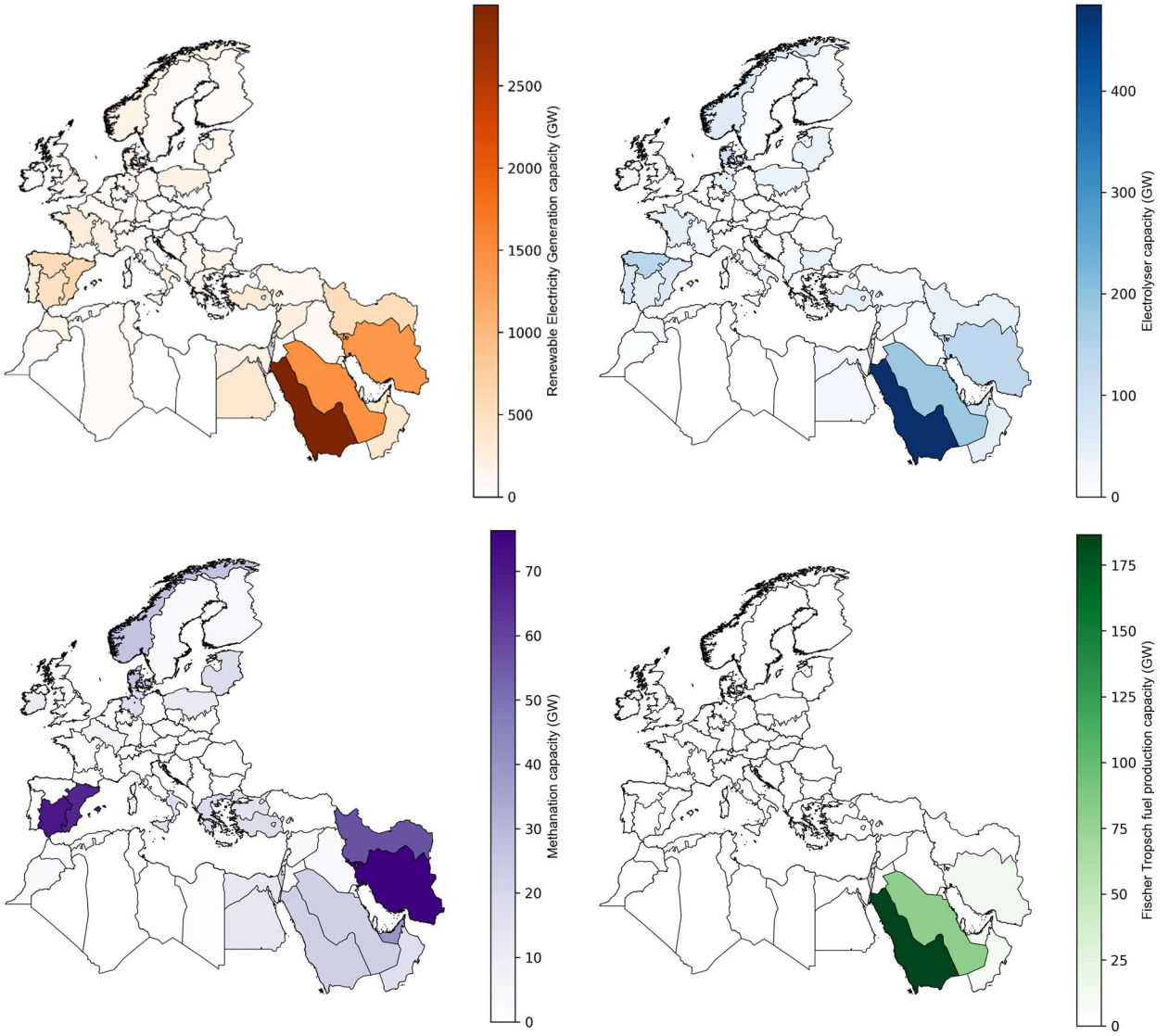

Figure 4-33 Total installed RES (top left), hydrogen (top right), methanation (bottom left) and FT fuel production (bottom right) capacities WACC (2050)

This pattern becomes even clearer when isolating the net annual flows on network links that connect MENA and Europe. Annual flows through new and retrofitted hydrogen pipelines drop strongly compared to BASE, and methane flows across the intercontinental gas backbone are reduced as well (Figure 4-37). In other words, differentiated WACC weakens the physical corridor between MENA and Europe; less energy is moved via electricity, hydrogen and methane, and more of the value chain is either reshored to Europe or confined within a few low-risk MENA exporters.

On the carrier level, FT fuels become the dominant transport medium between MENA and the EU in WACC. With export-oriented hydrogen and methane projects discouraged in high-WACC countries, direct hydrogen pipeline trade shrinks and the system leans more heavily on shipping of liquid hydrocarbons from low-risk exporters such as Saudi Arabia, reflected in an increase of FT-fuel trade by about 14%. Liquefied hydrogen shipped by sea does not play a meaningful role in any of the model variants: liquid-hydrogen flows remain negligible in BASE, in the no-pipeline configuration and under differentiated WACC. Within the cost and performance ranges assumed here, liquefied hydrogen therefore does not become a preferred option for EU-MENA trade.

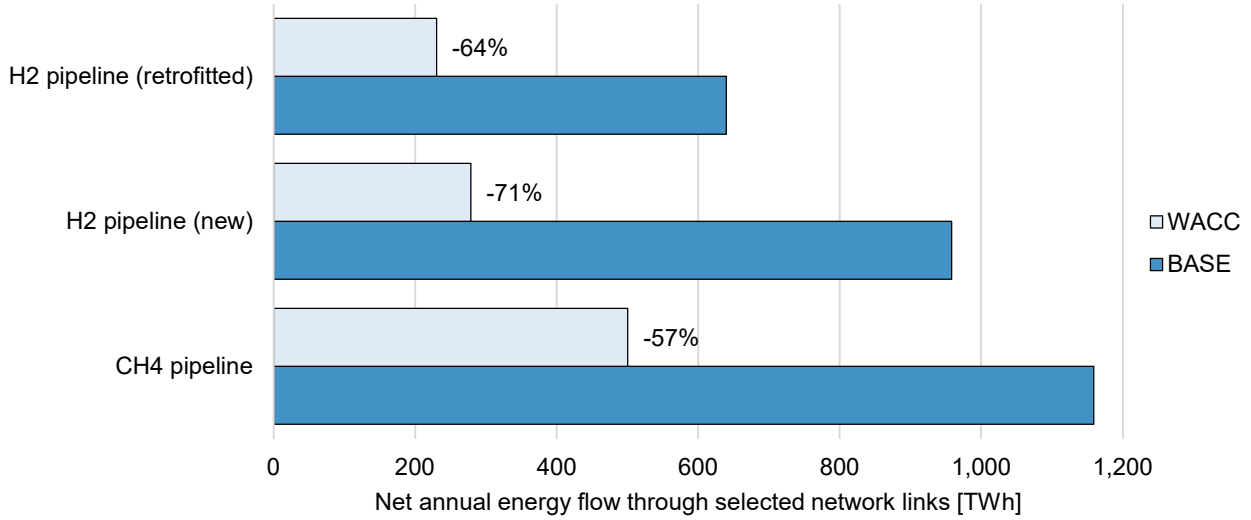

Figure 4-34 Net annual energy flow through EU-MENA network links (2050)

The cost decomposition reflects the asymmetry of these adjustments. European total system costs rise significantly by 35.1% as domestic renewable generation, electrolysis, methanation and storage capacity expanded to compensate for reduced imports. In MENA, by contrast, total system costs decline somewhat (-16.1%) despite higher WACC, because fewer capital-intensive export corridors are developed and part of the activity-related costs is offset by DAC revenues. Storage costs in MENA increase, as the region relies more on local buffering instead of cross-regional exchange, while Europe bears most of the additional investment burden. Overall, WACC leads to the highest total system cost of all scenario variants, with a TSC increase of 6.0%.

Taken together, these results answer Sub-question 3. Introducing country-specific costs of capital in the MENA region does not simply add noise around the BASE configuration; within the explored scenario space it materially alters the EU-MENA system. Higher WACC in key MENA entry countries weakens the physical corridor into Europe, reduces cross-border electricity, hydrogen and methane flows and triggers a reshoring of investment and system cost to Europe. At the same time, export-oriented activity in MENA concentrates in a small number of low-risk countries, with Saudi Arabia emerging as the main FT-fuel supplier and Iran covering its own demands. FT fuels become the dominant remaining long-distance carrier, while liquefied hydrogen does not become competitive in any of the model runs. Financing risk therefore reduces the scale and diversity of EU-MENA energy trade and redistributes costs and rents, rather than simply scaling the BASE architecture up or down.

5. Discussion

The model results suggest a clear qualitative picture under the assumptions of this thesis. Across the analysed scenarios, the cost-optimal EU-MENA system tends to be MENA-centred, with Europe remaining structurally import-dependent for synthetic methane, hydrogen and FT fuels by 2050. Cross-regional trade is economically attractive and its basic pattern survives substantial infrastructure shocks and differentiated financing conditions in the explored scenario space.

At the same time, these results are products of a specific model configuration and parameter set. They depend in particular on assumptions about technology costs and performance, water and CO_2 availability, transport cost projections, financing conditions and the evolution of CO_2 prices. This chapter therefore discusses how robust the main conclusions are to these assumptions, how they compare to findings by a study of similar scope in Krüger et al. [24], and what they imply politically for an EU-MENA energy partnership.

5.1 Uncertainty in underlying assumptions

The model uses exogenous techno-economic input data that are harmonised across regions and time. While this is necessary to keep the scenario space tractable, it also hides important uncertainties. Technology development curves and costs differ within studies, especially in the long-term after 2040. If capital or operating costs for renewable hydrogen and synfuels in MENA turn out higher than assumed, the economic advantage of shifting production south would be reduced. On the contrary, targeted political or financial support schemes could lead to an even more pronounced shift towards the MENA region. Moreover, as this thesis has shown, absolute trading volumes depend heavily on available transport infrastructure. Plans to enhance the connectivity between the EU and MENA (e.g., [76]) could lead to a further shift in network architecture.

Water and CO_2 are also stylised in the model. In reality, freshwater scarcity, competing uses and local environmental impacts could affect where electrolysers and DAC plants are accepted and how expensive they become. In the current configuration, water constraints mainly enter through additional electricity demand for SWRO. If desalination turns out significantly more expensive or socially contested, the attractiveness of some coastal production hubs and associated DAC rents might be overstated.

Transport of FT fuels and liquefied hydrogen is also only estimated based on a single cost and efficiency trajectory. Together with the penny-switching tendencies within ESOMs, liquefied hydrogen, which does not play a role according to the current findings, could become a viable transport method under a potentially only slightly different set of techno-economic assumptions.

Financial and policy assumptions

Financial assumptions are among the most influential drivers of model behaviour in this study. In the BASE configuration, all regions share a uniform 8% cost of capital. This implicitly assumes comparable risk perceptions by investors across the EU and MENA and stable long-term policy and currency conditions. Only in the WACC scenario are country-specific premia introduced for renewable, hydrogen and synfuel investments in MENA, while European projects retain the 8% rate. Even this stylised differentiation already has strong effects: it suppresses capital-intensive export projects in high-WACC MENA countries, weakens

electricity and methane trade into Europe, and shifts part of the generation and conversion chain back to European nodes (Chapter 4.3).

The WACC experiment should therefore be read less as a marginal parameter variation and more as a structural stress test. Within otherwise identical physical assumptions, changing only the cost of capital is sufficient to weaken the EU–MENA corridor, leading to a concentration of export activity into a small number of low-risk countries. This indicates that conclusions about the magnitude and distribution of hydrogen and synfuel trade are highly sensitive to how financing risks are represented, to which technologies they apply and in which regions they are allowed to vary. Because European WACC is held constant in all scenarios, the results also reflect an asymmetric treatment of risk that favours European reshoring whenever MENA risk premia are high. In reality, higher or more heterogeneous costs of capital inside Europe would narrow the gap between domestic and imported options and could restore some of the trade volumes that are lost in the WACC case.

Policy assumptions about CO_2 emission prices add another layer of abstraction. The model uses an exogenous, rising CO_2 price path applied uniformly within the system boundary and treats DAC credits symmetrically. Under this trajectory, DAC becomes a profitable activity in MENA because cheap renewable electricity combines with high CO_2 prices to generate substantial negative-cost DAC revenues. The TRANS_no_pipeline case illustrates that these revenues are large enough to offset part of MENA's activity-related costs, and that the net total system cost can decrease even as the gross emissions bill rises. The qualitative consideration in Chapter 4.2.3 suggests that if CO_2 prices were uniformly lowered, two opposing effects would emerge: residual emissions would become cheaper, but DAC credits would lose value. In a configuration where DAC is already deployed at scale and is net-beneficial, the loss of DAC revenue dominates.

Regional differentials in CO_2 prices could further complicate the picture. If CO_2 prices in MENA were substantially lower than in Europe, the incentive to deploy DAC in MENA would weaken, and emission-intensive stages of the value chain might shift back towards high-price European nodes where CO_2 avoidance is more strongly rewarded. Given that only a subset of MENA countries currently has government-administered carbon crediting mechanisms in place, a wide range of effective CO_2 cost levels across the EU-MENA system appears plausible [75]. In such settings, DAC deployment, carrier choice and the regional distribution of rents would be expected to differ markedly from the stylised uniform-price case represented here.

Taken together, the WACC and CO_2 assumptions used in this thesis should be viewed as defining one corner of a broader parameter space. Uniform financing conditions in the BASE configuration, a single differentiated-WACC stress test in MENA and a high and harmonised CO_2 price path favour large-scale DAC deployment. Within that space, the MENA-centred trade architecture emerges robustly, but the WACC and CO_2 experiments clearly show that the scale of trade and the allocation of costs and rents are highly sensitive to how these levers are set.

Model configuration and structural uncertainty

Regional aggregation and the central-planner formulation omit important real-world constraints. Local acceptance, permitting times, labour and supply-chain bottlenecks are not modelled explicitly; they are only indirectly approximated via generic build-rate limits for network infrastructure. This tends to represent an optimistic upper bound on the feasible speed

and spatial concentration of infrastructure deployment. Similarly, demand paths for hydrogen and synfuels are taken from external scenario datasets rather than emerging endogenously from technology competition in end-use sectors. As a result, fuel switching patterns and final energy demand levels reflect prior scenario assumptions instead of price- and cost-driven substitution within the model, limiting the scope for feedbacks between infrastructure expansion, fuel prices and sectoral technology choice.

5.2 Results in the context of a comparison study by Krüger et al.

When comparing the results of this study against Krüger et al. [24], comparable storylines emerge, though the scale differs. In a first step, it is important to highlight the differences between the two studies. Krüger et al. model the system under greenfield conditions, with 25 representative time steps per year and only 13 modelling regions. Furthermore, Krüger et al. capture only industry and transportation demand, compared to this study's more comprehensive scope.

Nonetheless, in the baseline cases without differentiated finance risks, both models produce a decisively MENA-centred architecture, with Europe relying heavily (82%) on synfuel imports. While the total European import dependency is lower in this study (48%), it still implies a strong structural dependence. As in this study, electricity imports play only a very minor role. However, Krüger et al. conclude that electricity transport costs offset MENA production advantages, leading to electricity production close to the sink, whereas this study points more towards infrastructure bottlenecks limiting EU-MENA electricity trade. Regarding the specific export countries, both models identify Algeria, Egypt and the Middle Eastern countries as the main exporters.

The handling of investment risk marks the clearest quantitative difference. In Krüger et al., introducing risk-adjusted financing costs reduces Europe's import quota from 82% to 0% in the most pessimistic case. In this thesis, by contrast, higher WACC only reduces cross-regional energy flows but does not eliminate trade. Long-distance energy trade in FT fuels even increases by 14%.

Taken together, the two studies show that while a MENA-based corridor often appears cost-effective, its strength is highly sensitive to financing assumptions.

5.3 Political relevance for an EU-MENA energy partnership

Politically, the combined evidence points to structural interdependence between the EU and MENA in many plausible futures. In the BASE configuration Europe remains a substantial net importer of synthetic fuels in 2050. Decarbonisation changes the origin and composition of energy imports, but does not automatically remove dependence on external suppliers. For MENA, the results suggest that a role as renewable-fuel exporter is economically attractive given its resource advantage, land availability and proximity to Europe.

The AUTARKY case illustrates the trade-offs of pursuing strong self-sufficiency. Europe can minimise external dependence by expanding domestic renewables, electrolysis and storage, at the trade-off of higher system costs. The question is therefore less whether autarky is technically possible and more whether the additional cost and lost partnership opportunities are politically preferable.

Financing conditions emerge as a central political lever. In the model, higher WACC in MENA exporters reduces export volumes, weakens corridors and shifts system costs towards Europe. In reality, risk premia are endogenous to policy: they depend on regulatory stability,

contract enforcement, credit support and diplomatic relations. If EU and MENA actors design risk-sharing instruments that lower the cost of capital for clean-energy investments in exporting countries, many of the benefits of a MENA-centred architecture remain accessible at lower total cost. Conversely, if perceived risks remain high, much of the cost-efficient trade potential identified here may not materialise, regardless of technical potential.

Finally, the modelling approach abstracts from non-economic dimensions such as social acceptance, distributional justice, environmental impacts beyond CO_2 and security concerns. An EU-MENA energy partnership, however, cannot be evaluated on techno-economic grounds alone. The corridor architectures derived in this thesis should therefore be read as inputs into a broader political debate, not as prescriptions. They provide a structured picture of what is technically and economically possible under specific assumptions; whether and how such architectures are pursued will depend on how Europe and MENA balance cost efficiency against sovereignty, resilience, equity and development goals, as well as accounting schemes at the European border.

The key message from this discussion is that, within the scenario variants explored here, an EU-MENA hydrogen and synfuel partnership is structurally plausible and, in many cases, economically attractive. However, its eventual scale, carrier mix and cost distribution are likely to depend less on physical resource constraints than on how infrastructure expansion, financing risk and political priorities are managed in practice.

6. Conclusion

This thesis has assessed long-term hydrogen and synfuel trade between the EU and the MENA region under alternative infrastructure and financing conditions. Using a brownfield energy system optimisation model with a broad carrier portfolio and a spatially explicit electricity and gas network, it has examined how a cost-minimising central planner would configure EU-MENA energy trade and how sensitive this configuration is to transport constraints and differentiated costs of capital.

Within the explored scenario space, the trends across all scenarios point towards the same overarching insights. Under uniform financing conditions and unconstrained infrastructure development, the cost-optimal energy system for the EU is MENA-centred. Superior solar and, to a lesser extent, wind resources make MENA the most economical location for renewable electricity generation, hydrogen production and synfuel conversion. Europe remains structurally import-dependent in this least-cost configuration. By 2050, hydrogen, synthetic methane and Fischer-Tropsch fuels are imported via interconnected gas and hydrogen pipelines, shipping corridors and land links.

The resulting architecture assigns distinct roles to the main energy carriers. Hydrogen is primarily used to redistribute energy within and between regions through a retrofitted intra-European backbone and selected cross-regional links. Fischer-Tropsch fuels act as long-distance carriers that bridge bottlenecks in the grid and gas network and supply hard-to-abate sectors via shipping and land logistics. Synthetic methane provides large-scale seasonal flexibility by exploiting cavern storage to absorb summer surpluses and meet winter peaks. Electricity remains mostly locally consumed but underpins all conversion chains. Taken together, these outcomes answer Sub-question 1: under favourable infrastructure and financing assumptions, a MENA-centred, import-dependent architecture is the cost-optimal configuration for the EU.

The AUTARKY scenario shows that European self-sufficiency is technically feasible once cross-regional molecular trade is removed. However, it also makes explicit the associated economic and structural costs. Total system expenditure increases relative to the BASE case, Europe incurs a sizeable autarky penalty and the system shifts towards a more inward-looking configuration. Hydrogen's role changes from a spatial redistribution vector to a seasonal storage medium, supported by expanded cavern capacity and a larger domestic renewable fleet. Imports are replaced by local generation, conversion and storage.

Transport constraints further reshape, but do not overturn, this picture. Delaying the roll-out of new hydrogen pipelines reduces long-distance hydrogen trade and relocates more generation, conversion and storage assets to Europe. Removing cross-regional hydrogen pipelines altogether forces the system to rely more heavily on legacy natural-gas infrastructure and FT-fuel shipping, with FT fuels taking over a larger share of long-distance transport. In both cases, EU-MENA corridors are retained. Overall, infrastructure constraints reduce the scale of cross-regional exchange and alter the carrier mix, while preserving the fundamental economic rationale for trade. This addresses Sub-question 2: hydrogen pipeline corridors and FT-fuel shipping are central enablers of the cost-optimal architecture, and constraining them systematically raises system costs and reshores investment towards Europe.

Introducing country-specific costs of capital in MENA materially changes the optimal system. Higher WACC in key MENA entry countries weakens export-oriented projects there and shift new investment towards lower-risk MENA producers, especially Saudi Arabia, while Europe

accelerates domestic build-out of PV, wind, electrolysis, methanation and hydrogen storage. Cross-border electricity, hydrogen and methane flows decline, FT fuels become the only remaining long-distance carrier and liquefied hydrogen does not emerge as a competitive option in any variant. The WACC scenario produces the highest total system cost of all cases. Sub-question 3 can therefore be answered as follows: differentiated financing conditions in MENA do not eliminate EU-MENA trade, but they significantly reduce its scale, concentrate export activity in a few low-risk countries and reallocate costs and investment back towards Europe.

A central insight from this study is that, across a wide range of explored assumptions, long-term EU-MENA trade in hydrogen and synfuels is structurally attractive from a system-cost perspective. Good renewable resources in MENA, combined with existing and expandable transmission and transport links, are sufficient to generate a MENA-centred architecture in cost-optimal models. At the same time, this implies a persistent European import dependence: in the BASE configuration, several EU member states retain high import shares for synthetic fuels in 2050, even though the aggregate EU import dependency falls below today's levels. Decarbonisation therefore changes the origin and composition of imports rather than removing dependence on external suppliers.

From a policy perspective, three implications follow. First, an EU-MENA energy partnership can form an efficient component of a European decarbonisation strategy, but only if infrastructure development and permitting keep pace with cost-optimal deployment pathways. Second, pursuing strong autarky has a non-trivial cost: it requires substantially higher investment in domestic generation, conversion and storage and reduces opportunities for MENA to use hydrogen and synfuels as a diversification strategy. Third, financing conditions in potential exporter countries are a critical bottleneck. Without instruments that lower the cost of capital, many technically attractive export projects may not materialise, and the overall system becomes more expensive and more EU-centric.

Methodologically, the thesis demonstrates the value of combining a brownfield network representation, a broad carrier portfolio and regionally differentiated financing assumptions within a single integrated energy-system model. It shows that assumptions about existing infrastructure and financial risk are not peripheral details but can materially alter system-optimal outcomes. Future work on hydrogen and synfuel trade should therefore avoid purely greenfield representations and uniform financing assumptions and instead embed trade analyses in more holistic network and financing contexts.

Within these limits, the thesis provides a structured answer to the main research question: under the assumptions used here, the cost-optimal architecture for EU-MENA hydrogen and synfuel trade up to 2050 is a MENA-centred system in which Europe remains a substantial net importer and hydrogen, methane and FT fuels play distinct roles along shared corridors. This architecture is robust to a range of infrastructure and financing shocks, but its precise scale, carrier mix and cost distribution depend sensitively on pipeline availability, shipping options, CO_2-price trajectories and, above all, the cost of capital in exporting countries. The corridors emerging from the optimisation should therefore be regarded as candidate architectures rather than blueprints, offering a quantitative benchmark against which future policy, investment and diplomacy around EU-MENA hydrogen partnerships can be assessed.

References

[1] H. Lee *et al.,* “IPCC, 2023: Climate Change 2023: Synthesis Report. Contribution of Working Groups I, II and III to the Sixth Assessment Report of the Intergovernmental Panel on Climate Change [Core Writing Team, H. Lee and J. Romero (eds.)]. IPCC, Geneva, Switzerland,” 2023.

[2] European Commission and Directorate-General for Climate Action, *Going climate-neutral by 2050: A strategic long-term vision for a prosperous, modern, competitive and climate-neutral EU economy*: Publications Office, 2019.

[3] R. Béres, W. Nijs, A. Boldrini, and M. van den Broek, “Will hydrogen and synthetic fuels energize our future? Their role in Europe's climate-neutral energy system and power system dynamics,” *Applied Energy*, vol. 375, p. 124053, 2024, doi: 10.1016/j.apenergy.2024.124053.

[4] A. Nuñez-Jimenez and N. de Blasio, “Competitive and secure renewable hydrogen markets: Three strategic scenarios for the European Union,” *International Journal of Hydrogen Energy*, vol. 47, no. 84, pp. 35553–35570, 2022, doi: 10.1016/j.ijhydene.2022.08.170.

[5] E. Curmi *et al.,* “Hard to Abate Sectors & Emissions II: The Road to Decarbonization,” Jul. 2024. Accessed: Nov. 4 2025. [Online]. Available: https://www.citigroup.com/global/insights/hard-to-abate-sectors-and-emissions-ii

[6] European Commission, *Renewable Hydrogen.* [Online]. Available: https://energy.ec.europa.eu/topics/eus-energy-system/hydrogen/renewable-hydrogen_en (accessed: Oct. 9 2025).

[7] N. Johnson, M. Liebreich, D. M. Kammen, P. Ekins, R. McKenna, and I. Staffell, “Realistic roles for hydrogen in the future energy transition,” *Nat. Rev. Clean Technol.*, vol. 1, no. 5, pp. 351–371, 2025, doi: 10.1038/s44359-025-00050-4.

[8] European Commission, *Hydrogen.* [Online]. Available: https://energy.ec.europa.eu/topics/eus-energy-system/hydrogen_en (accessed: Aug. 27 2025).

[9] European Commission, “A hydrogen strategy for a climate-neutral Europe,” Brussels, Jul. 2020.

[10] M. Frömel, F. Sensfuß, B. Lux, G. Deac, and W. Männer, “Langfristszenarien für die Transformation des Energiesystems in Deutschland: Treibhausgasneutrale Orientierungsszenarien - Modul Energieangebot,” Fraunehofer-Institut für System- und Innovationsforschung; Consentec GmbH, Karlsruhe, Mar. 2025. Accessed: Aug. 27 2025. [Online]. Available: https://langfristszenarien.de/enertile-explorer-wAssets/docs/LFS3_O45-Energieangebot_final.pdf

[11] M. Wietschel, B. Weißenburger, J. Wachsmith, and V. Paul Müller, “What do we know about importing green hydrogen and its derivatives and what can be derived from this for Germany’s import strategy,” Fraunehofer-Institut für System- und Innovationsforschung, Karlsruhe, HYPAT Position paper 1/2024, Feb. 2024. Accessed: Aug. 27 2025.

[12] L. Genge, F. Scheller, and F. Müsgens, “Supply costs of green chemical energy carriers at the European border: A meta-analysis,” *International Journal of Hydrogen Energy*, vol. 48, no. 98, pp. 38766–38781, 2023, doi: 10.1016/j.ijhydene.2023.06.180.

[13] F. Dalla Longa and B. van der Zwaan, “Autarky penalty versus system cost effects for Europe of large-scale renewable energy imports from North Africa,” *Energy Strategy Reviews*, vol. 51, p. 101289, 2024, doi: 10.1016/j.esr.2023.101289.

[14] M. C. Pinto, S. G. Simões, and P. Fortes, “How can green hydrogen from North Africa support EU decarbonization? Scenario analyses on competitive pathways for trade,” *International Journal of Hydrogen Energy*, vol. 79, pp. 305–318, 2024, doi: 10.1016/j.ijhydene.2024.06.395.
[15] L. Sens, U. Neuling, K. Wilbrand, and M. Kaltschmitt, “Conditioned hydrogen for a green hydrogen supply for heavy duty-vehicles in 2030 and 2050 – A techno-economic well-to-tank assessment of various supply chains,” *International Journal of Hydrogen Energy*, vol. 52, pp. 1185–1207, 2024, doi: 10.1016/j.ijhydene.2022.07.113.
[16] A. Fattahi, F. Dalla Longa, and B. van der Zwaan, “Opportunities of hydrogen and ammonia trade between Europe and MENA,” *International Journal of Hydrogen Energy*, vol. 83, pp. 967–974, 2024, doi: 10.1016/j.ijhydene.2024.08.021.
[17] B. Lux, M. Frömel, G. Resch, F. Hasengst, and F. Sensfuß, “Effects of different renewable electricity diffusion paths and restricted european cooperation on Europe's hydrogen supply,” *Energy Strategy Reviews*, vol. 56, p. 101589, 2024, doi: 10.1016/j.esr.2024.101589.
[18] B. Lux, J. Gegenheimer, K. Franke, F. Sensfuß, and B. Pfluger, “Supply curves of electricity-based gaseous fuels in the MENA region,” *Computers & Industrial Engineering*, vol. 162, p. 107647, 2021, doi: 10.1016/j.cie.2021.107647.
[19] M. Hoffmann *et al.,* “A review of mixed-integer linear formulations for framework-based energy system models,” *Advances in Applied Energy*, vol. 16, p. 100190, 2024, doi: 10.1016/j.adapen.2024.100190.
[20] F. Egli, B. Steffen, and T. S. Schmidt, “Bias in energy system models with uniform cost of capital assumption,” *Nature communications*, vol. 10, no. 1, p. 4588, 2019, doi: 10.1038/s41467-019-12468-z.
[21] J. Terrapon-Pfaff, J. Braun, S. R. Ersoy, M. Prantner, J. Kern, and P. Viebahn, “Country risk impacts on export costs of green hydrogen and its synthetic downstream products from the Middle East and North Africa,” *Front. Energy Res.*, vol. 13, 2025, doi: 10.3389/fenrg.2025.1546876.
[22] M. Taylor, P. Beiter, and F. Egli, “The cost of financing for renewable power,” Abu Dhabi, May. 2023. Accessed: Sep. 1 2025. [Online]. Available: https://www.irena.org/Publications/2023/May/The-cost-of-financing-for-renewable-power
[23] M. Moritz, M. Schönfisch, and S. Schulte, “Estimating global production and supply costs for green hydrogen and hydrogen-based green energy commodities,” *International Journal of Hydrogen Energy*, vol. 48, no. 25, pp. 9139–9154, 2023, doi: 10.1016/j.ijhydene.2022.12.046.
[24] C. Krüger, L. Doré, T. Janßen, M. Saurat, A. Nebel, and P. Viebahn, “Providing the transport sector in Europe with fossil free energy - a model-based analysis under consideration of the MENA region,” *Front. Energy Res.*, vol. 13, 2025, doi: 10.3389/fenrg.2025.1524907.
[25] S. Pfenninger, A. Hawkes, and J. Keirstead, “Energy systems modeling for twenty-first century energy challenges,” *Renewable and Sustainable Energy Reviews*, vol. 33, pp. 74–86, 2014, doi: 10.1016/j.rser.2014.02.003.
[26] M. Wetzel *et al.,* “REMix: A GAMS-based framework for optimizing energy system models,” *JOSS*, vol. 9, no. 99, p. 6330, 2024, doi: 10.21105/joss.06330.
[27] M. Wetzel, H. C. Gils, and V. Bertsch, “Green energy carriers and energy sovereignty in a climate neutral European energy system,” *Renewable Energy*, vol. 210, pp. 591–603, 2023, doi: 10.1016/j.renene.2023.04.015.

[28] M. Wetzel, H. C. Gils, and V. Bertsch, “From ambition to reality: The impact of limited capacity expansion rates on the transformation pathway to a climate-neutral European energy system,” *Submitted to Renewable Energy*, Jun. 2025.
[29] European Network of Transmission System Operator for Gas, *European Gas Flow Dashboard.* [Online]. Available: https://gasdashboard.entsog.eu/ (accessed: Sep. 11 2025).
[30] P. R. Shukla, J. Skea, and A. R. Reisinger, Eds., *Climate change 2022: Mitigation of climate change*. Geneva: IPCC, 2022. [Online]. Available: https://www.ipcc.ch/report/ar6/wg3/downloads/report/IPCC_AR6_WGIII_FullReport.pdf
[31] T. Junne, “Constructing and evaluating energy futures: life cycle environmental impacts, material demand and transparency of energy scenarios,” 2021.
[32] A. Alkhalidi, H. Battikhi, M. Almanasreh, and M. K. Khawaja, “A review of renewable energy status and regulations in the MENA region to explore green hydrogen production – Highlighting the water stress effect,” *International Journal of Hydrogen Energy*, vol. 67, pp. 898–911, 2024, doi: 10.1016/j.ijhydene.2024.01.249.
[33] N. Nesterenko *et al.,* “Methane-to-chemicals: a pathway to decarbonization,” *National science review*, vol. 10, no. 9, nwad116, 2023, doi: 10.1093/nsr/nwad116.
[34] S. Bube, N. Bullerdiek, S. Voß, and M. Kaltschmitt, “Kerosene production from power-based syngas – A technical comparison of the Fischer-Tropsch and methanol pathway,” *Fuel*, vol. 366, p. 131269, 2024, doi: 10.1016/j.fuel.2024.131269.
[35] *Commission Delegated Regulation (EU) 2023/1185 of 10 February 2023 supplementing Directive (EU) 2018/2001 of the European Parliament and of the Council by establishing a minimum threshold for greenhouse gas emissions savings of recycled carbon fuels and by specifying a methodology for assessing greenhouse gas emissions savings from renewable liquid and gaseous transport fuels of non-biological origin and from recycled carbon fuels*, 2023. Accessed: Oct. 6 2025. [Online]. Available: https://eur-lex.europa.eu/eli/reg_del/2023/1185/oj
[36] J. Hampp, M. Düren, and T. Brown, “Import options for chemical energy carriers from renewable sources to Germany,” *PloS one*, vol. 18, no. 2, e0262340, 2023, doi: 10.1371/journal.pone.0281380.
[37] InflationTool, *Inflation calculator: Euro.* [Online]. Available: https://www.inflation-tool.com/euro (accessed: Sep. 30 2025).
[38] European Commission, *A European strategic long-term vision for a prosperous, modern, competitive and climate neutral economy*. Brussels, 2018.
[39] N. Wulff *et al.,* “Energy system implications of demand scenarios and supply strategies for renewable transportation fuels,” *Energy Strategy Reviews*, vol. 58, p. 101606, 2025, doi: 10.1016/j.esr.2024.101606.
[40] J. Braun, T. Pregger, J. Kern, and Y. Scholz, “Costs and export potentials of green synthetic fuels produced in the MENA region,” *Front. Energy Res.*, vol. 13, 2025, doi: 10.3389/fenrg.2025.1550419.
[41] R. G. Sargent, “Verification and validation of simulation models,” *Journal of Simulation*, vol. 7, no. 1, pp. 12–24, 2013, doi: 10.1057/jos.2012.20.
[42] A. Pluta, W. Medjroubi, J. Diettrich, J. Dasenbrock, and H.-P. Tetens, “SciGRID_gas -- Data Model of the European Gas Transport Network,” 2022.
[43] B. Xiong, D. Fioriti, F. Neumann, I. Riepin, and T. Brown, “Modelling the high-voltage grid using open data for Europe and beyond,” *Scientific data*, vol. 12, no. 1, p. 277, 2025, doi: 10.1038/s41597-025-04550-7.

[44] World Ports Organization, *Worlports.org.* [Online]. Available: https://www.worldports.org/ (accessed: Oct. 11 2025).
[45] J. Gaffuri and J. Korhonen, *SeaRoute*, 2022. Accessed: Oct. 9 2025. [Online]. Available: https://github.com/eurostat/searoute
[46] S. Ramakrishnan, M. Delpisheh, C. Convery, D. Niblett, M. Vinothkannan, and M. Mamlouk, “Offshore green hydrogen production from wind energy: Critical review and perspective,” *Renewable and Sustainable Energy Reviews*, vol. 195, p. 114320, 2024, doi: 10.1016/j.rser.2024.114320.
[47] The Engineering ToolBox, *Higher Calorific Values of Common Fuels: Reference & Data.* [Online]. Available: https://www.engineeringtoolbox.com/fuels-higher-calorific-values-d_169.html (accessed: Oct. 4 2025).
[48] A. Soler *et al.,* “E-Fuels: A techno-economic assessment of European domestic production and imports towards 2050: Update,” Brussels, Mar. 2024. Accessed: Sep. 18 2025. [Online]. Available: https://www.concawe.eu/publication/e-fuels-a-techno-economic-assessment-of-european-domestic-production-and-imports-towards-2050-update/
[49] Danish Energy Agency, “Renewable fuels: Technology descriptions and projections for long-term energy system planning.,” Copenhagen, Aug. 2016.
[50] C. Bollmeyer *et al.,* “Towards a high-resolution regional reanalysis for the European CORDEX domain,” *Quart J Royal Meteoro Soc*, vol. 141, no. 686, pp. 1–15, 2015, doi: 10.1002/qj.2486.
[51] J. Walter, L. Fischer, S. Venghaus, and A. Moser, “Integrating water availability for electrolysis into energy system modeling,” *Advances in Applied Energy*, vol. 17, p. 100208, 2025, doi: 10.1016/j.adapen.2025.100208.
[52] S. Kuzma *et al.,* “Aqueduct 4.0: Updated Decision-Relevant Global Water Risk Indicators,” *WRIPUB*, 2023, doi: 10.46830/writn.23.00061.
[53] U. Caldera, D. Bogdanov, and C. Breyer, “Local cost of seawater RO desalination based on solar PV and wind energy: A global estimate,” *Desalination*, vol. 385, pp. 207–216, 2016, doi: 10.1016/j.desal.2016.02.004.
[54] H. E. Garcia *et al.,* “World Ocean Atlas 2023, Volume 3: Dissolved Oxygen, Apparent Oxygen Utilization, and Dissolved Oxygen Saturation,” 2024.
[55] U. Caldera and C. Breyer, “Learning Curve for Seawater Reverse Osmosis Desalination Plants: Capital Cost Trend of the Past, Present, and Future,” *Water Resources Research*, vol. 53, no. 12, pp. 10523–10538, 2017, doi: 10.1002/2017WR021402.
[56] P. Schmidt, V. Batteiger, A. Roth, W. Weindorf, and T. Raksha, “Power-to-Liquids as Renewable Fuel Option for Aviation: A Review,” *Chemie Ingenieur Technik*, vol. 90, 1-2, pp. 127–140, 2018, doi: 10.1002/cite.201700129.
[57] A. Galadima and O. Muraza, “From synthesis gas production to methanol synthesis and potential upgrade to gasoline range hydrocarbons: A review,” *Journal of Natural Gas Science and Engineering*, vol. 25, pp. 303–316, 2015, doi: 10.1016/j.jngse.2015.05.012.
[58] Danish Energy Agency, “Carbon Capture, transport and storage: Technology descriptions and projections for long-term energy system planning.,” Copenhagen, Nov. 2021.
[59] H. Basma and F. Rodríguez, “A total cost of ownership comparison of truck decarbonization pathways in Europe,” The International Council on Clean Transportation, Nov. 2023. Accessed: Oct. 10 2025. [Online]. Available: https://theicct.org/publication/total-cost-ownership-trucks-europe-nov23/

[60] S. Yang, *What is the price of an oil tanker trailer?* [Online]. Available: https://www.cncdcryotank.com/blog/what-is-the-price-of-an-oil-tanker-trailer-744172.html (accessed: Oct. 10 2025).
[61] M. Hurskainen and J. Ihonen, “Techno-economic feasibility of road transport of hydrogen using liquid organic hydrogen carriers,” *International Journal of Hydrogen Energy*, vol. 45, no. 56, pp. 32098–32112, 2020, doi: 10.1016/j.ijhydene.2020.08.186.
[62] *On the harmonisation of certain social legislation relating to road transport: Regulation (EC) No 561/2006*, 2006. Accessed: Oct. 11 2025. [Online]. Available: https://eur-lex.europa.eu/legal-content/EN/TXT/?uri=CELEX%3A02006R0561-20200820
[63] S. Tamhankar, *Terminal Operations for Tube Trailer and Liquid Tanker Filling: Status, Challenges and R&D Needs: DOE Hydrogen Transmission and Distribution Workshop.* [Online]. Available: https://www.energy.gov/sites/default/files/2014/07/f17/fcto_2014_h2_trans_dist_wkshp_tamhankar.pdf (accessed: Oct. 11 2025).
[64] Mærsk Mc-Kinney Møller Center for Zero Carbon Shipping, *Total Cost of Ownership (TCO) model*. Copenhagen, 2021. Accessed: Oct. 12 2025. [Online]. Available: https://www.zerocarbonshipping.com/publications/calculate-total-cost-of-ownership-tco-for-decarbonization-of-vessels
[65] A. N. Alkhaledi, S. Sampath, and P. Pilidis, “A hydrogen fuelled LH2 tanker ship design,” *Ships and Offshore Structures*, vol. 17, no. 7, pp. 1555–1564, 2022, doi: 10.1080/17445302.2021.1935626.
[66] G. Bandoc, R. Prăvălie, C. Patriche, and M. Degeratu, “Spatial assessment of wind power potential at global scale. A geographical approach,” *Journal of Cleaner Production*, vol. 200, pp. 1065–1086, 2018, doi: 10.1016/j.jclepro.2018.07.288.
[67] D. Franzmann *et al.,* “Green hydrogen cost-potentials for global trade,” *International Journal of Hydrogen Energy*, vol. 48, no. 85, pp. 33062–33076, 2023, doi: 10.1016/j.ijhydene.2023.05.012.
[68] P. Lopion, P. Markewitz, D. Stolten, and M. Robinius, “Cost Uncertainties in Energy System Optimization Models: A Quadratic Programming Approach for Avoiding Penny Switching Effects,” *Energies*, vol. 12, no. 20, p. 4006, 2019, doi: 10.3390/en12204006.
[69] Gas Infrastructure Europe, *Aggregated Gas Storage Inventory.* [Online]. Available: https://agsi.gie.eu/ (accessed: Nov. 12 2025).
[70] B. van der Zwaan, S. Lamboo, and F. Dalla Longa, “Timmermans’ dream: An electricity and hydrogen partnership between Europe and North Africa,” *Energy Policy*, vol. 159, p. 112613, 2021, doi: 10.1016/j.enpol.2021.112613.
[71] European Commission, *Dashboard for EU energy bill 2024.* [Online]. Available: https://energy.ec.europa.eu/data-and-analysis/energy-prices-and-costs-europe/dashboard-eu-energy-bill-2024_en (accessed: Nov. 16 2025).
[72] H. E. Delgado *et al.,* “Techno-economic analysis and life cycle analysis of e-fuel production using nuclear energy,” *Journal of CO2 Utilization*, vol. 72, p. 102481, 2023, doi: 10.1016/j.jcou.2023.102481.
[73] M. Fasihi, D. Bogdanov, and C. Breyer, “Techno-Economic Assessment of Power-to-Liquids (PtL) Fuels Production and Global Trading Based on Hybrid PV-Wind Power Plants,” *Energy Procedia*, vol. 99, pp. 243–268, 2016, doi: 10.1016/j.egypro.2016.10.115.
[74] Eurostat, “Simplified energy balances,” 2022.
[75] International Bank of Reconstruction and Redevelopment and International Development Association, *State and Trends of Carbon Pricing Dashboard.* [Online]. Available:

https://carbonpricingdashboard.worldbank.org/credits/instrument-detail (accessed: Nov. 19 2025).
[76] H. Schult *et al.,* “Advancing Cross-Border Energy Infrastructure between Europe and the MENA region,” Berlin, Mar. 2025. Accessed: Nov. 23 2025. [Online]. Available: https://energypartnership-uae.org/fileadmin/vae/publications/EU-MENA_Energy_Infrastructure_Guidehouse.pdf
[77] K. Alanazi, S. Mittal, A. Hawkes, and N. Shah, “Renewable hydrogen trade in a global decarbonised energy system,” *International Journal of Hydrogen Energy*, vol. 101, pp. 712–730, 2025, doi: 10.1016/j.ijhydene.2024.12.452.
[78] G. Brändle, M. Schönfisch, and S. Schulte, “Estimating long-term global supply costs for low-carbon hydrogen,” *Applied Energy*, vol. 302, p. 117481, 2021, doi: 10.1016/j.apenergy.2021.117481.
[79] B. Breitschopf *et al., The role of renewable H2 import & storage to scale up the EU deployment of renewable H2*. Luxembourg, Luxembourg: Publications Office of the European Union, 2022. [Online]. Available: https://op.europa.eu/o/opportal-service/download-handler?identifier=7ab70e32-a5a0-11ec-83e1-01aa75ed71a1&format=pdf&language=en&productionSystem=cellar&part=
[80] P. S.-L. Chen, H. Fan, and N. Abdussamie, “Evaluation of hydrogen shipping cost for potential trade routes,” *WMU J Marit Affairs*, vol. 24, no. 2, pp. 315–338, 2025, doi: 10.1007/s13437-025-00365-w.
[81] R. Dickson, A. Abbas, Y. Lee, J. Liu, and H. Niaz, “A global perspective on solar-driven hydrogen economy and 2050 carbon neutrality,” *Chemical Engineering Journal*, vol. 516, p. 164144, 2025, doi: 10.1016/j.cej.2025.164144.
[82] T. Galimova, M. Fasihi, D. Bogdanov, and C. Breyer, “Feasibility of green ammonia trading via pipelines and shipping: Cases of Europe, North Africa, and South America,” *Journal of Cleaner Production*, vol. 427, p. 139212, 2023, doi: 10.1016/j.jclepro.2023.139212.
[83] V. Guillot and E. Assoumou, “Power and green hydrogen trade potential between North African and European countries: Conditions, challenges, and sustainability prospects,” *Applied Energy*, vol. 382, p. 125209, 2025, doi: 10.1016/j.apenergy.2024.125209.
[84] Hydrogen Import Coalition, “Shipping sun and wind to Belgium is key in climate neutral economy,” Jan. 2021. Accessed: Sep. 2 2025. [Online]. Available: https://www.demegroup.com/sites/default/files/2021-01/Hydrogen%20Import%20Coalition%20Final%20Report.pdf
[85] International Energy Agency, *The Future of Hydrogen*. Paris: OECD, 2019. Accessed: Sep. 2 2025.
[86] M. Jensterle, J. Schröder, F. Wahabzada, and K. Crone, “Grüner Wasserstoff: Internationale Kooperationspotenziale für Deutschland: Kurzanalyse zu ausgewählten Aspekten potenzieller Nicht-EU-Partnerländer,” Oct. 2019. Accessed: Sep. 2 2025. [Online]. Available: https://adelphi.de/en/system/files/mediathek/bilder/20191002%20Wasserstoff_Partnerl%C3%A4nder_Kurzgutachten%20FINAL.pdf
[87] V. L. Meca, R. d’Amore-Domenech, A. Crucelaegui, and T. J. Leo, “Large-Scale Maritime Transport of Hydrogen: Economic Comparison of Liquid Hydrogen and Methanol,” *ACS Sustainable Chemistry & Engineering*, vol. 10, no. 13, pp. 4300–4311, 2022, doi: 10.1021/acssuschemeng.2c00694.
[88] J. Neumann *et al.,* “Techno-economic assessment of long-distance supply chains of energy carriers: Comparing hydrogen and iron for carbon-free electricity generation,”

Applications in Energy and Combustion Science, vol. 14, p. 100128, 2023, doi: 10.1016/j.jaecs.2023.100128.
[89] F. Neumann, J. Hampp, and T. Brown, “Green energy and steel imports reduce Europe's net-zero infrastructure needs,” *Nature communications*, vol. 16, no. 1, p. 5302, 2025, doi: 10.1038/s41467-025-60652-1.
[90] M. Niermann, S. Timmerberg, S. Drünert, and M. Kaltschmitt, “Liquid Organic Hydrogen Carriers and alternatives for international transport of renewable hydrogen,” *Renewable and Sustainable Energy Reviews*, vol. 135, p. 110171, 2021, doi: 10.1016/j.rser.2020.110171.
[91] J. Perner, M. Unteutsch, and A. Lövenich, “Die zukünftigen Kosten strombasierter synthetischer Brennstoffe,” Agora Verkehrswende; Agora Energiewende; Frontier Economics, Mar. 2018. Accessed: Sep. 2 2025. [Online]. Available: https://www.agora-energiewende.de/fileadmin/Projekte/2017/SynKost_2050/Agora_SynCost-Studie_WEB.pdf
[92] T. H. Roos, “The cost of production and storage of renewable hydrogen in South Africa and transport to Japan and EU up to 2050 under different scenarios,” *International Journal of Hydrogen Energy*, vol. 46, no. 72, pp. 35814–35830, 2021, doi: 10.1016/j.ijhydene.2021.08.193.
[93] P. Runge, C. Sölch, J. Albert, P. Wasserscheid, G. Zöttl, and V. Grimm, “Economic Comparison of Electric Fuels Produced at Excellent Locations for Renewable Energies: A Scenario for 2035,” *SSRN Journal*, 2020, doi: 10.2139/ssrn.3623514.
[94] M. Sayer, A. Ajanovic, and R. Haas, “Economic and environmental assessment of different hydrogen production and transportation modes,” *International Journal of Hydrogen Energy*, vol. 65, pp. 626–638, 2024, doi: 10.1016/j.ijhydene.2024.04.073.
[95] F. Schorn *et al.,* “Methanol as a renewable energy carrier: An assessment of production and transportation costs for selected global locations,” *Advances in Applied Energy*, vol. 3, p. 100050, 2021, doi: 10.1016/j.adapen.2021.100050.
[96] K. Seeger *et al.,* “Techno-economic analysis of hydrogen and green fuels supply scenarios assessing three import routes: Canada, Chile, and Algeria to Germany,” *International Journal of Hydrogen Energy*, vol. 116, pp. 558–576, 2025, doi: 10.1016/j.ijhydene.2025.02.379.
[97] L. Sens, Y. Piguel, U. Neuling, S. Timmerberg, K. Wilbrand, and M. Kaltschmitt, “Cost minimized hydrogen from solar and wind – Production and supply in the European catchment area,” *Energy Conversion and Management*, vol. 265, p. 115742, 2022, doi: 10.1016/j.enconman.2022.115742.
[98] F. Staiß *et al., Optionen für den Import grünen Wasserstoffs nach Deutschland bis zum Jahr 2030: Transportwege - Länderbewertungen - Realisierungserfordernisse*. München, Halle (Saale), Mainz: acatech - Deutsche Akademie der Technikwissenschaften; Deutsche Akademie der Naturforscher Leopoldina e.V. - Nationale Akademie der Wissenschaften; Union der deutschen Akademien der Wissenschaften e.V, 2022. [Online]. Available: http://nbn-resolving.org/urn:nbn:de:gbv:3:2-903596
[99] D. Teichmann, W. Arlt, and P. Wasserscheid, “Liquid Organic Hydrogen Carriers as an efficient vector for the transport and storage of renewable energy,” *International Journal of Hydrogen Energy*, vol. 37, no. 23, pp. 18118–18132, 2012, doi: 10.1016/j.ijhydene.2012.08.066.
[100] B. Tiar, S. O. Fadlallah, D. E. Benhadji Serradj, P. Graham, and H. Aagela, “Navigating Algeria towards a sustainable green hydrogen future to empower North Africa and Europe's clean hydrogen transition,” *International Journal of Hydrogen Energy*, vol. 61, pp. 783–802, 2024, doi: 10.1016/j.ijhydene.2024.02.328.

[101] A. Wang *et al.,* “Analysing future demand, supply, and transport of hydrogen,” Jun. 2021. Accessed: Sep. 2 2025. [Online]. Available: https://www.ehb.eu/files/downloads/EHB-Analysing-the-future-demand-supply-and-transport-of-hydrogen-June-2021-v3.pdf
[102] A. Wietfeld, D. Krieg, T. Hajjar, S. Mitra, and R. Meier, “Competitiveness of green hydrogen import pathways for Germany in 2025,” Oct. 2021. Accessed: Sep. 2 2025. [Online]. Available: https://emvg.energie-und-management.de/filestore/newsimgorg/Illustrationen_Stimmungsbilder/Studien_als_PDF/Competitiveness_of_green_hydrogen_import_pathways_for_Germany_in_2025.orig.pdf
[103] L. Bühler and D. Möst, “Projecting technological advancement of electrolyzers and the impact on the competitiveness of hydrogen,” *International Journal of Hydrogen Energy*, vol. 98, pp. 1174–1184, 2025, doi: 10.1016/j.ijhydene.2024.12.078.
[104] W. Wang, Y. Wang, and D. Wang, “Review of Seawater Desalination Load Characteristics and its Application Integrated with Clean Energy,” in *2021 Power System and Green Energy Conference (PSGEC)*, Shanghai, China, 2021, pp. 368–372.
[105] M. Tommasi, S. N. Degerli, G. Ramis, and I. Rossetti, “Advancements in CO2 methanation: A comprehensive review of catalysis, reactor design and process optimization,” *Chemical Engineering Research and Design*, vol. 201, pp. 457–482, 2024, doi: 10.1016/j.cherd.2023.11.060.
[106] Q. Zhang, M. Bown, L. Pastor-Pérez, M. S. Duyar, and T. R. Reina, “CO2 Conversion via Reverse Water Gas Shift Reaction Using Fully Selective Mo-P Multicomponent Catalysts,” *Industrial & engineering chemistry research*, vol. 61, no. 34, pp. 12857–12865, 2022, doi: 10.1021/acs.iecr.2c00305.
[107] P. Schmidt and W. Weindorf, “Power-to-Liquids: Potentials and Perspectives for the Future Supply of Renewable Aviation Fuel,” Sep. 2016. Accessed: Oct. 14 2025. [Online]. Available: https://www.umweltbundesamt.de/sites/default/files/medien/377/publikationen/161005_uba_hintergrund_ptl_barrierrefrei.pdf
[108] TheProjectEstimate.com, *Steel Water Tank Price List.* [Online]. Available: https://www.theprojectestimate.com/steel-water-tank-price-list/ (accessed: Oct. 15 2025).
[109] K. Lauri, R. Jouko, N. Nicklas, and T. Sebastian, “Scenarios and new technologies for a North-European CO2 transport infrastructure in 2050,” *Energy Procedia*, vol. 63, pp. 2738–2756, 2014, doi: 10.1016/j.egypro.2014.11.297.
[110] Insights Global, *Tankterminals.com.* [Online]. Available: https://tankterminals.com/ (accessed: Oct. 14 2025).
[111] K. Mazloomi and C. Gomes, “Hydrogen as an energy carrier: Prospects and challenges,” *Renewable and Sustainable Energy Reviews*, vol. 16, no. 5, pp. 3024–3033, 2012, doi: 10.1016/j.rser.2012.02.028.
[112] M. Reuß, T. Grube, M. Robinius, P. Preuster, P. Wasserscheid, and D. Stolten, “Seasonal storage and alternative carriers: A flexible hydrogen supply chain model,” *Applied Energy*, vol. 200, pp. 290–302, 2017, doi: 10.1016/j.apenergy.2017.05.050.

Annex

Annex 1 Literature review Methodology

The selection methodology for relevant studies on the trade of hydrogen and hydrogen-derived synthetic fuels into the EU builds on the approach by Genge et al. [12]. In addition to reviewing the studies already identified in their meta-analysis, further studies were selected using the search key:

> **TITLE-ABS-KEY** ("Fischer-Tropsch" **OR** "Hydrogen" **OR** "chemical energy carrier" **OR** "e-fuels" **OR** "power-to-fuel" **OR** "power-to-gas" **OR** "hydrogen energy" **OR** "Ammonia" **OR** "Methanol" **OR** "Methane" **AND** "Middle East" **OR** "North Africa" **OR** "MENA" **AND** "Europe" **OR** "EU") **AND PUBYEAR** > 2014 **AND PUBYEAR** < 2026 **AND** (**LIMIT-TO**(DOCTYPE,"ar")) **AND** (**LIMIT-TO**(LANGUAGE, "English"))

The database used to identify additional studies was Scopus, with results limited to peer-reviewed articles written in English.

This search yielded 76 initial results. After a structured review of abstracts, the number was reduced to 32 potential studies. A further screening step narrowed this set to 14 studies considered directly relevant for the analysis. Out of the 34 studies listed in Genge et al. [12], 27 were also found to be relevant in the context of this thesis. In total, 41 studies were therefore included in the review.

The selected studies were assessed along three criteria:

- **Modelling scope**: Evaluation of the import network design, including spatial coverage and the number of analysed energy carriers.
- **Transportation scope**: Assessment of transport modelling, including the choice of transport modes and whether a greenfield or brownfield approach was applied. In cases where pipeline transport was excluded, greenfield/brownfield distinctions were often not applicable.
- **Country-sensitive financing risks**: Analysis of whether financing assumptions were applied uniformly across all countries or differentiated by national risk profiles.

The results of this review are displayed in A-1.

A-1 Overview reviewed studies. P = pipeline S = Ship, E = Electricity cable, R = Road transport

Authors	Modelling scope	No. of energy carriers	Transportation portfolio	Transportation value chain	Transportation modelling approach	Country sensitive financing risks
Alanazi et al. [77]	global	3	P, S	Fully modelled	Greenfield	Partially
Brändle et al. [78]	global	1	P, S	Fully modelled	Greenfield	No
Breitschopf et al. [79]	EU-MENA	4	P, S	Fully modelled	Brownfield	No
Chen et al. [80]	EU-global	5	S	Fully modelled	Not applicable	No
Dalla Longa et al. [13]	EU-NA	2	P, E	Partially modelled	Brownfield	No
Dickson et al. [81]	global	4	S, R	Fully modelled	Greenfield	No
Fattahi et al. [16]	EU-MENA	2	P, S	Fully modelled	Greenfield	No
Frömel et al. [10]	Europe	1	P, S	Fixed price assumption	Greenfield	No
Galimova et al. [82]	global	1	P, S	Fully modelled	Greenfield	No
Guillot and Assoumou [83]	EU-NA	2	S, E	Partially modelled	Brownfield	No
Hampp et al. [36]	EU-global	5	P, S, E	Fully modelled	Greenfield	No
Hydrogen Import Coalition [84]	EU-global	5	P, S	Fully modelled	Greenfield	No
International Energy Agency [85]	global	3	P, S	Fully modelled	Greenfield	No
Jensterle et al. [86]	EU-global	1	P, S	Fixed price assumption	Not applicable	No
Krüger et al. [24]	EU-MENA	8	P, S	Fully modelled	Greenfield	yes
Lux et al. [17]	EU-MENA	1	P, S	fixed import cost	Not applicable	No
Lux et al. [18]	EU-MENA	2	E	Fixed price assumption	Not applicable	No
Meca et al. [87]	global	2	S	Fully modelled	Not applicable	No
Moritz et al. [23]	EU-global	5	P, S	Fully modelled	Greenfield	Yes
Neumann et al. [88]	global	3	S	Fully modelled	Not applicable	No
Neumann et al. [89]	EU-global	7	P, S, E	Fully modelled	Brownfield	No

Niermann et al. [90]	EU-global	3	P, S, E	Fully modelled	Greenfield	No
Nuñez-Jimenez and Blasio [4]	EU-NA	2	P, S	Fully modelled	Greenfield	No
Perner et al. [91]	EU-global	3	S	Fully modelled	Not applicable	No
Pinto et al. [14]	EU-NA	1	P, S	Fixed price assumption	Greenfield	Yes
Roos [92]	EU-global	3	S	Fully modelled	Not applicable	No
Runge et al. [93]	global	3	S, T	Fully modelled	Not applicable	No
Sayer et al. [94]	EU-global	1	P, S	Fixed price assumption	Greenfield	No
Schorn et al. [95]	global	2	S	Fully modelled	Not applicable	No
Seeger et al. [96]	EU-global	4	P, S	Fully modelled	Greenfield	No
Sens et al. [15]	EU-global	4	P, S	Fully modelled	Greenfield	No
Sens et al. [97]	EU-global	1	P	Fully modelled	Greenfield	Unclear
Soler et al. [48]	EU-MENA	8	P, S	Fully modelled	Greenfield	No
Staiß et al. [98]	EU-NA	5	P, S	Fully modelled	Greenfield	No
Teichmann et al. [99]	EU-NA	1	S	Fully modelled	Not applicable	No
Terrapon-Pfaff et al. [21]	EU-MENA	1	S	Fully modelled	Not applicable	Yes
Tiar et al. [100]	NA	1	P	Not applicable	Brownfield	not applicable
van der Zwaan et al. [70]	EU-NA	2	P, E	Partially modelled	Greenfield	No
Wang et al. [101]	EU-NA	3	P	Fully modelled	Greenfield	No
Wetzel et al. [27]	EU-NA	3	P, S	Fixed price assumption	Brownfield	No
Wietfeld et al. [102]	EU-ME	3	S	Fully modelled	Greenfield	No

Annex 2 Objective function and further model constraints

The model is set up to optimise the system by minimizing the total system cost. For that, the total system cost (J_{Total}) is defined as the sum of all discounted and annualised cost components over the entire model horizon. The optimization minimizes this value by determining the least-cost configuration and operation of all generation, conversion, storage and transport technologies in the EU-MENA energy system. The model operates on a high temporal resolution (2,920) for each representative year $y \epsilon Y$ such that both investment and operational decisions are captured consistently

The fixed system cost (j_{Fix}) component captures annualised investment and fixed operation and maintenance (FOM) cost of all converter ($k \epsilon K$) and network ($n \epsilon N$) technologies, installed and node i in year y.

A-2 Objective function for fixed cost indicators

$$\boldsymbol{j_{Fix,i,y} = d_{i,k} * \sum_{k \epsilon K} INV^{+}_{i,y,k} + INV^{-}_{i,y,k} + FOM_{i,y,k} + d_{i,n} * \sum_{n \epsilon N} INV^{+}_{i,y,n} + INV^{-}_{i,y,n} + FOM_{i,y,n}}$$

Where:

- $d_{i,k}$ and $d_{i,n}$ are the node and technology specific annuity factors,
- INV^{+} and INV^{-} represent annualised investment and decommissioning cost,
- and FOM represents fixed operation and maintenance costs.

The variable cost (j_{var}) includes operational expenses that depend on the dispatch decisions of converter and network technologies per timestep. Each converter technology k performs one or more activities $m \epsilon M_k$ (e.g. conversion of electricity and water to hydrogen) while each network element n performs activities $p \epsilon P_n$ transferring energy or material between nodes i and l. As such the variable system cost are captured in A-3, where $G_{i,h,y,k,m}$ is the activity output and $VOM_{i,y,k,m}$ the variable operation cost. Similarly, $F_{i,h,y,n,p,l}$ represents the flow of energy or material along the network link between nodes i and j, as well as the associated specific transport cost $STC_{i,y,n,p,l}$.

A-3 Objective function for variable cost indicators

$$\boldsymbol{j_{Var,i,y} = d_{i,k} * \sum_{h \epsilon H_y, k \epsilon K, m \epsilon M_k} G_{i,h,y,k,m} * VOM_{i,y,k,m} + d_{i,n} * \sum_{h \epsilon H_y, n \epsilon N, p \epsilon P_n, l \epsilon L} F_{i,h,y,n,p,l} * STC_{i,y,n,p,l}}$$

Storage cost (j_{stor}) contribute to the total system cost through both capacity-related and operation-related components.

A-4 Objective function for storage cost indicators

$$\boldsymbol{j_{stor,i,y} = d_{i,s} * \left(\sum_{s \epsilon S} INV^{+}_{i,y,s} + INV^{-}_{i,y,s} + FOM_{i,y,s} + \sum_{s \epsilon S, h \epsilon H} CH^{+}_{i,h,y,s} * VOM^{+}_{i,y,s} + CH^{-}_{i,h,y,s} * VOM^{-}_{i,y,s} \right)}$$

Where:

- $s \epsilon S$ denotes the set of storage technologies,
- CH^{+} and CH^{-} represent charging and discharging volumes per timestep, and
- VOM^{+} and VOM^{-} are the associated charging and discharging costs.

The import ($e \in E$) of energy across system boundaries creates external import cost (j_{Import}):

A-5 Objective function for nodal import and export cost indicators

$$\boldsymbol{j_{Import,i,y} = d_{y,i} * \sum_{h \epsilon H, e \epsilon E} q_{i,h,e} * IMP^{+}_{i,y,e}}$$

Where:

- $q_{i,h,e}$ is the imported energy quantity and
- $IMP^{+}_{i,y,e}$ the import price.

Lastly, slack cost (j_{Slack}) are included in the model via the sum of all slack cost components ($z \in Z$):

A-6 Objective function for slack cost indicators

$$\boldsymbol{j_{Slack,i,y} = \sum_{z \epsilon Z} p_{i,y,z} * Slack_{i,y,z}}$$

Where:

- $p_{i,y,z}$ is the amount of slack and
- $Slack_{i,y,z}$ the respective slack price.

The total system cost is calculated by summing all node-level cost components across space and time. All annual totals are discounted to the base year y_0 using the social discount rate ϕ:

A-7 Objective function of the total system cost

$$J_{Total} = \sum_{y \epsilon Y} \frac{1}{(1+\phi)^{(y-y_0)}} * \sum_{i \epsilon I} j_{Fix,i,y} + j_{Var,i,y} + j_{Stor,i,y} + j_{Import,i,y} + j_{Slack,i,y}$$

Annex 3 Pre-processed input maps

A-8 Pre-processed HVAC grid

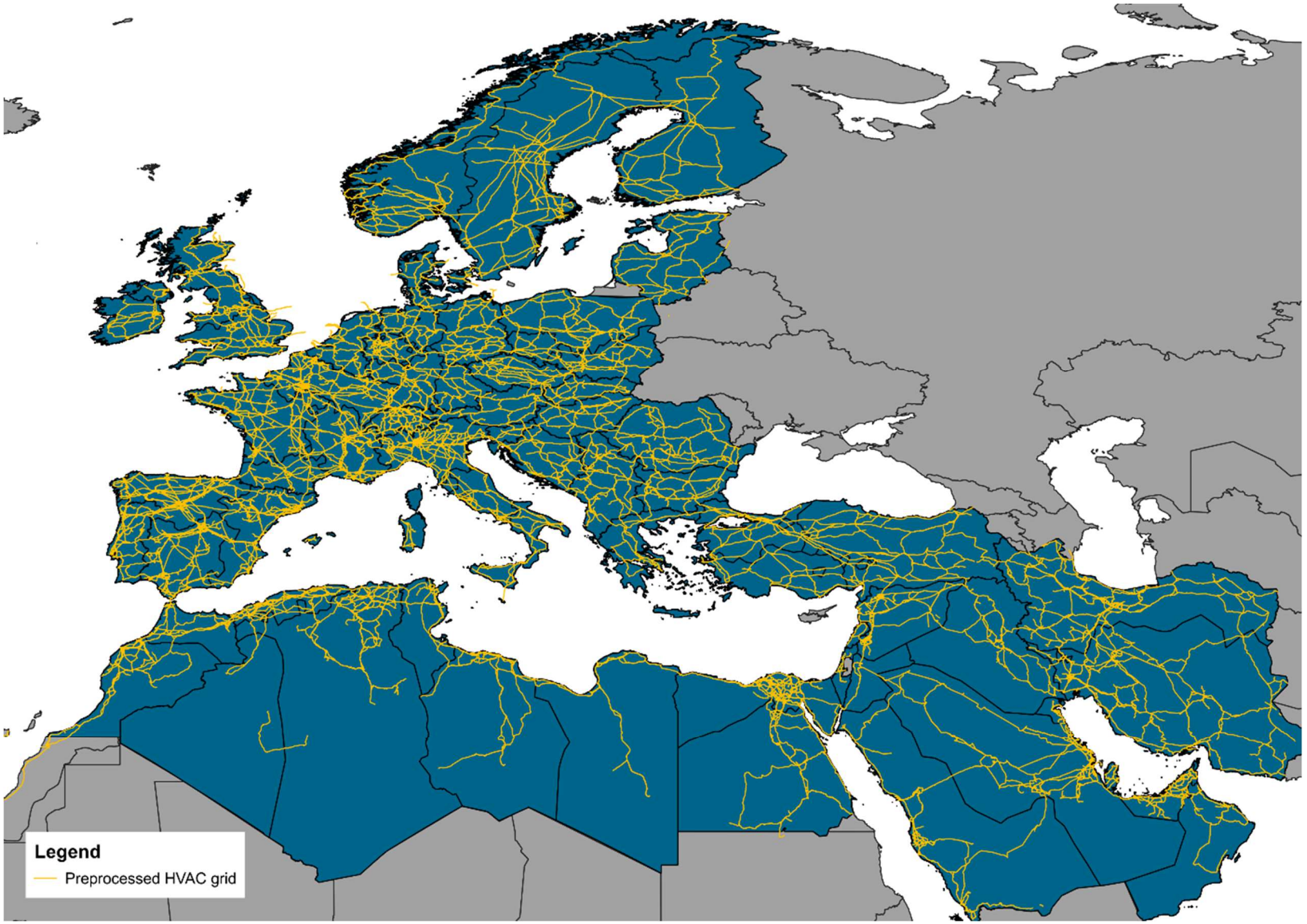

A-9 Pre-processed HVDC grid

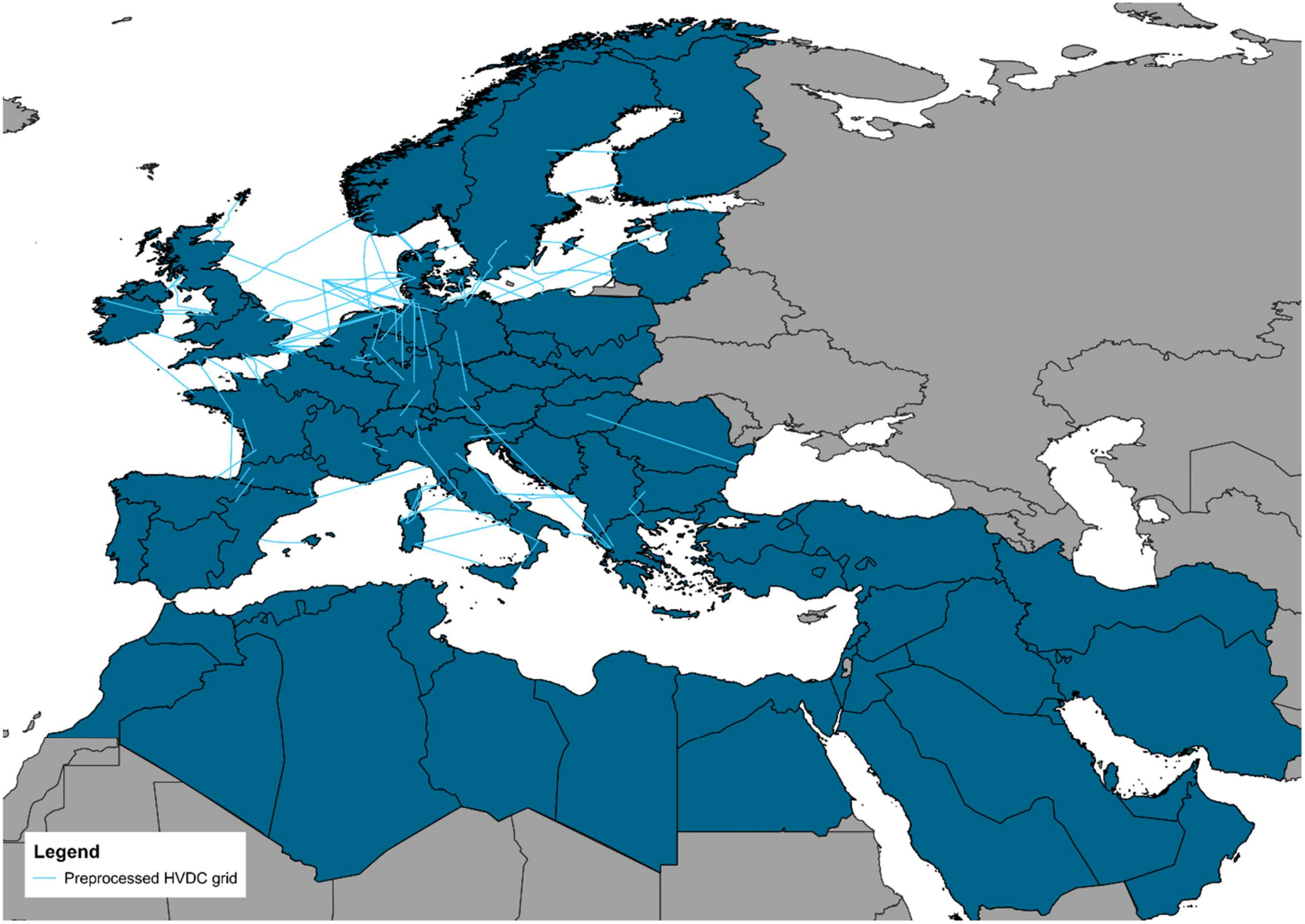

A-10 Pre-processed gas grid

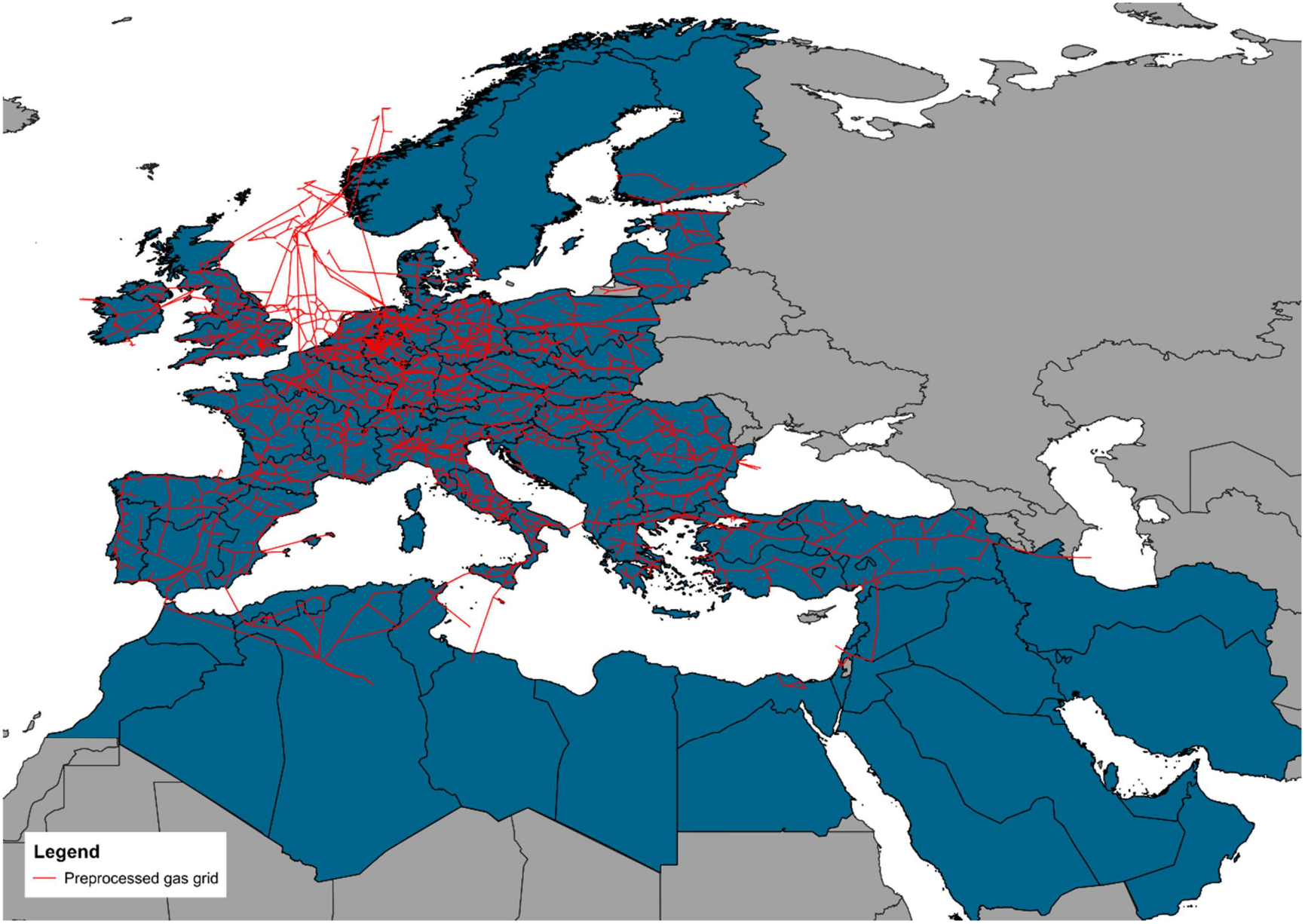

Annex 4 List of technology assumptions

Electricity generation

- Base model instance technology envelope:
    - Solar PV (rooftop and land-mounted)
    - Concentrated Solar PV (electricity – quality class 1 and 2 and heat)
    - Onshore wind (quality class 1, 2 and 3)
    - Offshore wind (foundation and floating)
    - Run-of-river hydro power
    - Pumped hydro storage (electricity generation module)
    - Hydro reservoir (electricity generation module)
    - OCGT
    - CCGT
    - Coal
    - Lignite coal
    - Nuclear

- Added/changed technologies:
    - None

Hydrogen conversion

- Base model instance technology envelope:
    - Steam methane reforming (with and without carbon capture & storage)
    - Autothermal reforming

- Added and changed technologies
    - PEM Electrolysis (updated values)
    - AEL Electrolysis (added)
    - SOEC Electrolysis (added)
    - Sea Water Reverse Osmosis (added)

- Methodological selection decisions:

A mix of Electrolysis options is chosen to represent common current and future electrolysis options [103]. SWRO is selected for its relatively low energy demand and wide industrial adoption [104].

Synfuel pathways

- Added/changed technologies:
    - Catalytic methanation (added)
    - Fischer-Tropsch Synthesis (added)
    - Methanol-to-hydrocarbon (added)

- Methodological selection decisions:

Synthetic methane is produced via the Sabatier process, i.e., the catalytic reaction of CO_2 and H_2 to CH_4 and H_2O [36]. While alternative methods exist, such as direct biogas methanation (BHM), this study choses to model only the catalytic methane pathway. Direct biogas methanation promises a potentially higher economical production pathway, has however a generally lower technology readiness level than direct the direct hydrogenation pathway [105].

A-11 Sabatier reaction [36]

$$CO_2 + 4H_2 \leftrightarrows CH_4 + 2H_2O$$

Excess heat generated throughout the methanation process is not captured in the model given the system scale. While it is assumed that production and demand clusters are co-located within a model region, such that intra-regional transport is neglected, process heat is mainly traded on a sub-regional scale. Accurately assessing opportunities to use excess heat elsewhere would therefore require a more spatially resolved model to preserve realistic boundary conditions. The resulting CH_4 is assumed to be grid-quality, meaning that no further downstream processes are needed to transport the methane through the existing gas grid.

The production of FT-fuels is modelled via two routes: (i) low-temperature FT synthesis of long-chain hydrocarbons from synthesis gas (syngas) and (ii) a methanol-to-hydrocarbon (MTH) route.

In the low-temperature FT synthesis, CO_2 and hydrogen are first used to create syngas through the reverse water gas shift reaction (RWGS) [36]. The syngas is then upgraded to synthetic crude oil (syncrude) through the Fischer-Tropsch synthesis before being further refined into a range of hydrocarbons. The low-temperature version of the Fischer-Tropsch synthesis was chosen, as it favours the production of liquid hydrocarbons. [49] As with the methane pathway, excess heat is not accounted for. The heat needed for the RWGS (T=100-200 °C) is assumed to be electrified (η = 100%) [49].

A-12 Reverse water gas shift reaction [106].

$$CO_2 + H_2 \leftrightarrows CO + H_2O$$

Alternative to the Fischer-Tropsch synthesis, a methanol-to-hydrocarbon (MTH) pathway is also modelled. The benefit of including the methanol production pathway lies in higher technology readiness levels and thus lower current costs [107]. In this study, the MTH route is modelled analogously to the methanol-to-kerosene process. First, methanol (CH_3OH) is synthesized via direct catalytic hydrogenation of CO_2, then upgraded to kerosene-range hydrocarbons. During this process, methanol is initially transformed into water and dimethyl ether (DME), which is then catalytically converted into hydrocarbons and water [57].

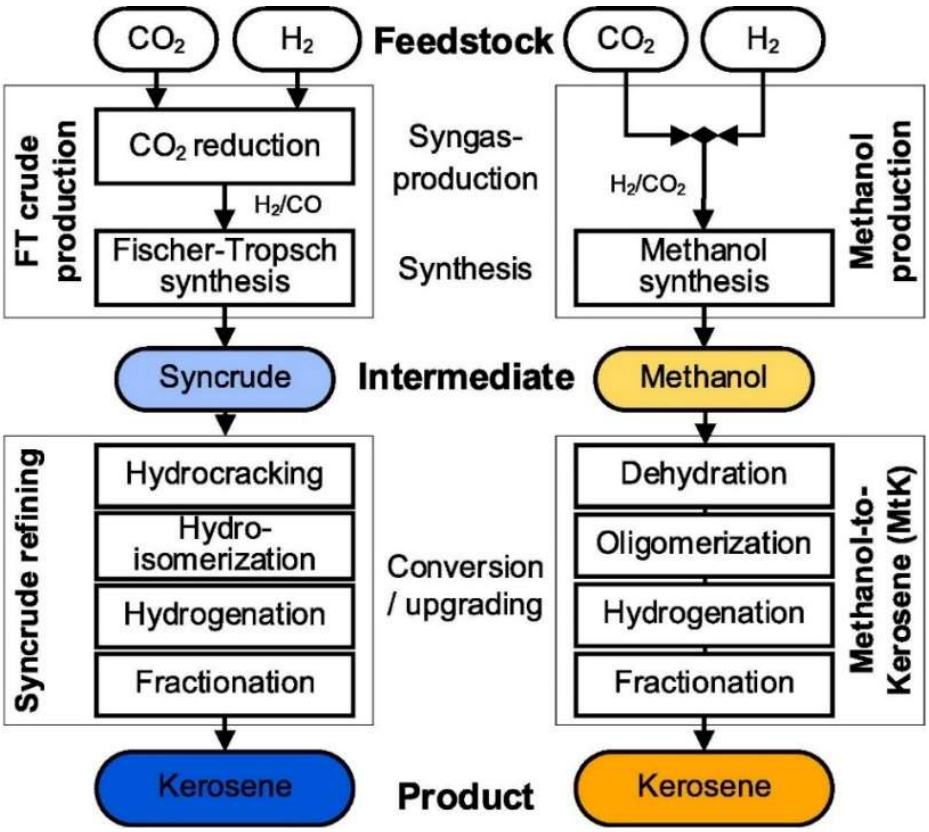

A-13 Process diagram Fischer-Tropsch and Methanol-to-kerosene synthesis [34]

The needed CO_2 for all processes must, in the model, be sourced through solid adsorption direct air capture (DAC), as sourcing the CO_2 from point sources does not enable true carbon neutrality, since the fossil carbon gets recycled, rather than removed from the ecosystem. Capturing CO_2 from the atmosphere also ensures consistency with future CO_2 point source devaluation after 2041 [35]. Input heat demand is, similar to other processes electrified (η = 100%, T = 100°C) [48].

Storage

- Base model instance technology envelope:
  - Lithium-Ion batteries
  - CH_4 cavern storage
  - H_2 cavern storage
  - H_2 tank storage
- Added/changed technologies:
  - H_2O buffer storage (added)
  - CO_2 buffer storage (added)
  - General hydrocarbon storage (added)

Transportation

- Base model instance technology envelope:
  - HVAC
  - HVDC
  - CH_4 gas pipeline
  - H_2 pipeline (new)

    - H_2 pipeline (retrofitted)
- Added/changed technologies:
    - Land transport for hydrocarbons and liquefied hydrogen (added)
    - Maritime transport for hydrocarbons and liquefied hydrogen (added)

Annex 5 Matched model region ids

A-14 Model nodes

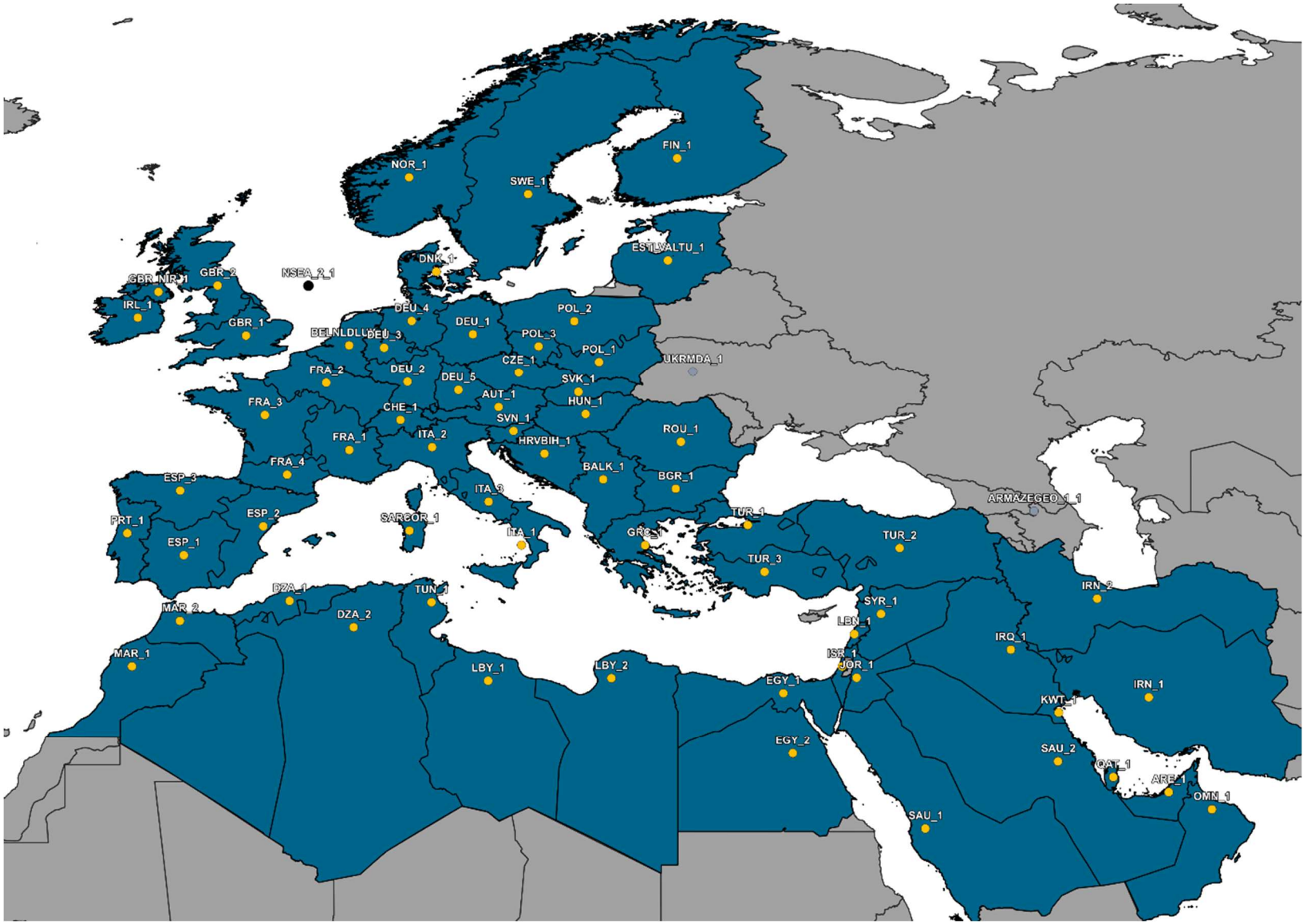

A-15 Port nodes

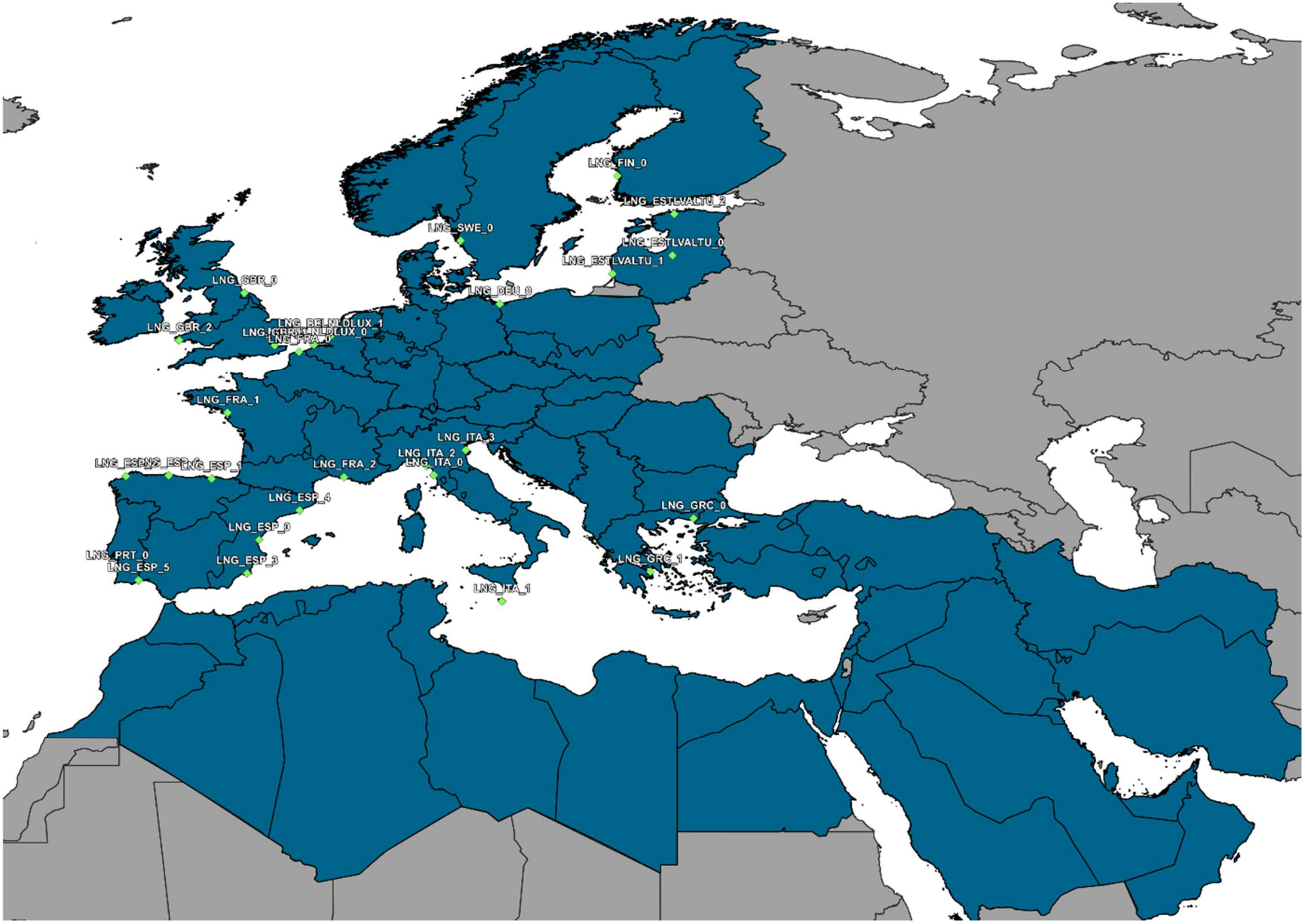

Annex 6 Post-processed network maps

A-16 Reduced HVAC grid

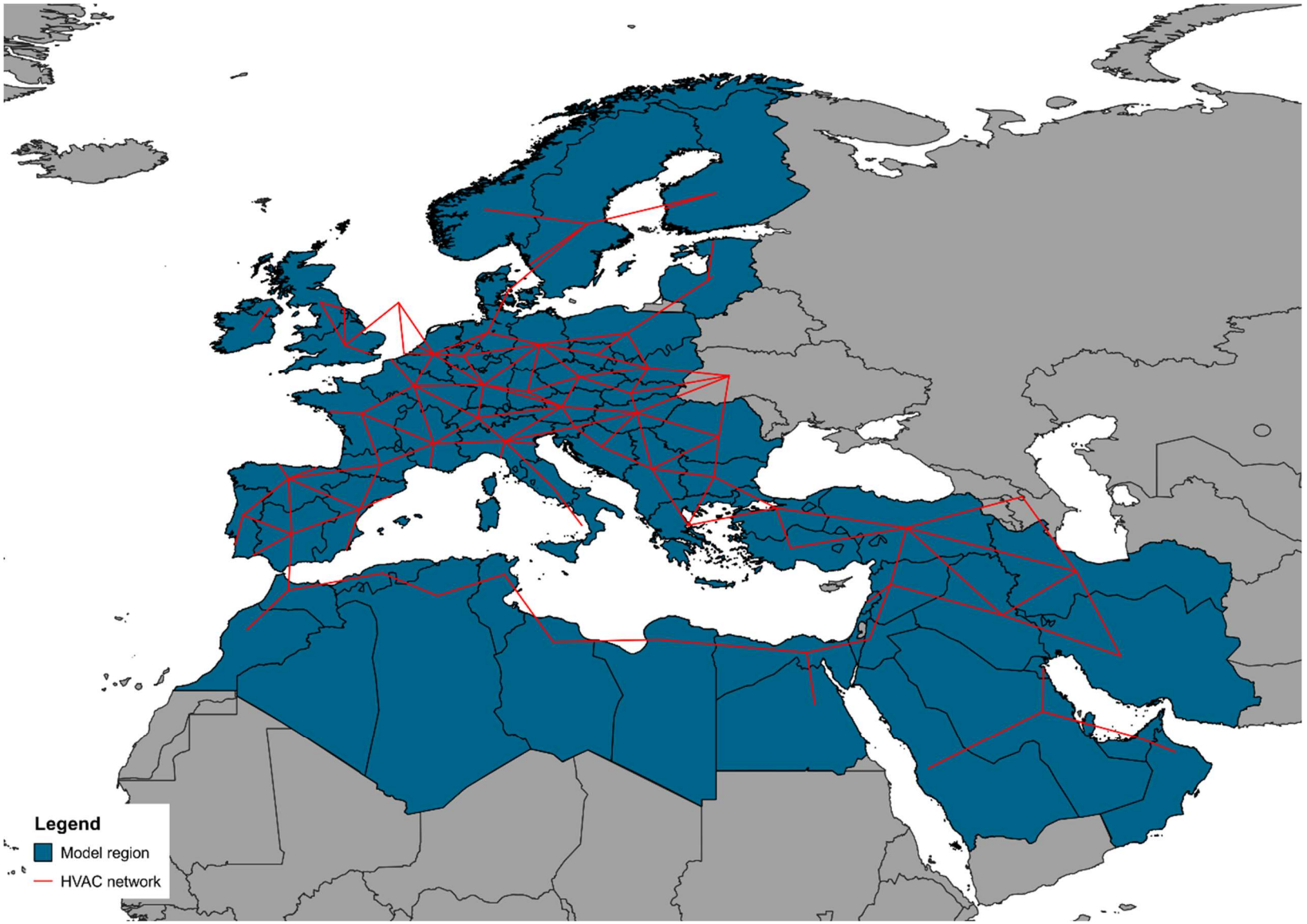

A-17 Reduced HVAC grid including link capacity

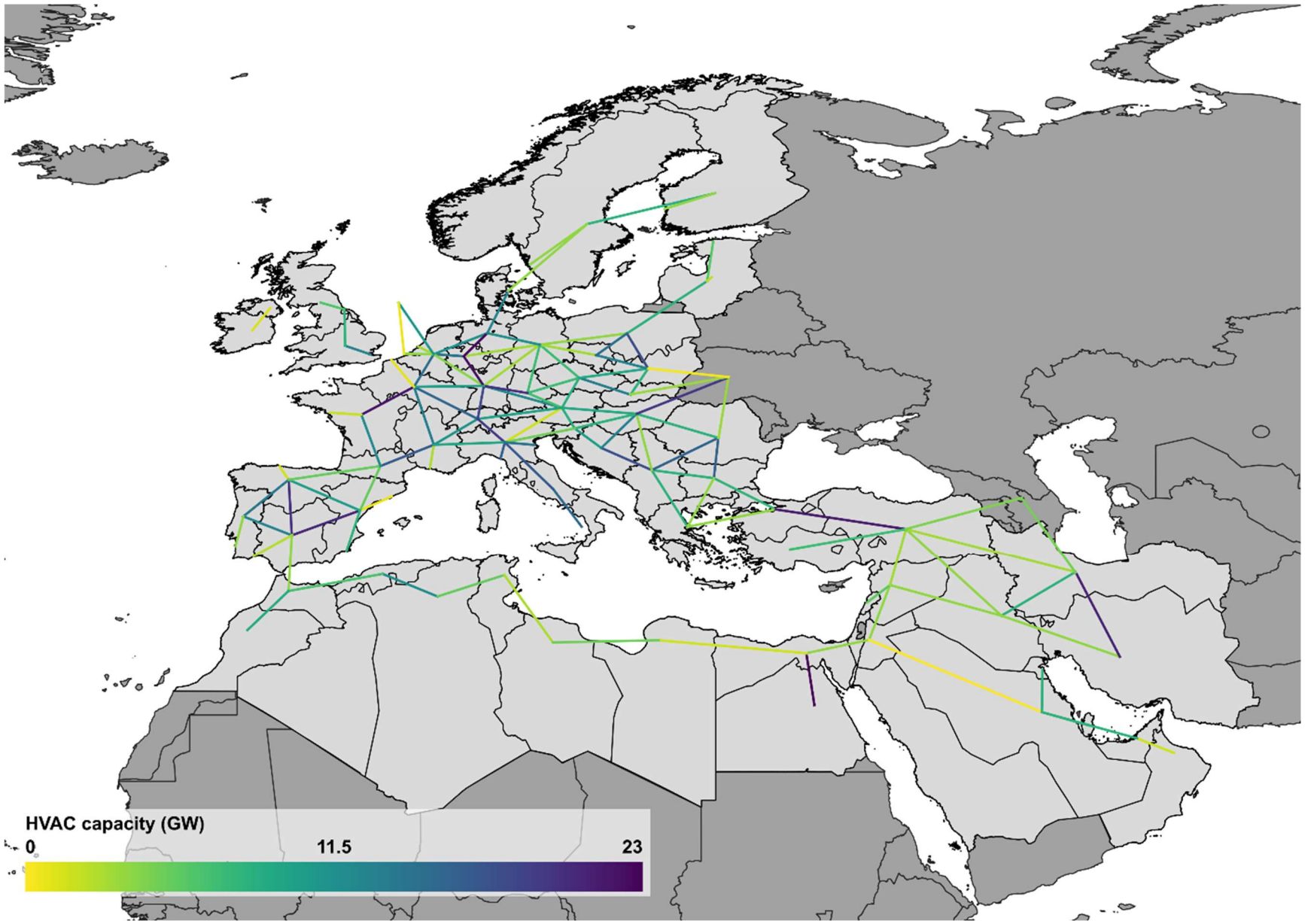

A-18 Reduced HVDC network

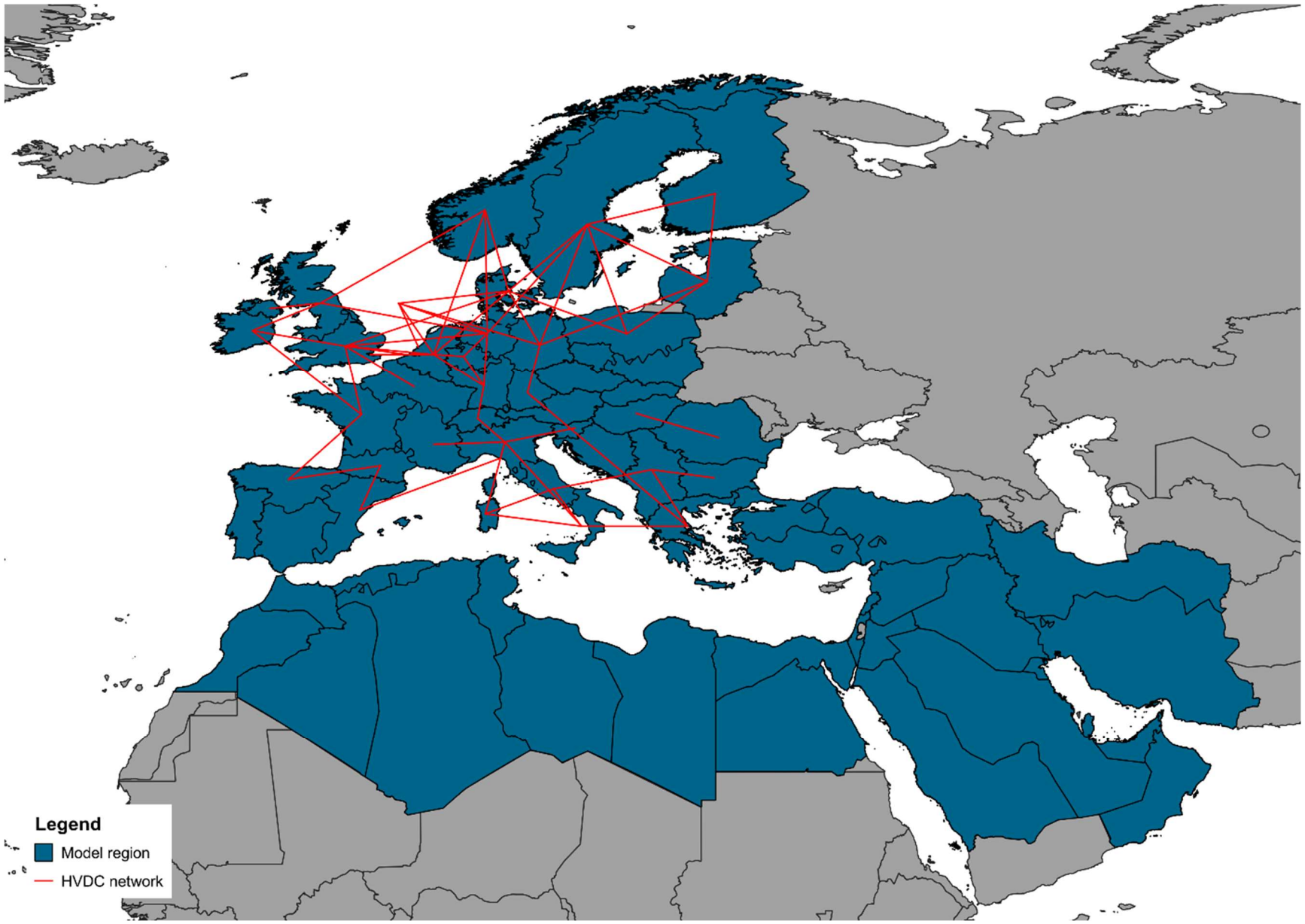

A-19 Reduced HVDC network including link capacity

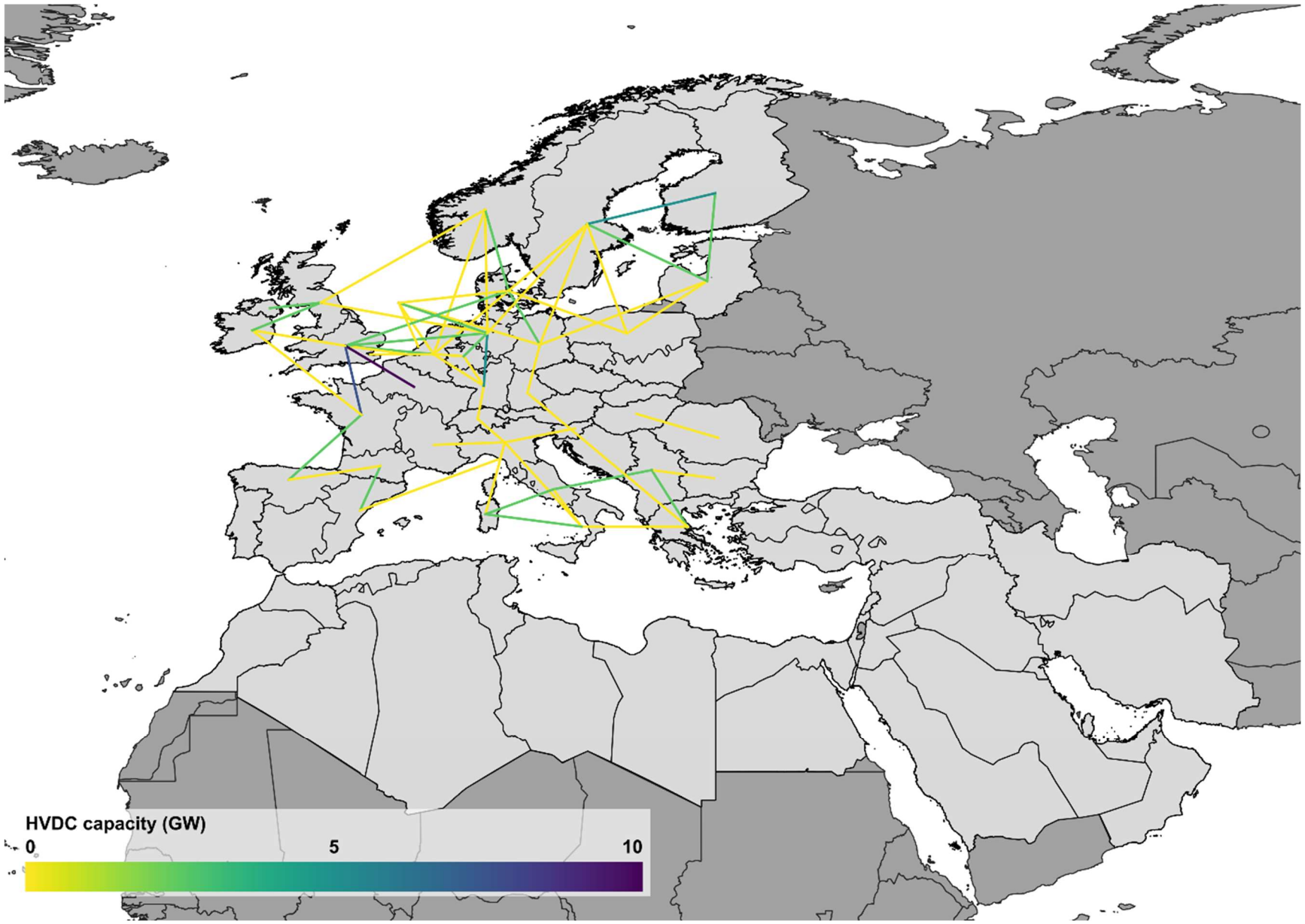

A-20 Reduced gas network

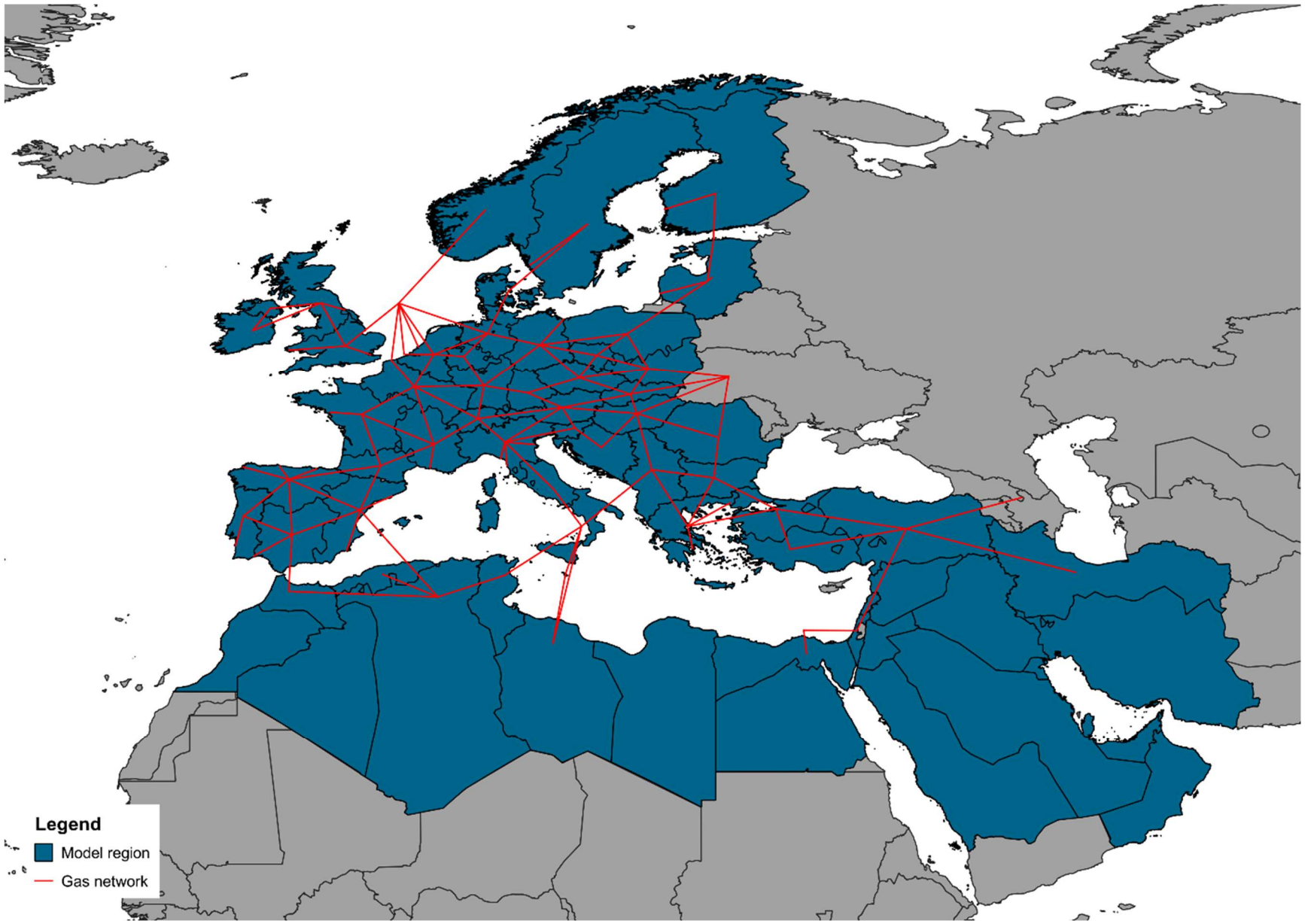

A-21 Reduced gas network including link capacity

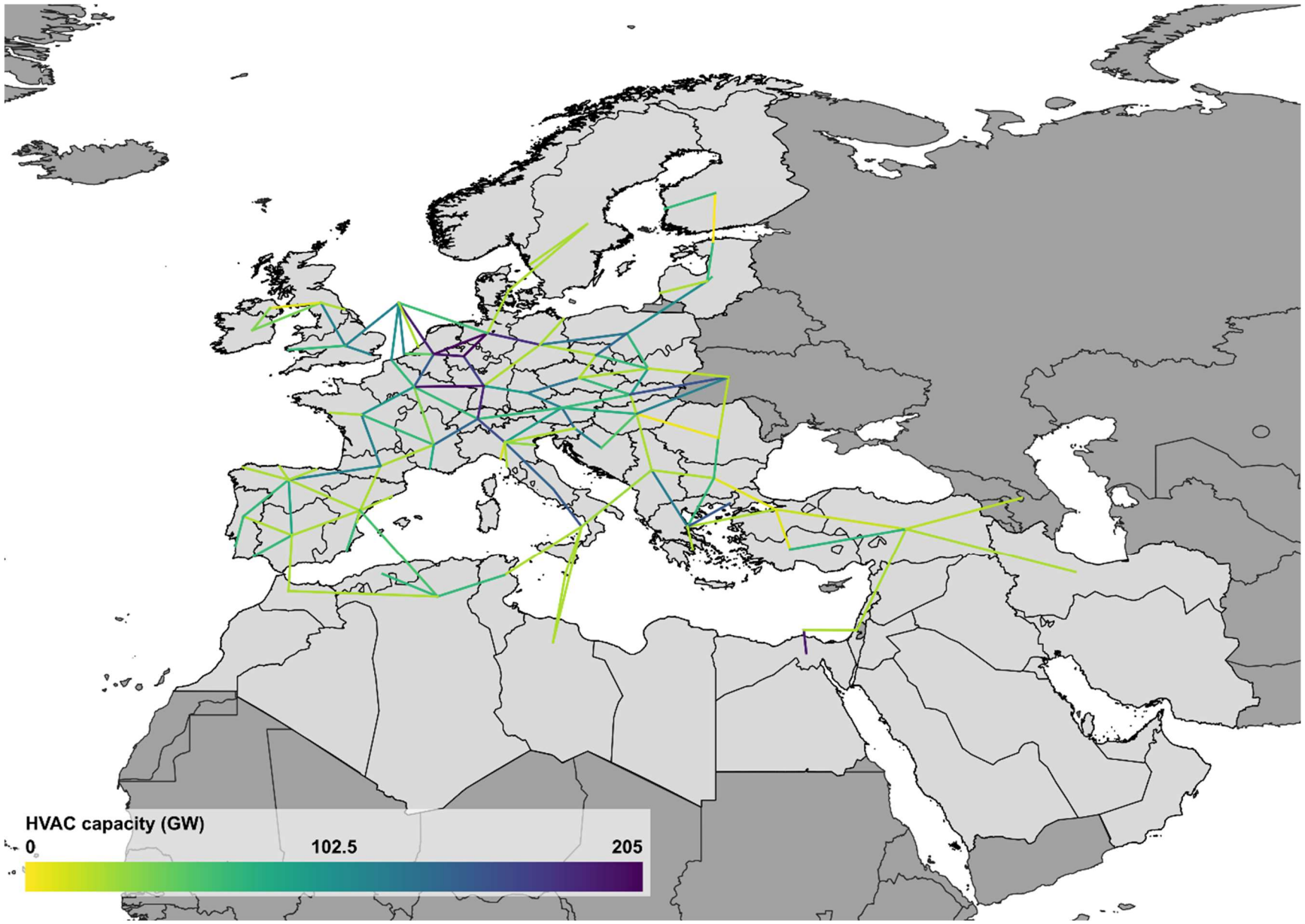

A-22 Reduced land network

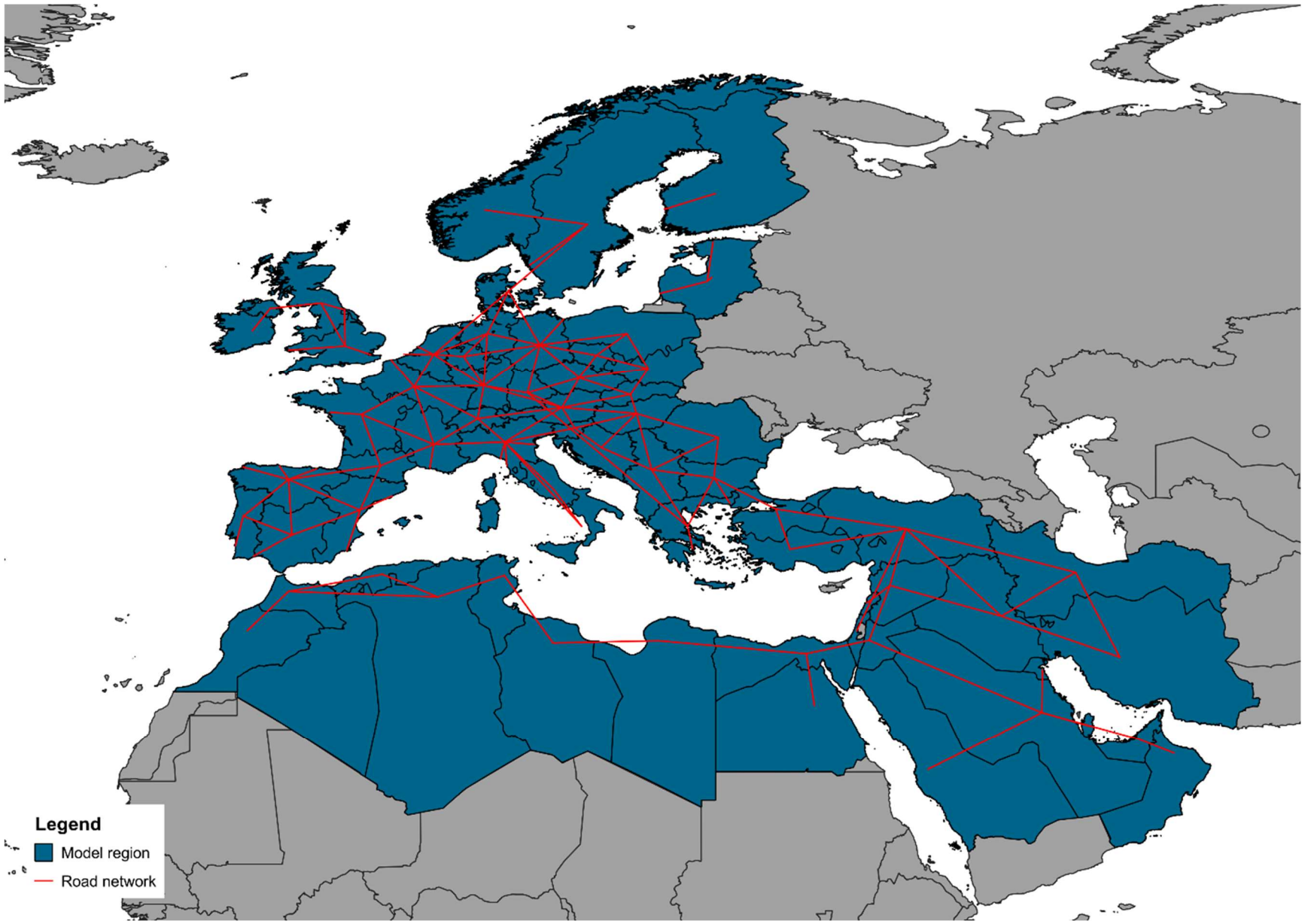

A-23 Reduced waterways network

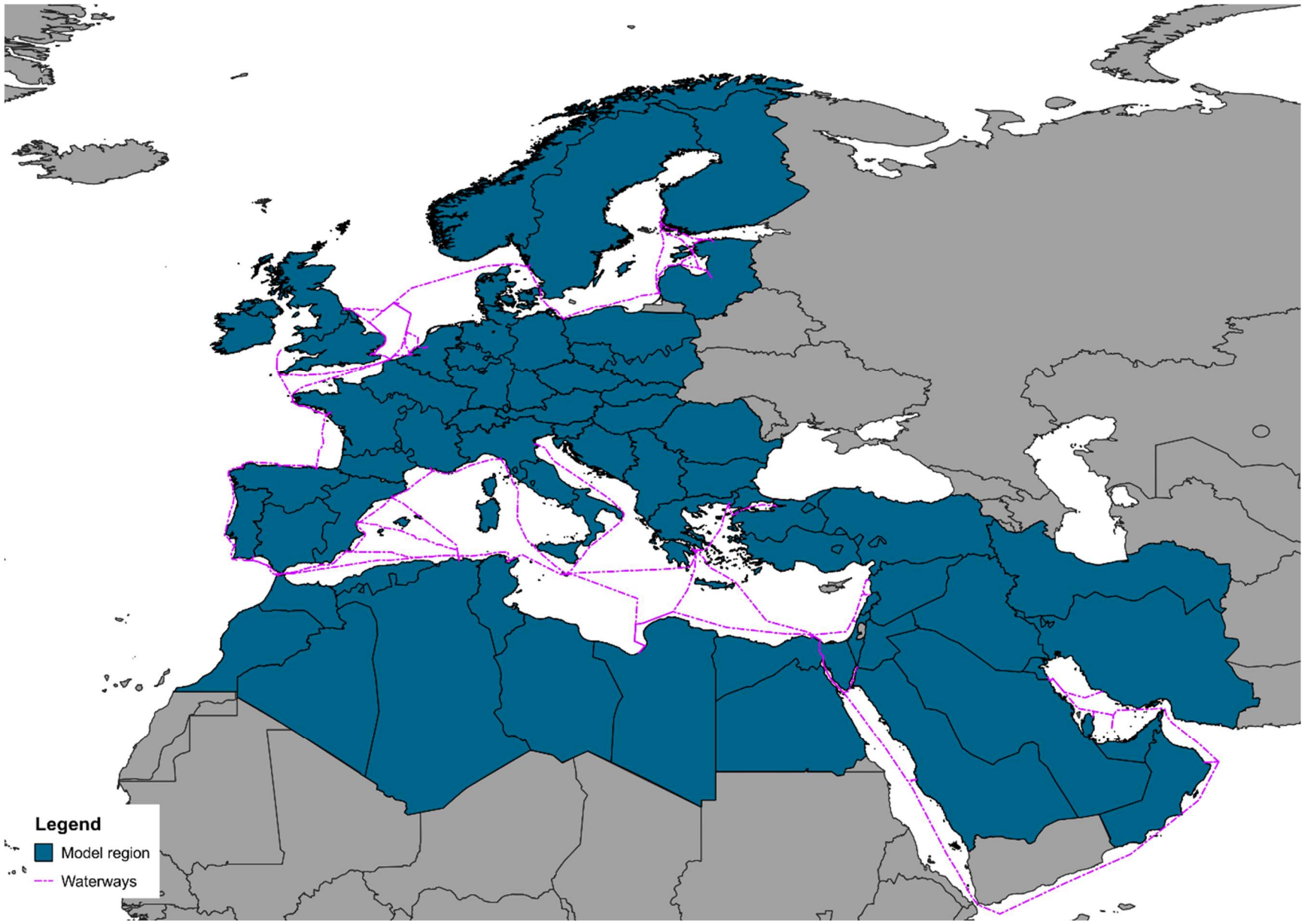

Annex 7 Waterways

Origin port	Destination port	Origin lon-gitude	Origin latitude	Destination longitude	Destination latitude
MAR_2	LNG_ESP_5	-5.78332	35.7999	-7.518	37.211
MAR_2	LNG_ESP_3	-5.78332	35.7999	-0.966526	37.62754
LNG_ESP_5	LNG_ESP_3	-7.518	37.211	-0.966526	37.62754
DZA_1	LNG_ESP_3	3.07714	36.77138	-0.966526	37.62754
MAR_2	DZA_1	-5.78332	35.7999	3.07714	36.77138
LNG_ESP_3	LNG_ESP_0	-0.966526	37.62754	-0.235301	39.641627
DZA_1	LNG_ESP_0	3.07714	36.77138	-0.235301	39.641627
DZA_1	TUN_1	3.07714	36.77138	10.310726	36.80462
LNG_ESP_0	LNG_ESP_4	-0.235301	39.641627	2.20347833	41.4247853
DZA_1	LNG_ESP_4	3.07714	36.77138	2.20347833	41.4247853
LNG_ESP_4	LNG_FRA_2	2.20347833	41.4247853	4.89018714	43.4269899
LNG_FRA_2	LNG_ITA_2	4.89018714	43.4269899	9.8574425	44.0904305
LNG_ITA_2	LNG_ITA_0	9.8574425	44.0904305	10.311025	43.547519
LNG_ITA_0	LNG_ITA_1	10.311025	43.547519	14.424149	35.93143
TUN_1	LNG_ITA_1	10.310726	36.80462	14.424149	35.93143
LNG_ITA_1	LBY_2	14.424149	35.93143	20.02652	32.11325
LNG_ITA_1	LNG_ITA_3	14.424149	35.93143	12.2347206	45.0480048
LNG_ITA_1	LNG_GRC_1	14.424149	35.93143	23.3840165	37.7243015
LBY_2	LNG_GRC_1	20.02652	32.11325	23.3840165	37.7243015
LNG_GRC_1	LNG_GRC_0	23.3840165	37.7243015	25.994099	40.939928
LNG_GRC_0	TUR_1	25.994099	40.939928	29.272627	40.66283
LBY_2	EGY_1	20.02652	32.11325	31.1976371	31.9842104
LNG_GRC_1	EGY_1	23.3840165	37.7243015	31.1976371	31.9842104
EGY_1	ISR_1	31.1976371	31.9842104	34.638238	31.829967
ISR_1	LBN_1	34.638238	31.829967	35.51717	33.90817
EGY_1	SAU_1	31.1976371	31.9842104	39.14746	21.46655
SAU_1	OMN_1	39.14746	21.46655	56.36848	25.171098
OMN_1	ARE_1	56.36848	25.171098	54.6475877	24.3574665
ARE_1	QAT_1	54.6475877	24.3574665	51.64284	25.91328
QAT_1	KWT_1	51.64284	25.91328	48.17091	29.05278
KWT_1	IRN_1	48.17091	29.05278	52.200821	27.695922
MAR_2	ESH_1	-5.78332	35.7999	-14.49593	26.10981
LNG_ESP_5	LNG_PRT_0	-7.518	37.211	-8.797	37.937
LNG_PRT_0	LNG_ESP_2	-8.797	37.937	-8.277	43.475
LNG_ESP_2	LNG_ESP_6	-8.277	43.475	-5.695359	43.5271955
LNG_ESP_6	LNG_ESP_1	-5.695359	43.5271955	-3.100987	43.3336625
LNG_ESP_1	LNG_FRA_1	-3.100987	43.3336625	-2.1383025	47.3133415
LNG_FRA_1	LNG_GBR_2	-2.1383025	47.3133415	-5.61350667	51.724077
LNG_FRA_1	LNG_FRA_0	-2.1383025	47.3133415	2.175771	51.1755
LNG_GBR_2	LNG_FRA_0	-5.61350667	51.724077	2.175771	51.1755
LNG_FRA_0	LNG_GBR_1	2.175771	51.1755	0.69427886	51.414549
LNG_FRA_0	LNG_BELNLD LUX_0	2.175771	51.1755	3.67771	51.4487408

LNG_BELNLD LUX_0	LNG_BELNLD LUX_1	3.67771	51.4487408	4.6889	51.959378
LNG_GBR_1	LNG_GBR_0	0.69427886	51.414549	-1.129514	54.571158
NSEA_2_1	LNG_GBR_0	2.69160387	55.0290693	-1.129514	54.571158
NSEA_2_1	LNG_GBR_1	2.69160387	55.0290693	0.69427886	51.414549
NSEA_2_1	LNG_FRA_0	2.69160387	55.0290693	2.175771	51.1755
NSEA_2_1	LNG_BELNLD LUX_0	2.69160387	55.0290693	3.67771	51.4487408
NSEA_2_1	LNG_BELNLD LUX_1	2.69160387	55.0290693	4.6889	51.959378
NSEA_2_1	LNG_SWE_0	2.69160387	55.0290693	11.9284657	57.7232583
LNG_SWE_0	LNG_DEU_0	11.9284657	57.7232583	14.294722	53.909167
LNG_DEU_0	LNG_ESTLVA LTU_1	14.294722	53.909167	21.101954	55.7253
LNG_ESTLVA LTU_1	LNG_FIN_0	21.101954	55.7253	21.4045365	61.635196
LNG_ESTLVA LTU_1	LNG_ESTLVA LTU_0	21.101954	55.7253	24.7157915	56.8352214
LNG_ESTLVA LTU_1	LNG_ESTLVA LTU_2	21.101954	55.7253	24.8231514	59.3377056
LNG_FIN_0	LNG_ESTLVA LTU_0	21.4045365	61.635196	24.7157915	56.8352214
LNG_FIN_0	LNG_ESTLVA LTU_2	21.4045365	61.635196	24.8231514	59.3377056

Annex 8 Enlarged model network map

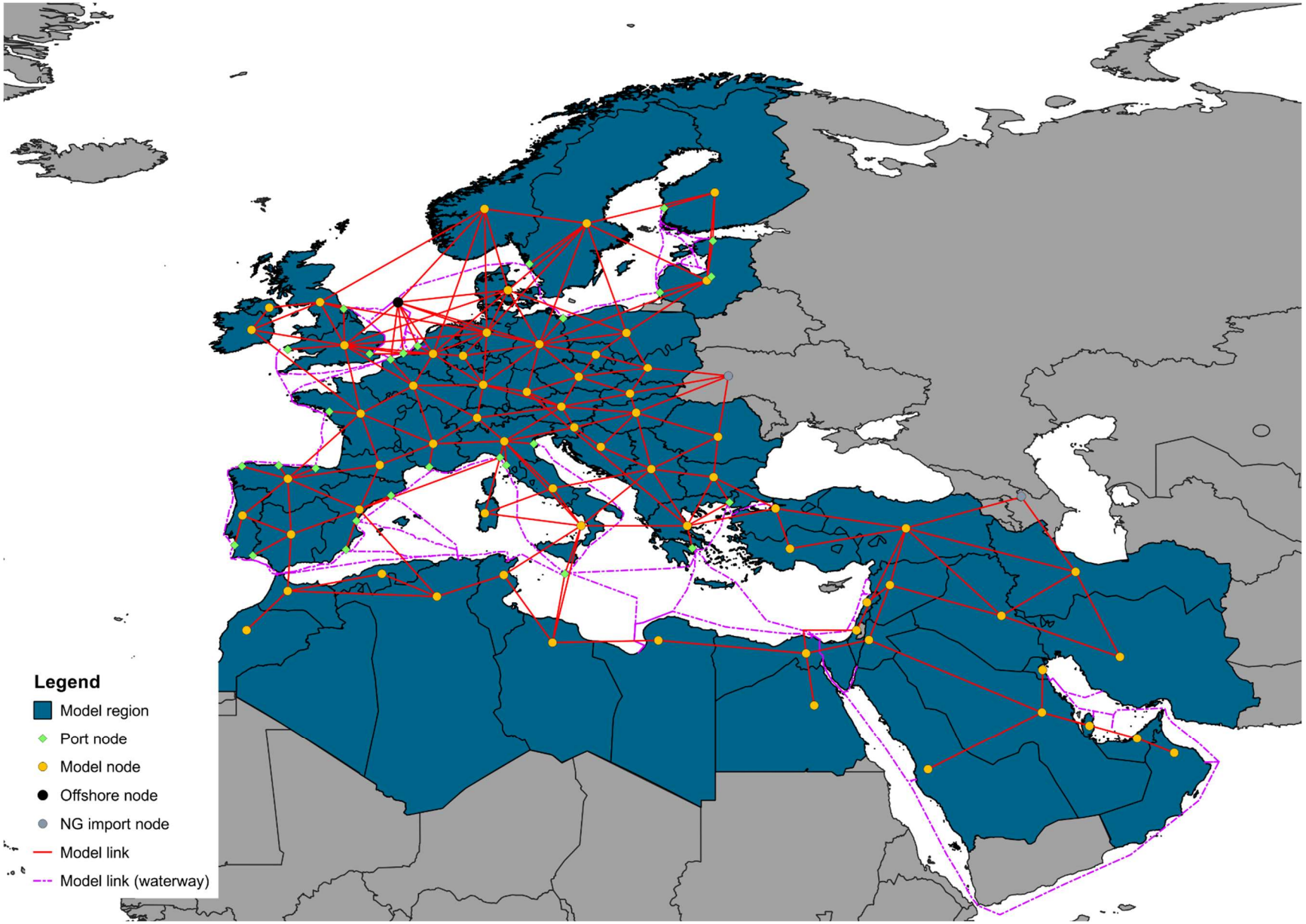

Annex 9 Techno-economic technology assumptions

Hydrogen production

A-24 Alkaline electrolyser (1 GW), techno-economic input data

Parameter	2030	2040	2050	Source
Electricity demand [MWh/MWh$_{H2}$]	1.608	1.531	1.431	[49]
Water demand [t/MWh$_{H2}$]	0.185	0.195	0.298	[49]
Lifetime [a]	25			[49]
Capacity factor [-]	1			[49]
Ramping rate [%/h]	100			[49]
Capital expenditure cost [k€/MW$_{el}$]	615	429	338	[49]
Fixed operation cost [%$_{CAPEX}$]	4			[49]

A-25 Proton-exchange membrane electrolyser (100 MW), techno-economic input data

Parameter	2030	2040	2050	Source
Electricity demand [MWh/MWh$_{H2}$]	1.709	1.623	1.506	[49]
Water demand [t/MWh$_{H2}$]	0.178	0.187	0.202	[49]
Lifetime [a]	25			[49]
Capacity factor [-]	1			[49]
Ramping rate [%/h]	100			[49]
Capital expenditure cost [k€/MW$_{el}$]	800	615	430	[49]
Fixed operation cost [%$_{CAPEX}$]	2			[49]

A-26 Solid-oxide electrolyser (10 MW), techno-economic input data

Parameter	2030	2040	2050	Source
Electricity demand [MWh/MWh$_{H2}$]	1.437	1.418	1.379	[49]
Water demand [t/MWh$_{H2}$]	0.237	0.240	0.248	[49]
Lifetime [a]	25			[49]
Capacity factor [-]	1			[49]
Ramping rate [%/h]	12	15	20	[49]
Capital expenditure cost [k€/MW$_{el}$]	1538	1292	984	[49]
Fixed operation cost [%$_{CAPEX}$]	12			[49]

Storage technologies

A-27 H_2O storage tank (6,000 L), techno-economic input data

Parameter	2030	2040	2050	Source
Lifetime [a]	30			Assumption
Ramping rate [%/h]	100			Assumption
Self-discharge rate [%/d]	0			Assumption
Capital expenditure cost [€/t$_{H2O}$]	23.3			[108]
Fixed operation cost [%$_{CAPEX}$]	0			Assumption

A-28 Storage tank for liquid hydrocarbons, techno-economic input data

Parameter	2030	2040	2050	Source
Lifetime [a]	25			[36]
Ramping rate [%/h]	100			Assumption
Self-discharge rate [%/d]	0			Assumption
Capital expenditure cost [k€/MWh$_{FT}$]	2.77			[36]
Fixed operation cost [%$_{CAPEX}$]	6.25			[36]

A-29 CO_2 storage tank, techno-economic input data

Parameter	2030	2040	2050	Source
Lifetime [a]	25			[109]
Ramping rate [%/h]	100			Assumption
Capital expenditure cost [k€/MWh_{CO2}]	2,580			[109]
Fixed operation cost [$\%_{CAPEX}$]	2			[109]

TCO land and ship calculation

The TCO for trucks is based on Basma and Rodríguez [59], selecting the e-diesel-powered cross-border long-haul class as a reference. Including fuel cost, the truck TCO amounts to 1.33 €/km. Trailer investment cost are assumed at 100,000 € for synfuel tank trailers and 780,000 € for liquid hydrogen tank trailers [48, 60]. No additional operational costs are attributed to trailer usage. Assuming a 15-year trailer lifetime and the same average annual mileage as reported by Basma and Rodríguez, the resulting total TCO per truck-trailer unit is 1.57 €/km for synfuel and 1.79 €/km for liquid hydrogen [61].

Each trailer is assumed to carry 0.472 GWh of synfuel or 0.117 GWh of liquid hydrogen, corresponding to specific transport costs of 3.33 €/GWh*km and 15.30 €/GWh*km, respectively [48, 49, 60]. The average travel speed and driving hours per day are assumed at 80 km/h and 9 hours of travel time per 24 hour period, as outlined in Regulation (EC) No 561/2006 [62]. The duration of loading and unloading time spent filling the trailers is assumed to be <1 h for synfuels and 6 h total for liquefied hydrogen [63].

The ship transport is modelled analogous. TCO parameters are derived using the *Total Cost of Ownership (TCO) model* of the Mærsk Mc-Kinney Møller Center for Zero Carbon Shipping [64].

For the transport of synfuels the tanker ship class, using a heavy fuel oil (HFO) internal combustion engine (ICE) as main and auxiliary engine, is selected. E-Diesel sourced from DAC is selected as fuel for both engines. For the electricity and oil price scenario “Path we are on” is chosen, no CO_2 price is assumed.

The yearly TCO of amounts to 39.99 M€ (2030) and decreases to 31.22 M€ (2050). With an assumed annual traveling distance of 64,800 nm per year and a carrying capacity of 34,380 tonnes (60,671 dead weight tonnage (DWT), 57% load factor) the total specific TCO is 0.80 €/GWh*km which decreases down to 0.62 €/GWh*km in 2050. The travelling speed assumed is 13 nm/hr. Loading is expected to take up 16 hours based on the average visiting duration at the oil terminals in the port of Rotterdam (calculated with data from [110]).

For the transport of liquified hydrogen, the gas carrier class is selected as it represents currently operational LNG tankers. Since the volumetric energy density of liquified hydrogen is roughly half that of LNG, it is assumed that construction characteristics cannot be mapped to allow the transport of liquified hydrogen without adjustment [111].

The cargo capacity of the tanker is therefore modelled after Alkhaledi et al. [65], who explore the design of large liquified hydrogen tankers. The cargo capacity per tanker is, based on [65], assumed to be 20,000 tonnes of liquified hydrogen. With an initial TCO between 56.88 M€ (2030) and 50.21 M€ (2050) and an assumed travel distance of 102,000 nm, the specific TCO totals to 0.45 €/GWh*km and 0.40 €/GWh*km respectively. The traveling speed is assumed to be 17 nm/hr. Loading time for liquified hydrogen is higher than synfuels, as

evidenced by the average visit duration at the HyTouch Kobe terminal which is 103.6 hours [110].

Hydrogen liquefaction is scaled to deliver 1 GWh/h from annual values and includes respective pump cost, also from [112].

A-30 Hydrogen liquefaction, techno-economic input data

Parameter	2030	2040	2050	Source
Electricity demand [MWh/MWh$_{LH2}$]	0.206			[112]
Hydrogen demand [MWh$_{H2}$/MWh$_{LH2}$]	1.05			Assumption
Lifetime [a]	20			[112]
Capacity factor [-]	1			Assumption
Ramping rate [%/h]	100			[112]
Capital expenditure cost [k€/MW$_{el}$]	1,726			[112]
Fixed operation cost [%$_{CAPEX}$]	8			[112]

Annex 10 Water stressed model regions

A-31 Water scarce model regions Europe

Europe	
Country	**Node_ID**
Benelux	BELNLDLUX_1
Spain	ESP_1
	ESP_2
France	FRA_2
Greece	GRC_1
Italy	ITA_1
	ITA_3

A-32 Water scarce model regions Middle East

Middle East	
Country	**ID**
Iran	IRN_1
	IRN_2
Iraq	IRQ_1
Jordan	JOR_1
Kuwait	KWT_1
Lebanon	LBN_1
Oman	OMN_1
Qatar	QAT_1
Saudi Arabia	SAU_1
	SAU_2
Syria	SYR_1
Turkey	TUR_1
	TUR_2
	TUR_3

A- 33 Water scarce model regions North Africa

North Africa	
Country	**ID**
Algeria	DZA_1
	DZA_2
Egypt	EGY_1
	EGY_2
Morocco	MAR_1
	MAR_2
Tunisia	TUN_1
Libya	LBY_1
	LBY_2

Annex 11 Energy and mass balances of synfuel pathways

A-34 Energy and mass balance catalytic methanation (including SWRO)

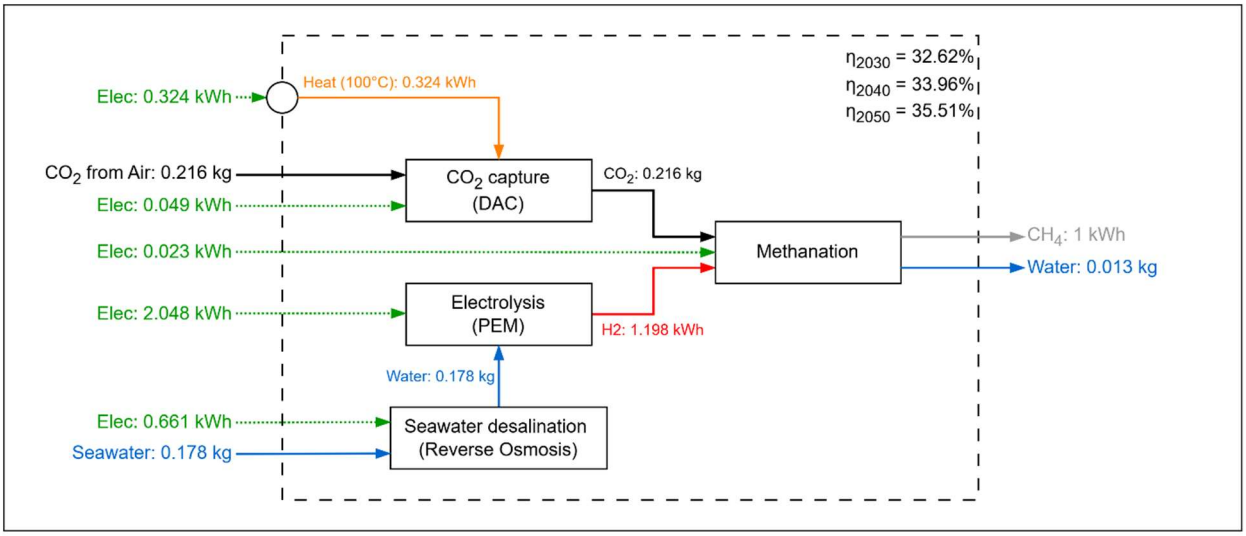

A-35 Energy and mass balance catalytic methanation

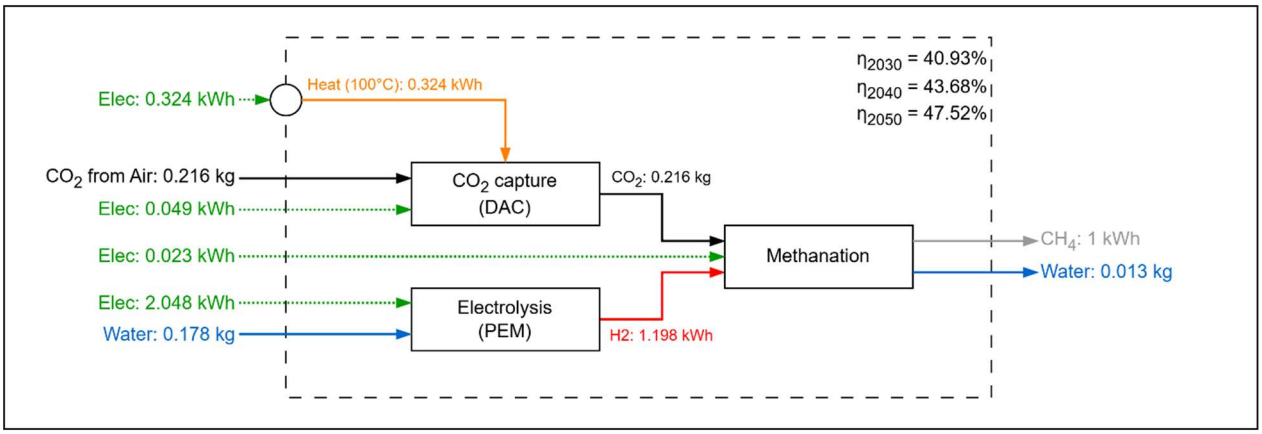

A-36 Energy and mass balance Fischer-Tropsch synthesis (including SWRO)

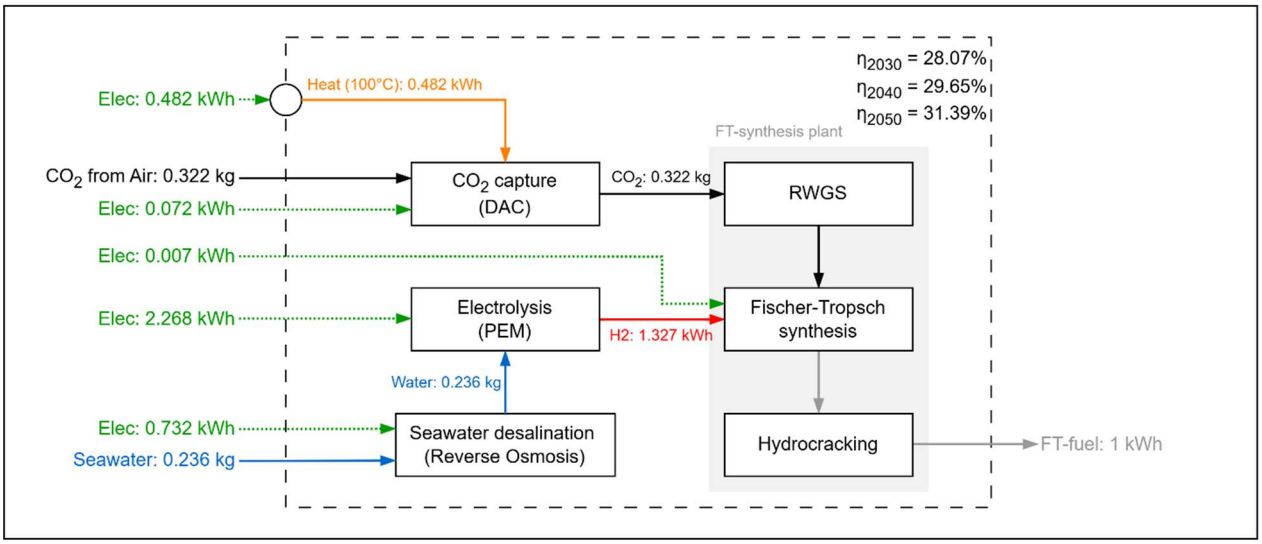

A-37 Energy and mass balance Fischer-Tropsch synthesis

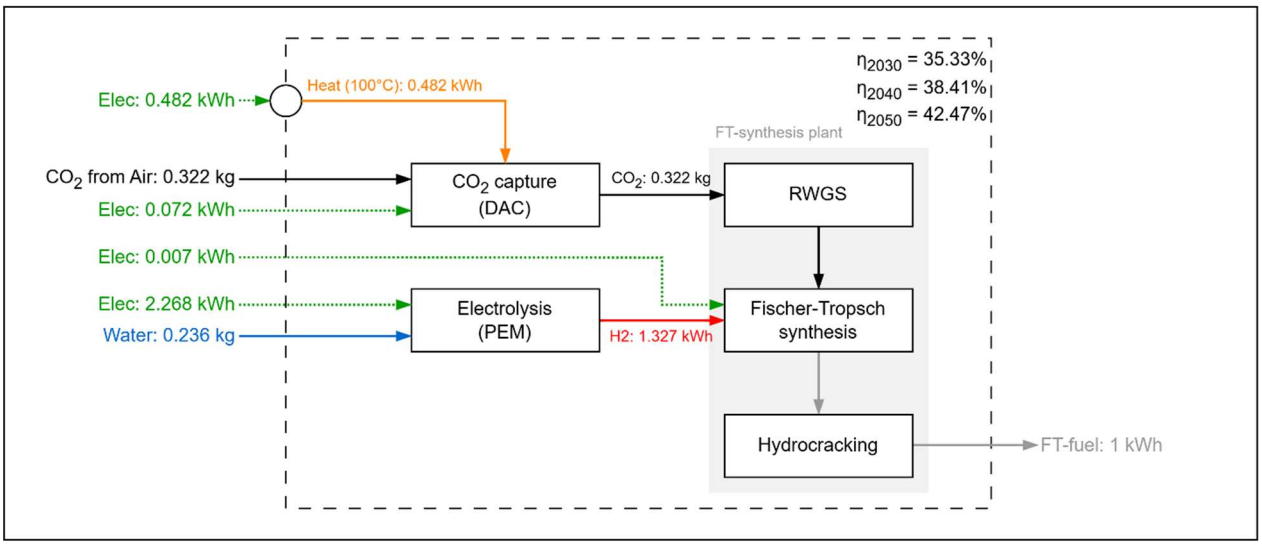

A-38 Energy and mass balance Methanol-to-hydrocarbon (including SWRO)

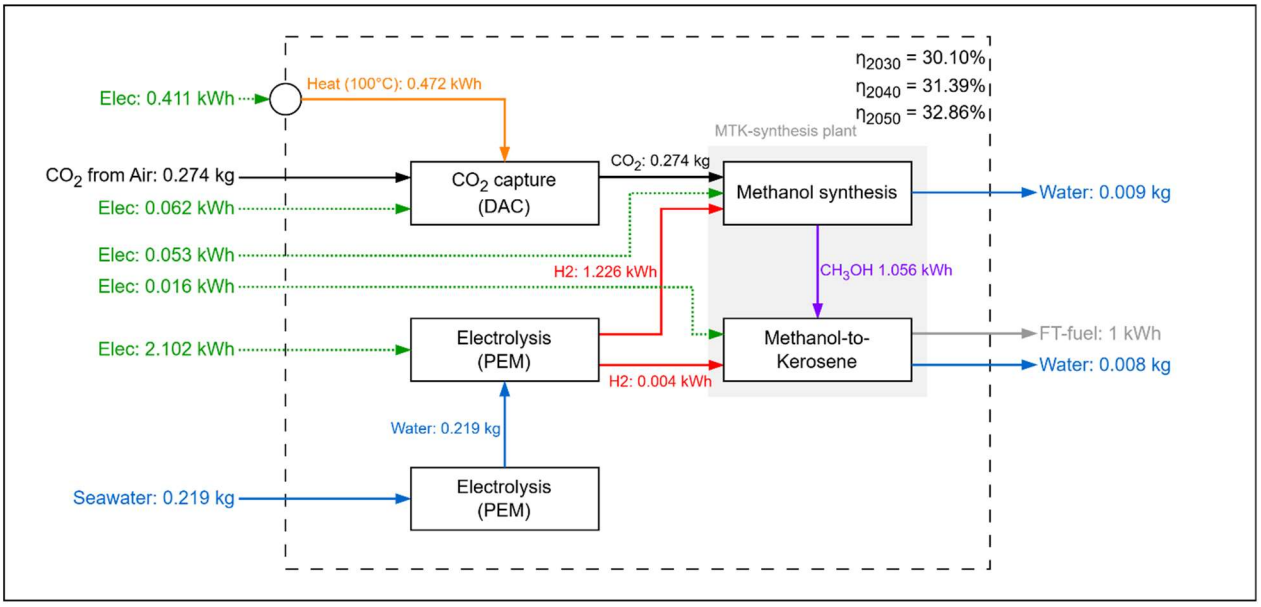

A-39 Energy and mass balance Methanol-to-hydrocarbon

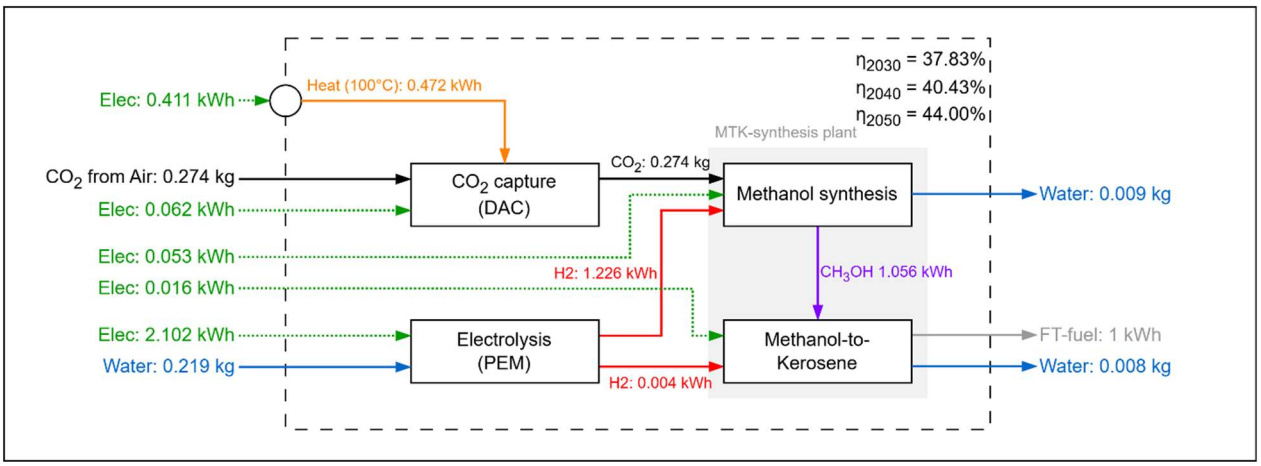

Annex 12 Country sensitive WACC assumptions from Braun et al.

A- 40 MENA country-specific cost of capital assumptions, based on scenario WACC_bau from [21]

Country	Cost of capital RES [%]	Cost of capital hydrogen and other synfuels [%]
Algeria	15.69	18.67
Egypt	13.86	16.78
Iran	15.69	18.21
Iraq	17.53	20.59
Jordan	12.02	15.21
Lebanon	22.32	25.77
Libya	21.18	24.27
Morocco	8.34	10.68
Oman	9.27	11.32
Qatar	4.87	6.25
Saudi Arabia	5.05	6.45
Syria	24.84	28.21
Tunisia	13.86	16.64
United Arab Emirates	4.67	6.05

Annex 13 Additional figures

BASE scenario

A- 41 Installed onshore wind capacity per region (BASE)

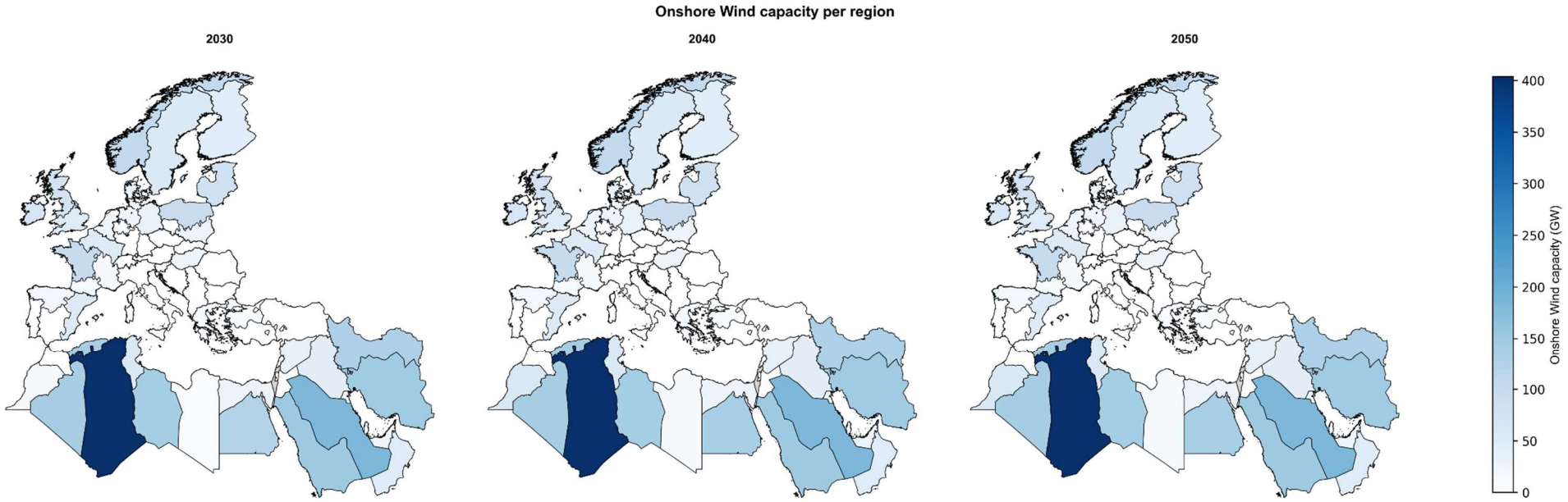

A- 42 Hydrogen network flows divided into retrofitted (left) and new (right) pipelines BASE (2050)

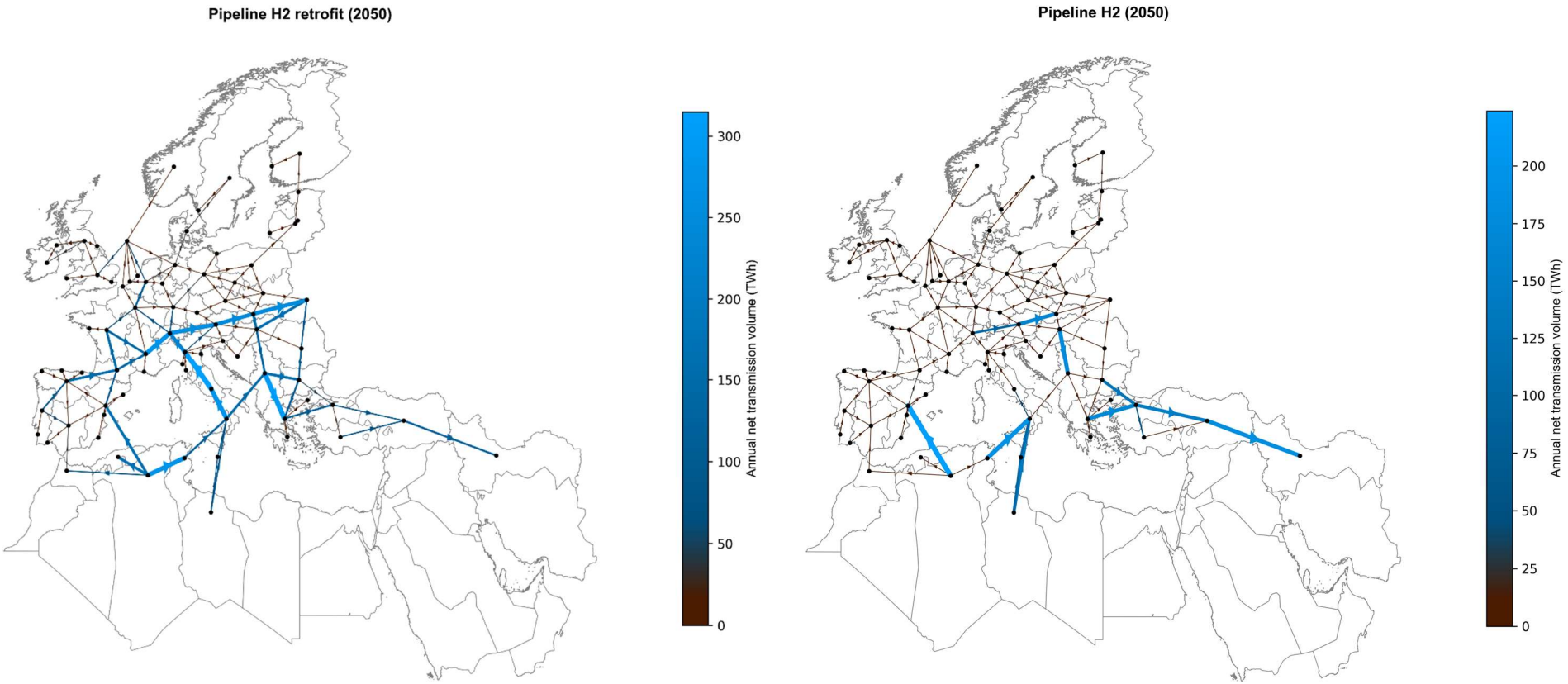

A- 43 Installed methane storage capacity BASE (2050)

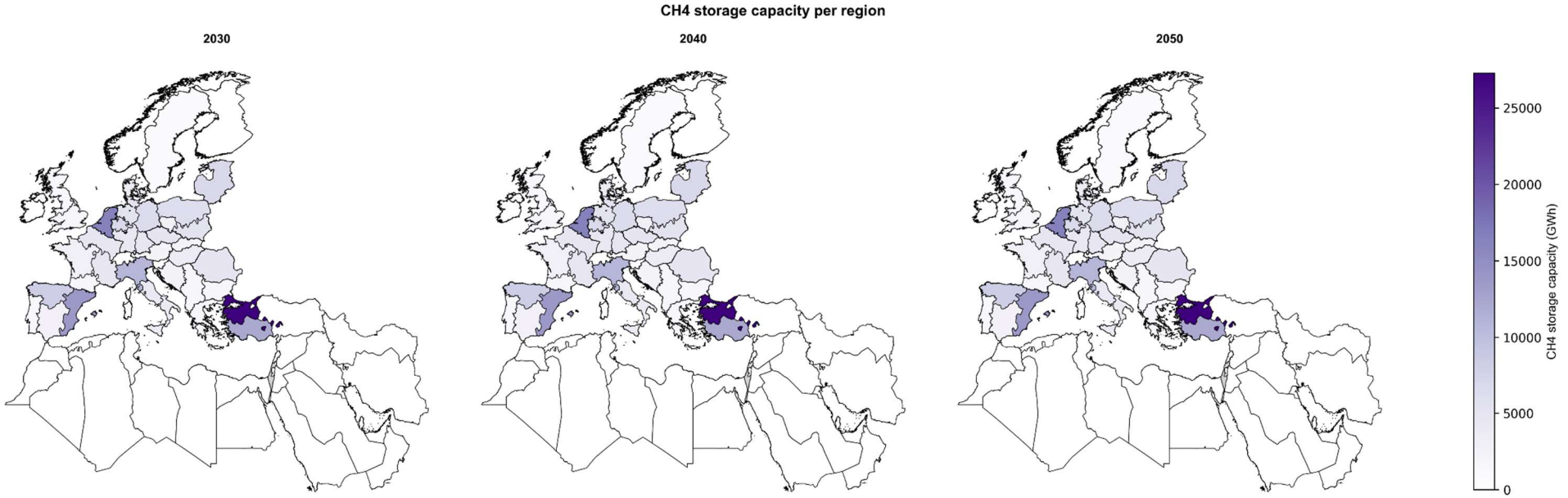

A- 44 EU (left) and MENA (right) mean hydrogen demand duration curves

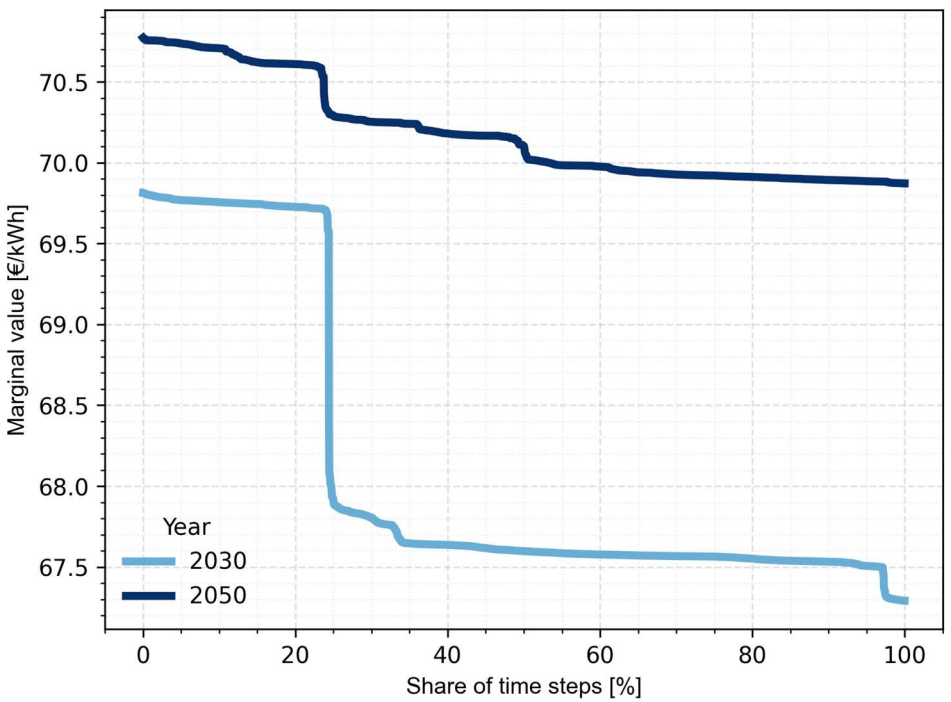

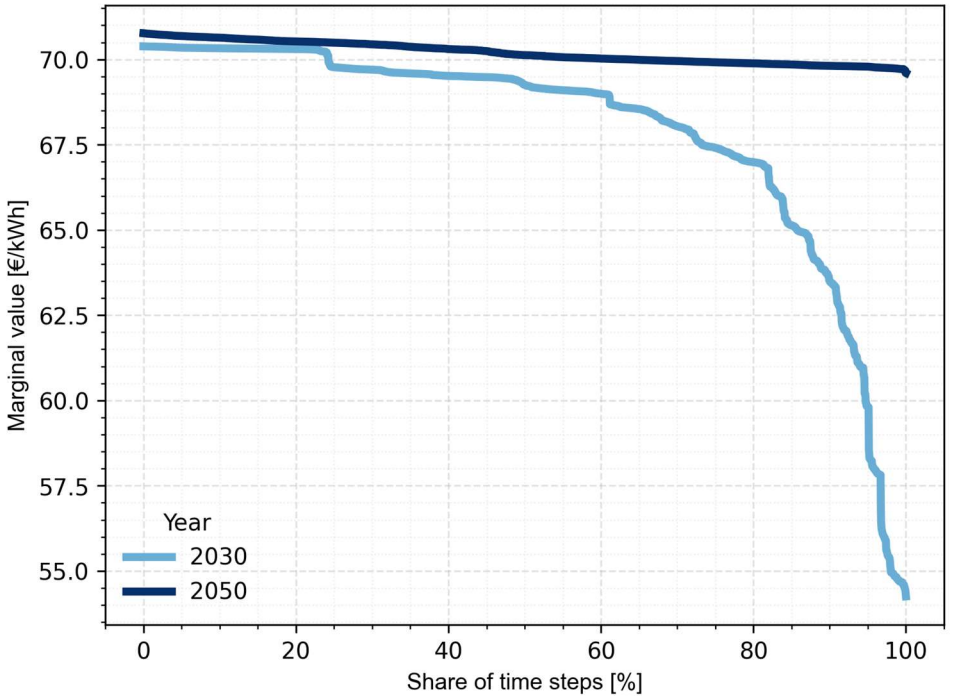

A- 45 EU (left) and MENA (right) mean FT fuel demand duration curves

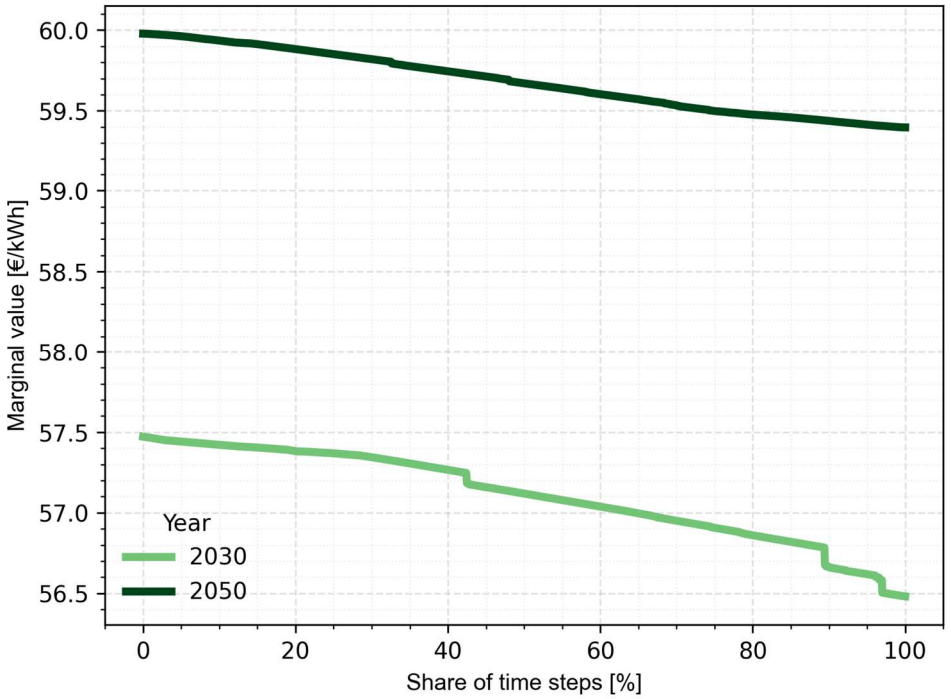

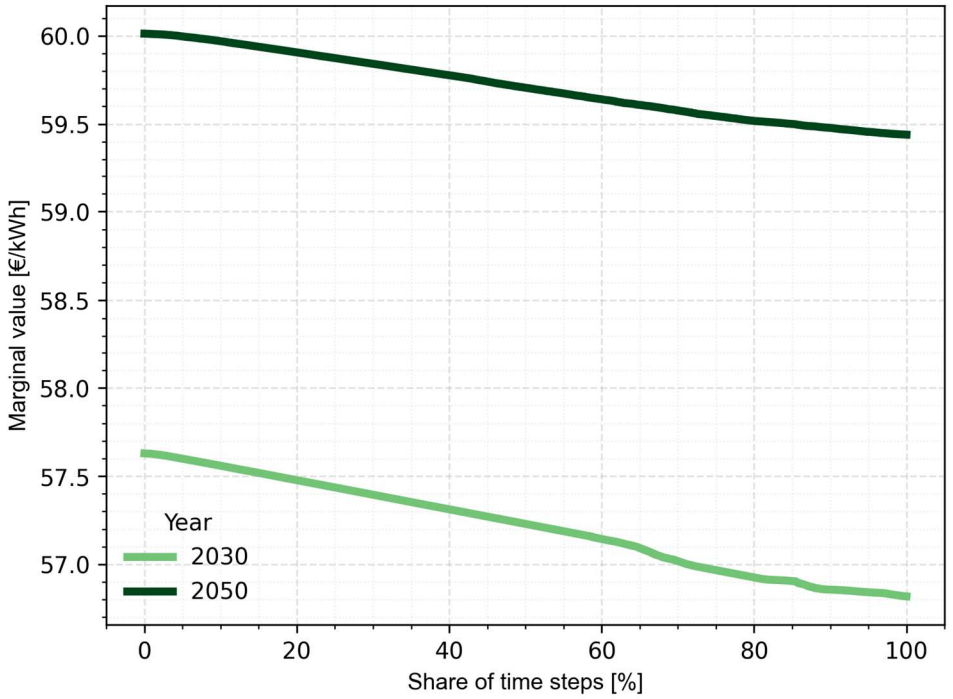

A- 46 EU and MENA marginal demand duration curves BASE (2030)

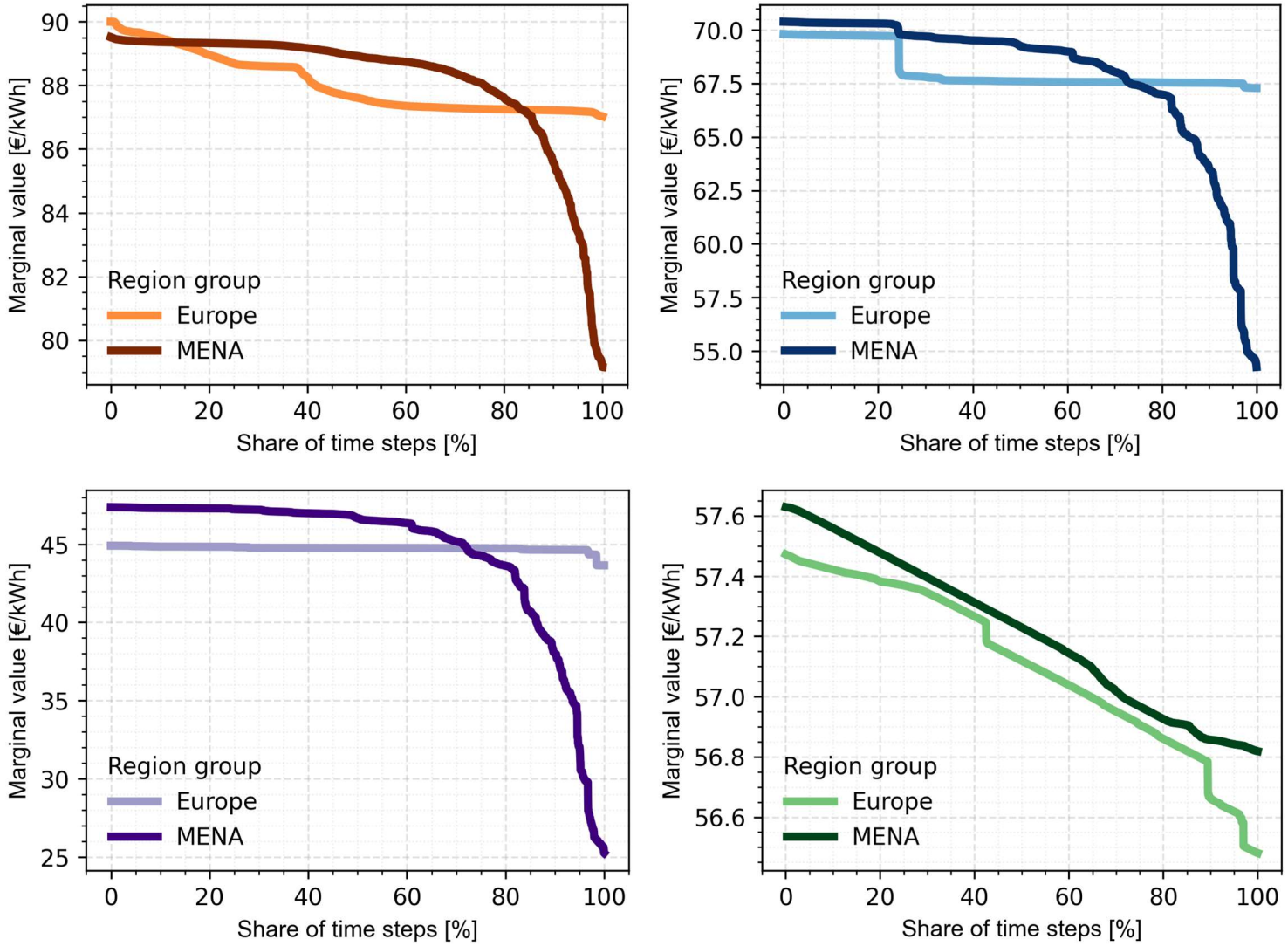

A- 47 Marginal methane production cost Δ BASE (2030-2050)

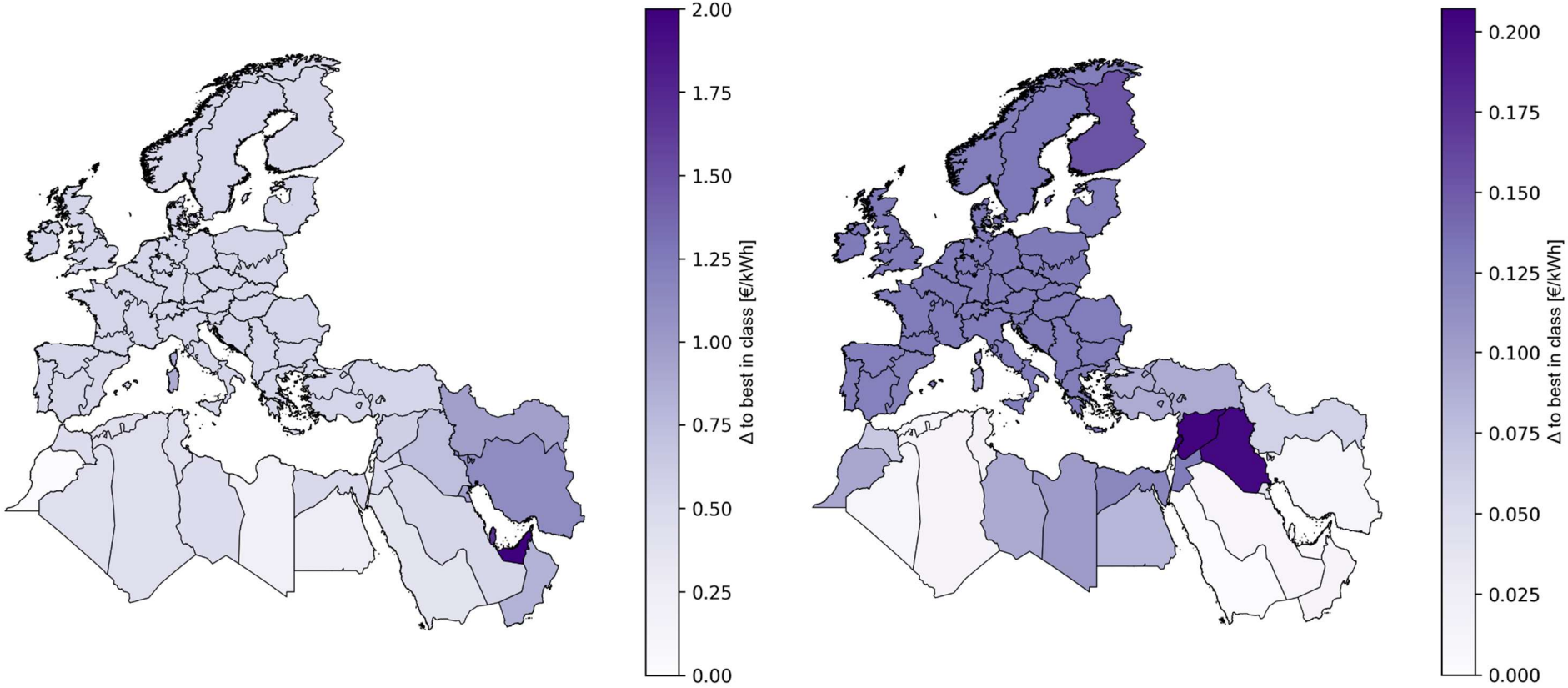

A- 48 Marginal FT fuel production cost Δ BASE (2030-2050)

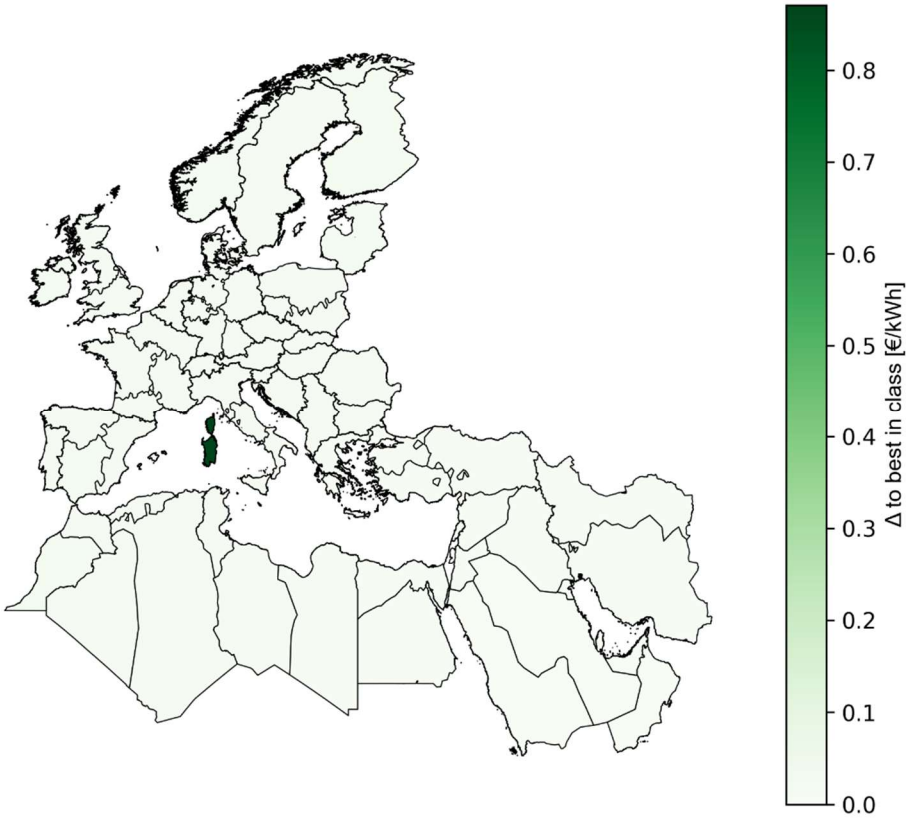

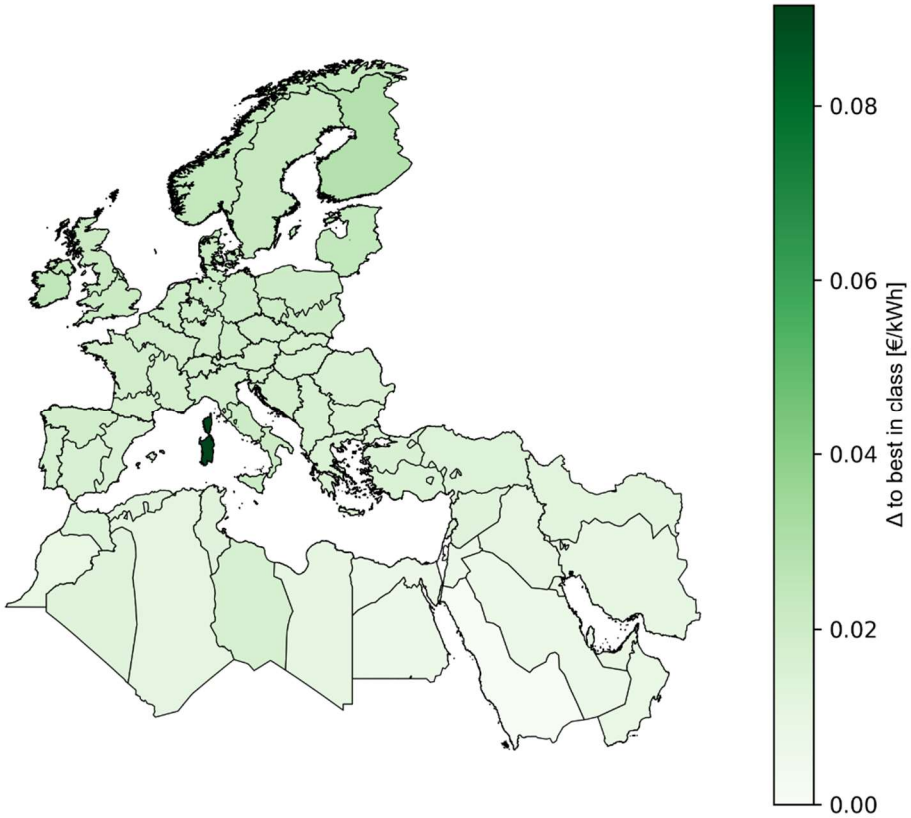

A- 49 Hydrogen cavern installation difference between BASE and AUTARKY (2050)

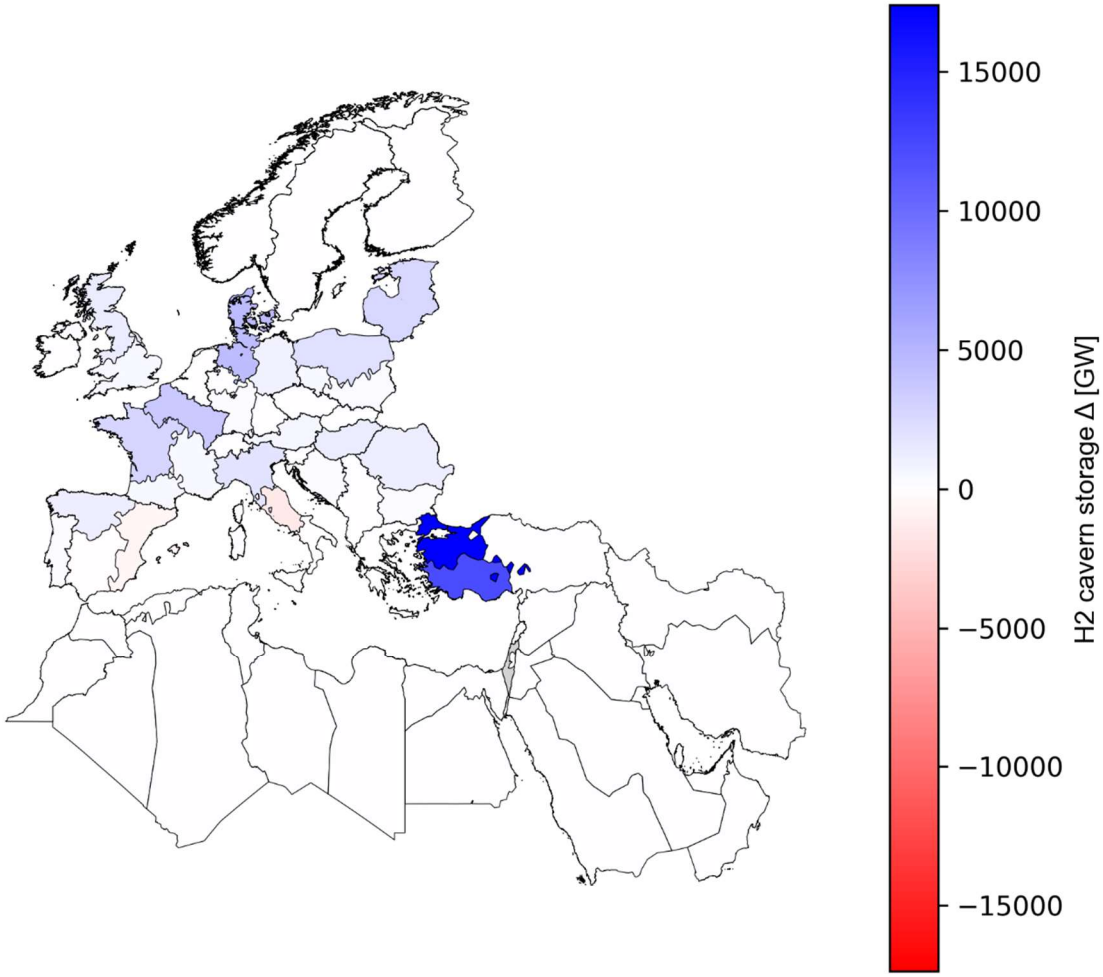

A- 50 Methane import dependency top 15 countries BASE (2050)

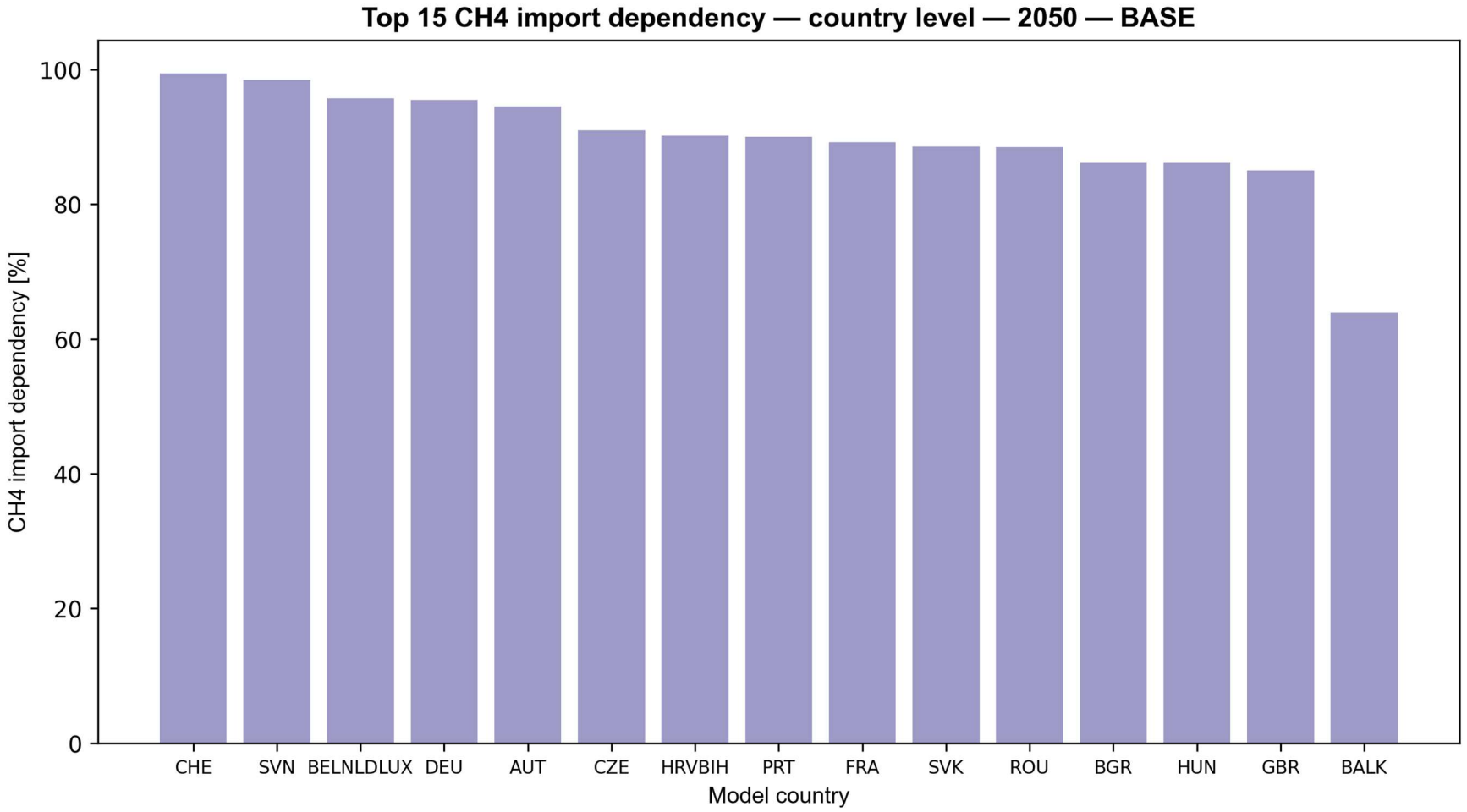

A- 51 FT fuel import dependency top 15 countries BASE (2050)

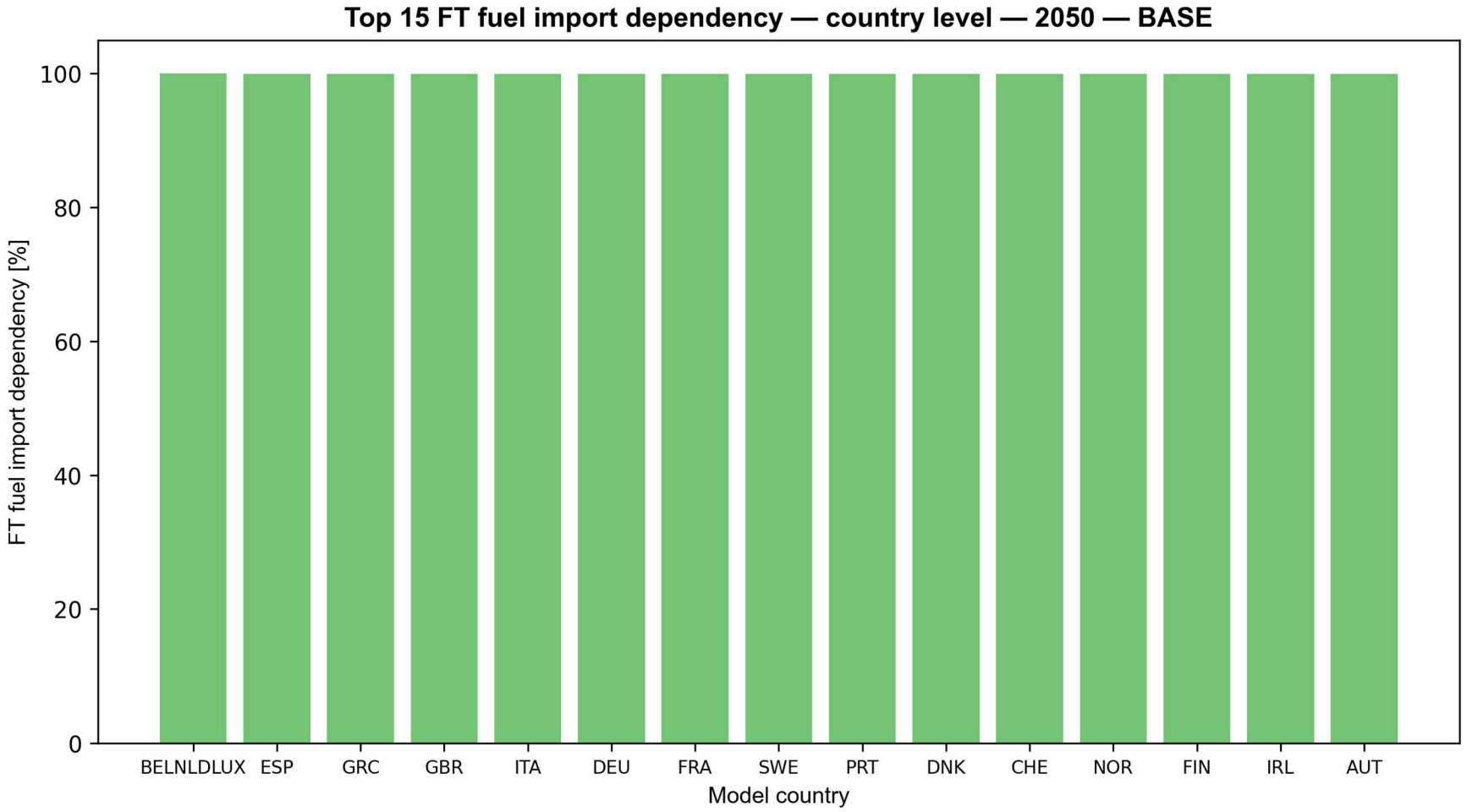

A- 52 Net annual hydrogen flows TRANS_delay, top 75% of flows (2050)